



**Hugo Filipe Orfão da
Silva**

**Implementação numa FPGA de Técnicas MIMO para
os futuros sistemas de transmissão wireless-
(Sistemas de 4G/LTE)**

**Hugo Filipe Orfão da
Silva**

**Implementação numa FPGA de Técnicas MIMO para
os futuros sistemas de transmissão wireless-
(Sistemas de 4G/LTE)**

**MIMO techniques implementation on FPGA for future
wireless transmission systems (4G/LTE)**

Dissertação apresentada à Universidade de Aveiro para cumprimento dos requisitos necessários à obtenção do grau de Mestre em Engenharia Electrónica e Telecomunicações, realizada sob a orientação científica do Professor Doutor Manuel Alberto Reis de Oliveira Violas e do Professor Doutor Adão Paulo Soares da Silva, Professores Auxiliares do Departamento Electrónica, Telecomunicações e Informática da Universidade de Aveiro

**Agradecimentos /
acknowledgements**

Dedico este trabalho à minha família e amigos pelo incansável apoio.

Um agradecimento ao Professor Doutor Manuel Alberto Reis de Oliveira Violas, ao Professor Doutor Adão Paulo Soares da Silva, ao Engenheiro João Filipe Lopes Seabra Lourenço e ao Engenheiro José Eduardo Reis Assunção pela incansável ajuda e disponibilidade.

o júri

presidente

Prof. Dr. José Rodrigues Ferreira da Rocha
professor catedrático da Universidade de Aveiro

arguente

Dr. Carlos Miguel Nogueira Gaspar Ribeiro
professor adjunto do Instituto Politécnico de Leiria

orientador

Prof. Dr. Alberto Reis de Oliveira Violas
professor associado da Universidade de Aveiro

Palavras-chave

LTE, MIMO, Matlab, Simulink , Xilinx System Generator, OFDM, SC-FDMA, OFDMA, MISO, Zero-forcing, MMSE, Alamouti, PAPR.

Resumo

O presente trabalho faz alusão à tecnologia 4G LTE. São descritas técnicas usadas na mesma tecnologia nomeadamente de precoding e codificação e descodificação Alamouti.

É introduzido um sistema Alamouti 4G implementado para FPGAs usando o programa System Generator da Xilinx. O trabalho também aborda o problema do PAPR devido aos pilotos de referência na plataforma estarem sendo gerados todos em fase. Neste trabalho, um gerador aleatório de pilotos foi implementado que combate a potência de pico (PAPR). No receptor levou-se em conta o método desta nova geração para realizar a estimativa de canal corretamente.

Keywords

LTE, MIMO, Matlab, Simulink , Xilinx System Generator, OFDM, SC-FDMA, OFDMA, MISO, Zero-forcing, MMSE, Alamouti, PAPR.

Abstract

This work alludes to 4G LTE technology. Techniques used for the same technology are described namely precoding and Alamouti coding and decoding. An Alamouti's 4G system implemented to FPGA using the Xilinx System is introduced. The work also addresses the PAPR problem due to the reference pilots in the platform being generated all in phase. In this work a random pilot generator was implemented which combats the high peak power. In the receiver it was taken into account the new generation method to perform channel estimation correctly. A technique is discussed to increase the energy efficiency of the system based on PAPR reduction.

Contents

CONTENTS.....	XIII
FIGURES LIST.....	XV
TABLES LIST.....	XVI
ACRONYMS.....	XVI
1. THESIS INTRODUCTION	1
1.1. MOTIVATION AND OBJECTIVES.....	3
2. INTRODUCTION TO BROADBAND WIRELESS	4
2.1. FIRST GENERATION	4
2.2. SECOND GENERATION	5
2.3. THIRD GENERATION.....	6
2.4. FOURTH GENERATION.....	7
3. NETWORK ARCHITECTURE.....	9
3.1. CORE NETWORK.....	10
3.2. ACCESS NETWORK	12
4. OFDM.....	14
4.1.1 BASIC PRINCIPLES OF OFDM.....	14
4.1.2 OFDM APPLIED ON LTE.....	17
4.1.2.1 ORTHOGONALITY	20
4.1.3. CYCLIC PREFIX	21
4.2. OFDMA AND SC-FDMA	22
4.2.1. OFDMA.....	22
4.2.2. SC-FDMA	23
4.3. MIMO SYSTEMS.....	25
4.3.1. MULTIPATH DIVERSITY	25
4.3.2. MACRO DIVERSITY	26
4.3.3. TIME DIVERSITY	27
4.3.4. FREQUENCY DIVERSITY	27

4.3.5.	RECEIVE ANTENNA DIVERSITY	27
4.3.6.	TRANSMIT DIVERSITY	28
4.4.	BENEFITS OF MIMO TECHNOLOGY.....	28
4.5.	MULTIPLE ANTENNA CONFIGURATIONS[56].....	29
4.5.1.	PRACTICAL IMPLEMENTATION	33
5	ALAMOUTI'S ENCODING AND DECODING	34
5.1.	SPACE-TIME BLOCK CODING ALAMOUTI	34
5.2.	SPACE-FREQUENCY BLOCK CODING ALAMOUTI [61]	36
5.3.	PRACTICAL SYSTEM	38
6.	PRECODING – PRACTICAL IMPLEMENTATION	41
6.1.	CELCOP CHAIN PRACTICAL IMPLEMENTATION	43
6.2.	ZERO-FORCING PRACTICAL IMPLEMENTATION - SYSTEM GENERATOR	49
7.	PAPR (PEAK-TO-AVERAGE POWER RATIO).....	55
7.1.	REDUCING PAPR – RANDOM REFERENCE PILOTS GENERATION PRACTICAL IMPLEMENTATION (TRANSMITTER SIDE).....	56
7.2.	REDUCING PAPR – RANDOM REFERENCE PILOTS GENERATION PRACTICAL IMPLEMENTATION (RECEIVER SIDE)	61
7.3.	PRACTICAL RESULTS (RECEIVER SIDE)	63
8.	CONCLUSION AND FUTURE WORK.....	68
	BIBLIOGRAPHY.....	69
	ANNEX	76
	ANNEX A.....	76
	ANNEX B.....	82
	ANNEX C.....	88
	ANNEX D.....	93

Figures List

Figure 1- FPGA board features [3].....	2
Figure 2 - Releases of 3GPP specifications for UTRA[15].....	7
Figure 3 - 3GPP cellular networks evolution [26].....	10
Figure 4 - Evolved Packet System architecture[26].....	12
Figure 5 - Evolved UMTS Terrestrial Radio Access Network architecture [29].....	13
Figure 6 - OFDM system in blocks [31].....	15
Figure 7 - OFDM symbol in time and frequency domain [15].....	16
Figure 8 - Bandwidth allocation [15].....	16
Figure 9 - OFDM concept[35].....	17
Figure 10- LTE frame [37].....	18
Figure 11 - Relationship between a LTE slot, symbols and Resource Blocks [39].....	19
Figure 12- Antenna pilots allocation[44].....	20
Figure 13 - Difference between OFDM and OFDMA[45].....	22
Figure 14- Differences between OFDM and SC-FDMA in terms of frequency/amplitude/time [48]	23
Figure 15-- Differences between OFDM and SC-FDMA in terms of overall system blocks [49].....	24
Figure 16- Multipath diversity[52].....	26
Figure 17- SISO, SIMO, MISO and MIMO[57].....	30
Figure 18- BER for 2x1, 2x2 and 1x1 systems.....	33
Figure 19- Transmitter side System Generator's Xilinx design.....	38
Figure 20- System reception block diagram.....	39
Figure 21 - Alamouti decoder Xilinx System Generator design.....	40
Figure 22 - BER comparing SISO to MIMO systems with ZF and MMSE precoders.....	43
Figure 23-Celcop Calibration tool V5.....	44
Figure 24- Celcop chain overall block diagram.....	45
Figure 25 - BER for cent-mmse precoding.....	48
Figure 26 - BER for ZF precoder.....	48
Figure 27- ZF Xilinx design system blocks.....	50
Figure 28 - Complex multiplier system blocks.....	51
Figure 29- Complex Division system blocks.....	52
Figure 30- Adjunct matrix creator system blocks.....	53
Figure 31- Input and Output system results.....	54
Figure 32 - Pilots insertion subsystem in antenna 1.....	56
Figure 33- Pilots insertion subsystem in antenna 2.....	57
Figure 34 - LFSR example sending in-phase values.....	58
Figure 35-LFSR example sending quadrature values.....	58
Figure 36 - Inside view of the pilots insertion subsystem.....	59
Figure 37- OFDM signals comparison at different time samples.....	60
Figure 38 - Overall system blocks of phase correction at reception.....	62
Figure 39 - Scope values.....	63
Figure 40 - Scope values for phase interpolation.....	64

Figure 41 - Pilots peak values comparison between old (red) and new system (blue)	64
Figure 42- QPSK output signal.....	65
Figure 43 - 16-QAM output signal.....	65
Figure 44- Testing graphic / received bits vs transmitted bits	66

Tables list

Table 1 - LTE specifications [7].....	8
Table 2 - Alamouti code 1	36
Table 3- Alamouti code 2.....	38
Table 4 - Phase correction values.....	61

Acronyms

16-QAM: 16-Quadrature Amplitude Modulation
1G: first generation
3G UTRA: Third Generation Universal Terrestrial Radio Access
3GPP: Third generation Partnership Project
3GPP2: Third generation Partnership Project
8-QAM: 8-Quadrature Amplitude Modulation
ACE: Active Constellation Extension
AMPS: • Advanced Mobile Phone System
ARIB: Association of Radio Industries and Businesses
ARP: Car Radio Phone
ATIS: Alliance for Telecommunications Industry Solutions
AWGN: Additive White Gaussian Noise
BER: Bit-Error Rate
CCSA: China Communications Standards Association
CDMA: Code-Division Multiple Access
CEPT: Conference of European Post and Telecommunications
CN: Core Network
CRF: Charging Rules Function
CS: Circuit Switched
CSI: Channel State Information
D-AMPS: Digital Analogue Mobile Phone System
DC-HSDPA: Dual Carrier-HSDPA

DFT: Discrete Fourier Transform
DL: Downlink
DVB: Digital Video Broadcasting
EDGE: Enhanced Data Rates for Global Evolution
EPC: Evolved Packet Core
EPS: Evolved Packet System
ETSI: European Telecommunication Standards Institute
E-UTRAN: Evolved-UMTS Terrestrial Radio Access Network
EVDO Rev B: Enhanced Voice-Data Only Revision B
FDD: Frequency Division Duplex
FDMA: Frequency Division Multiple Access
FFT: Fast Fourier Transform
FSK: Frequency Shift Keying
GGSN: Gateway GPRS Support Node
GMSK: Gaussian Minimum Shift Keying
GPRS: General Packet Radio Services
GSM: Global System for Mobile Communications
HSDPA: High Speed Downlink Packet Access
HSPA: High-Speed Packet Access
HSPA+: High Speed Packet Access Evolution
HSS: Home Subscriber Server
HSUPA: High Speed Uplink Packed Access
ICIC: Inter-cell Interference Coordination
IDFT: Inverse Discrete Fourier Transform
IFFT: Inverse Fast Fourier Transform
IMT-2000: International Mobile Telecommunications by 2000
IP: Internet Protocol
ISI: Intersymbol interference
ITU: International Telecommunication Union
LTE: Long Term Evolution
LTE FDD: LTE Frequency Division Duplex
MIMO: Multiple Input Multiple Output
MISO: Multiple Input single output
MME: Mobility Management Entity
MMSE: Minimum Mean Square Estimation

MS: Mobile Station
MSC: Mobile Service Switching Center
MTD: Mobile telephony system D
NAS: Non-Access Stratum
NMT: Nordic Mobile Telephone
NTT: Nippon Telephone & Telegraph
OFDM: Orthogonal Frequency-Division multiplexing
OFDMA: Orthogonal Frequency Division Multiple Access
OLT: Denmark and Public Land Mobile Telephony
PAPR: Peak-to-Average Power Ratio
PBCH: Physical Broadcast Channel
PCFICH: Physical Control Format Indicator Channel
PCRF: Policy and Charging Rules Function
PDCCH: Physical Downlink Control Channel
PDF: Policy Decision Function
PDN GW: Packet Data Network Gateway
PDSCH: Physical Downlink Shared Channel
P-GW: Packet-Gateway
PHICH: Physical Hybrid ARQ Indicator Channel
PMCH: Physical Multicast Channel
PRB: Probing Resource Block
PS: Packed Switched
PSK: Phase Shift Keying
QAM: Quadrature Amplitude Modulation
QoS: Quality of Service
QPSK: Quadrature Phase Shift Keying
RAM: Random Access Memory
RB: Resource Block
RNC: Radio Network Controller
RNS: Radio Network Subsystem
RRM: Radio Resource Management
SAE: System Architecture Evolution
SC-FDMA:; Single Carrier-Frequency Division Multiple Access
SFBC: Space-Frequency Block Coding
SGSN: Serving GPRS Support Node

S-GW: Serving-Gateway
SIMO: Single Input Single Output
SISO: Single Input Single Output
SMS: Short Message Services
SNR: Signal-to-Noise Ratio
SSDT: Site Selection Diversity Transmission
STTD: Space Time Transmit Diversity
TACS: Total Access Communications Systems
TDD: Time Division Duplex
TDMA: Time-Division Multiple Access
TD-SCDMA: Time Division Synchronous Code Division Multiple Access
TSTD: Time Switched Transmit Diversity
TTA: Telecommunications Technology Association
TTC: Telecommunication Technology Committee
UE: Universal User
UL: Uplink
UMTS: Universal Mobile Telecommunication Systems
UTRA: Universal Mobile Telephony System terrestrial radio access
UTRAN: Universal Terrestrial Radio Access Network
VLR: Visitor Location Register
VoIP: Voice over IP
W-CDMA: Wideband Code Division Multiple Access
WiMAX: Worldwide Interoperability for Microwave Access
WLAN: Wireless Local Area Network
XNOR: exclusive-nor
XOR: exclusive-or
ZF: Zero Forcing

Chapter 1

1. Thesis Introduction

Long distance communications started since the telegraphs and simple coded pulses were used for transmitting short messages wirelessly. Since that, technology has been progressively evolving leading to even better and advanced reliable ways of transferring information. Hardware connections and electronic switches have made transfer of digital data feasible. Internet also led it to another dimension in the way of the extensive processing of voice and data. Also, radio communication has been evolving [1].

All of this, changed the way of living and thinking of people. There are nearly 7 billion mobile subscriptions worldwide, estimates The International Telecommunication Union (May 2014), equivalent to 95.5 % of the world population. Now the growth is slowing, especially because mobile subscriptions in the developed world are reaching saturation point. New strategies need to be made, like incentivising people to join the newest technologies that are being launched [2].

In this thesis, the methods of study are proposed through Matlab simulations and also some are implemented for Virtex-6 FPGA ML605 Evaluation Kit to be added to a transceiver that follows closely the LTE physical layer specifications. We used the System Generator from Xilinx to develop and test the Simulink models.

The Virtex-6 FPGA ML605 from Xilinx is the base platform for high level applications programming for markets like wireless telecommunications. It provides an user friendly programming environment. A general view of the board is shown in figure below:

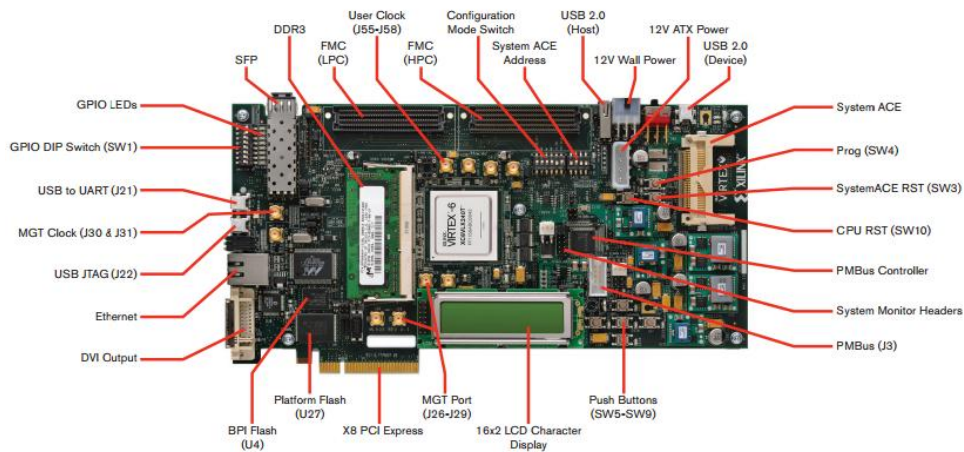


Figure 1- FPGA board features [3]

The thesis is organized through the main chapters that are briefly explained:

- Chapter 2
A brief historic explanation of the wireless technologies is done from the 1st Generation to 4th Generation wireless technologies. It is made some reference to the companies involved, and some specs are shown.
- Chapter 3
The network architecture of LTE system is superficially explained from Core Network to the Access Network, making reference to some of their components.
- Chapter 4
It is detailed the technologies used by LTE for downlink and uplink. Some methods to increase the efficiency (diversity) of the systems are detailed.
- Chapter 5
It is introduced Alamouti systems in order to encode and decode data in time or frequency domain.
- Chapter 6
Precoders implementations are made and simulated in order to take its advantages and disadvantages.

- Chapter 7

A PAPR reduction solution is proposed in Xilinx System Generator, in order to have more efficient transmission and reception systems for 4G communications through an FPGA.

1.1. Motivation and objectives

With the constant growing of wireless communications, the demands grow also in terms to provide users better transmission rates or better *Quality of Service* (QoS). Different methods that explore the increase of performance are explained in this thesis, according to diversity, increasing the number of antennas (with Alamouti's encoding and decoding) or using precoders.

Methods are proposed through Matlab simulations and also some are implemented for Virtex-6 FPGA ML605 Evaluation Kit to be added to a transceiver that follows closely the *Long Term Evolution* (LTE) physical layer specifications. It's used the System Generator from Xilinx to develop and test the Simulink models.

As the *Space-Frequency Block Coding* (SFBC) implementations require a high level of processing power, the use of a *Field Programmable Gate Array* (FPGA) have the potential of providing more comprehensive processing capability. Also, it is proposed a technique of a not too complex precoding scheme.

Not only increasing performance, but bumping the system's efficient in terms of power consumption is important to. Since *Orthogonal Frequency-Division multiplexing* (OFDM) modulation is known to have big *Peak-to-Average Power Ratio* (PAPR) values, leading to more power hungry devices, it is proposed a method to reduce it by dealing with the values of the pilots that are inserted into OFDM frames to the antennas in transmission.

Resuming, the principal objectives of this thesis are:

- Study of MIMO techniques such as *Space-Frequency Block Coding* (SFBC) and precoding;
- Study of the Alamouti decoder in a FPGA;
- Study of the Zero-forcing precoder for implementing in a FPGA;
- Study of PAPR reduction technique in a FPGA Xilinx pre-implemented chain.

In the following chapter, the main technologies for each generation are discussed.

Chapter 2

2. Introduction to broadband wireless

2.1. First Generation

The *first generation* (1G) systems started developing late 70's and deployed early 1980s [4]. Its design aimed to support analogue voice communication, with speeds up to 2.4kbps and provide the basic voice service to mobile users over large area. Meanwhile although the systems used were very similar, they were incompatible due to different frequencies of operation. The systems used were [5][6]:

- *Advanced Mobile Phone System* (AMPS) - USA, developed by Bell Labs (1979), it provided basic functions and structure for voice communication, such roaming and handover between cells;
- *Total Access Communications Systems* (TACS) - UK, a mostly obsolete variant of AMPS;
- *Nordic Mobile Telephone* (NMT) System - Scandinavian, it is the first fully automatic cellular phone system. It was specified by Nordic telecommunications administrations (PTTs) and started its service in 1 October 1981 in response to the increasing congestion and heavy requirements of the manual mobile phone networks *Car Radio Phone* (ARP) (operating on 150 MHz frequency) in Finland and *Mobile telephony system D* (MTD) (operating on 450 MHz frequency) in Sweden and Denmark and *Public Land Mobile Telephony* (OLT) in Norway. The NMT specifications were free and open, allowing many companies to produce NMT hardware and pushing the prices down;
- C450 - W. Germany, a first generation analogue cellular phone system deployed and operated in Germany, 1985;
- *Nippon Telephone & Telegraph* (NTT) system - Japan.

The analogue systems were based on *Frequency Division Multiple Access* (FDMA) scheme.

2.2. Second Generation

The evolution from *First Generation* (1G) (1980s) to *Second Generation* (2G) (1990s) was all about evolving from analogue to digital domain. However, the new system (although being completely different) was all about the same service: voice transmission. The data service speeds were about 9.6 kbps to 14.4 kbps [7] .

Developing mobile technologies changed from national or regional concern, and became an increasing task undertaken by global standards-developing organizations such as the *Third generation Partnership Project* (3GPP). The 3GPP is the union of telecommunications standard development organizations that specifies the *Third Generation Universal Terrestrial Radio Access* (3G UTRA) and *Global System for Mobile Communications* (GSM) systems. Its partnership project is formed by standard bodies like the *Association of Radio Industries and Businesses* (ARIB) and *Telecommunication Technology Committee* (TTC) from Japan, *Alliance for Telecommunications Industry Solutions* (ATIS) from USA, *China Communications Standards Association* (CCSA), *European Telecommunications Standards Institute* (ETSI) and *Telecommunications Technology Association* (TTA) from Korea [8] .

In Europe, the GSM system was developed in the mid 80's by telecommunication administrations in *Conference of European Post and Telecommunications* (CEPT) and later continued within the new *European Telecommunication Standards Institute* (ETSI).

Furthermore GSM technology takes advantage of *Gaussian Minimum Shift Keying* (GMSK) modulation technique which it is a special case of *Frequency Shift Keying* (FSK), providing good power and spectral efficiency.

Another 2G digital cellular systems were deployed, such as: *Digital Analogue Mobile Phone System* (D-AMPS) (IS-54) used in United States of America (USA). It was based in *Time-Division Multiple Access* (TDMA) and later development of a *Code-Division Multiple Access* (CDMA) standard called IS-95 was completed in USA in 1993.

The primary data service introduced in 2G was text *Short Message Services* (SMS), and data services enabling e-mail and other data applications, with data rates around 9.6 Kbit/s. Later, possible assigning to multiple time slots per user and modified coding schemes permitted elevate this last data rate.

In the second half of the 90's , *General Packet Radio Services* (GPRS) and *Enhanced Data Rates for Global Evolution* (EDGE) were added to GSM packet data transfer over cellular systems. GPRS systems are based in the same GMSK modulation used by GSM systems, although it has a network packet switched domain – *Packed*

Switched (PS). Its air interface allowed data and voice, through bit rate around 20 kbps (for each radio slot) . EDGE allowed peak data rate around 472 kbps using modulation *8-Phase Shift Keying* (8-PSK) with a faster coding scheme.

2.3. Third Generation

Bigger requirements for even higher rate data services, non-dropped connections, better interactivity and better spectrum use efficiency led into the appearance of the third generation mobile radio systems. The development started in *International Telecommunication Union* (ITU) in 1986. Also known as *International Mobile Telecommunications by 2000* (IMT-2000) at (ITU) or *Universal Mobile Telecommunication Systems* (UMTS) in Europe it provided full coverage and mobility for 144 kbps (preferably 384 kbps) and for limited coverage and mobility 2 Mbps. It is a much faster system than its preceding technologies and also insured a better spectrum efficiency and an higher flexibility to introduce new services [9].

With the introduction of CDMA scheme in 3GPP projects, UMTS kept the same GSM architecture, and the move to standards *Wideband Code Division Multiple Access* (W-CDMA) [10] and CDMA200 (first offered in 2002, standardized by *Third generation Partnership Project 2* (3GPP2), used especially in North America and South Korea, sharing infrastructure with the IS-95 2G standard) roaming capabilities improved. The latest release *Enhanced Voice-Data Only Revision B* (EVDO Rev B) offers peak rates of 14.7 Mbit/s downstream. Of course some obstacles emerged: to achieve more bandwidth and speed, carriers need more spectrum (the radio frequencies that carry data). For this licensing with federal governments had to be done and the costs are very high [11].

CDMA combined with *Frequency Division Duplex* (FDD), also referred to as UTRA-FDD, with UTRA standing for *Universal Mobile Telephony System terrestrial radio access*, allowed to achieve a two-way communication [12].

It was also used *Time Division Duplex* (TDD), also referred to as UTRA-TDD.

The chip rate between both was different, with TDD mode using 1.6 MHz bandwidth (low chip rate) and 5 MHz bandwidth for FDD (high chip rate)[13].

A slightly different air interface was used in China, *Time Division Synchronous Code Division Multiple Access* (TD-SCDMA) [14] radio interface was commercialized in 2009 and it also had slow chip rate and it uses *Synchronous-Code Division Multiple Access* (S-CDMA) access method across multiple time slots.

3GPP release 5 (Rel-5) deployed in March 2002 and it introduced *High Speed Downlink Packet Access* (HSDPA). Release 6 (Rel-6) deployed and introduced *High Speed Uplink Packed Access* (HSUPA). Both protocols together are known as *High Speed Packet Access* (HSPA). They afforded downlink speeds up to 14.4 Mbit/s and uplink speeds up to 5.76 Mbit/s. The modulation type introduced was *16-Quadrature Amplitude Modulation* (16-QAM), and it was good for achieving the speed rates mentioned before, and it also allowed fast adaptation to radio transmission changes.

HSPA evolution was deployed in 2007, with Rel-7, and it was known as *High Speed Packet Access Evolution* (HSPA+). It implemented the use of *Multiple Input Multiple Output* (MIMO), and use of higher modulation (64-QAM for downlink and 16-QAM for uplink) for radio transmission and reception.

A detailed illustration about 3GPP releases is shown in figure 2.

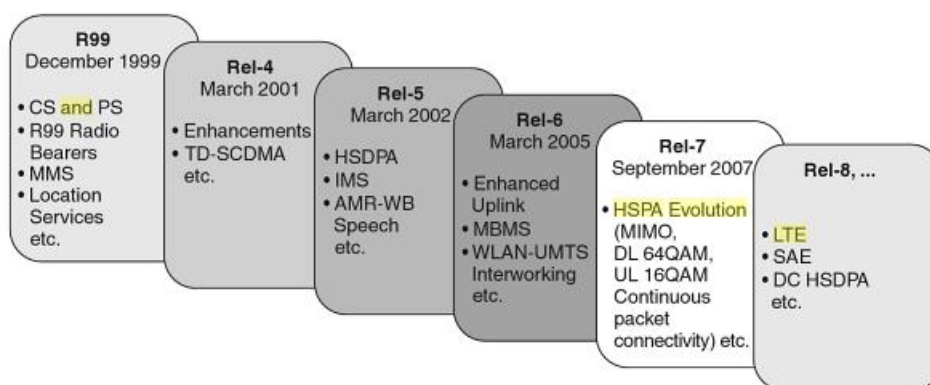


Figure 2 - Releases of 3GPP specifications for UTRA[15]

2.4. Fourth Generation

As a natural evolution of 3G, the *Long-Term Evolution* (LTE) used a completely new air interface. Its deployment was in 2010.

Better Spectrum usage and higher speeds were met without compromising one of the essentials: battery life. It was possible to have an access network with high spectral efficiency, high peak data rates and short round trip time [16].

The first release for LTE or *Evolved-Universal Terrestrial Access Network* (E-UTRAN) was released by 3GPP and it is called as Rel-8 in December 2008 and enhanced at Rel-9 in 2010. Rel-10 (march 2011) implemented the called "*LTE-Advanced*". In order for 4G to deserve that designation, to be a clear evolution from 3G, it had to bring some

clear changes. Some of them (according to performance [17]) were carrier aggregation, enhanced downlink and uplink MIMO (with simultaneous use of 64QAM), enhanced *Inter-cell Interference Coordination (ICIC)*, and *Dual Carrier-HSDPA (DC-HSDPA)* where two downlink carriers can be combined for a doubling of throughput and relays. A relay receives, demodulates and decodes the data, applies any error correction and then it re-transmits a new signal. The signal degradation from noise signals is smaller because there is a repeater [18].

An overall description about specifications are shown in table 1.

Bandwidth (MHz)	1.4, 3,5,10,15 and 20
Duplexing	FDD, TDD
Mobility	Optimized for 0-15Km/h High performance for 15-120Km/h Functional support for 120-350 Km/h
Multiple Access	DL: OFDMA UP: SC-FDMA
Channel Coding	Turbo coding
Modulation	QPSK, 16-QAM, 64-QAM
Multi-antenna support	DL: 2x2, 4x2, 4x4 UL: 1x2 1x4

Table 1 - LTE specifications [19]

Using a new air interface, it is based on *Orthogonal Frequency Division Multiple Access (OFDMA)* in the downlink and *Single Carrier-Frequency Division Multiple Access (SC-FDMA)* in the uplink allowing spectral efficiency improvement by a factor of 2-4, as compared to the *High-Speed Packet Access (HSPA)*, and it uses different transmission bandwidths from 1.4 MHz up to 20 MHz.

In order to meet even higher requirements, the LTE-Advanced was initially specified in Rel-10 of 3GPP and improved in Rel-11 and 12. It is expected to be fully implemented in 2014 [20].

It aims increased peak data rate[21], 3Gbps for downlink and 1.5 Gbps for uplink, higher spectral efficiency, increased number of simultaneously active subscribers and improved performance at cell edges[22].

In the following chapter the LTE's architecture will be detailed.

Chapter 3

3. Network architecture

3GPP cellular network has been progressively evolving (figure 3). The GSM simplified architecture is composed by *Core Network (CN)*, *Mobile Station (MS)* and *Radio Access Network (RAN)* [23].

With the 3G network and prior to the introduction of the HSPA system, some modifications were made and the CN was split in two domains: *Circuit Switched (CS)* domain and *Packet Switched (PS)* domain. GPRS standard introduced the packet switched component.

CN entities are chosen according to the service required by the end-user. The CS elements are *Mobile Service Switching Center (MSC)*, *Visitor Location Register (VLR)*, and *Gateway MSC*. The PS elements are *Serving GPRS Support Node (SGSN)* and *Gateway GPRS Support Node (GGSN)*.

Control and user plane flow between core and access networks through *Radio Network Controller (RNC)* which is connected to one or more NodeBs and in overall they form the *Radio Network Subsystem (RNS)*. One or more of this subsystems together, form the *Universal Terrestrial Radio Access Network (UTRAN)*.

The radio link is established to the *Universal User (UE)* by *Wideband-Code Division Multiple Access (W-CMDA)* and it is provided by the NodeB.

Some changes were made with the introduction of HSPA and HSPA+ to the Core and Access Network. The user data can flow between RNC and GGSN or directly to the NodeB. Also, some RNC functions have been moved to the NodeB (called evolved NodeB) making possible having faster *Radio Resource Management (RRM)* operations. Now control plane is separated with *Mobility Management Entity (MME)*.

Some non-radio aspects under the term *System Architecture Evolution (SAE)* including *Evolved Packet Core (EPC)* network evolved and together, LTE and SAE comprise the *Evolved Packet System (EPS)*. EPS provides a PDN to the user via IP for accessing to the internet or mass market *Internet Protocol (IP)* based services such *Voice over IP (VoIP)*[24] . All of this with better cost-efficiency and better network performance.

In addition, it supports interworking with circuit-switched systems [25]. EPS routes the IP packet, called EPS bearer, which uniquely identifies traffic flows that receive a common *Quality of Service (QoS)* treatment between *Packet Data Network Gateway (P-GW)* to UE [26].

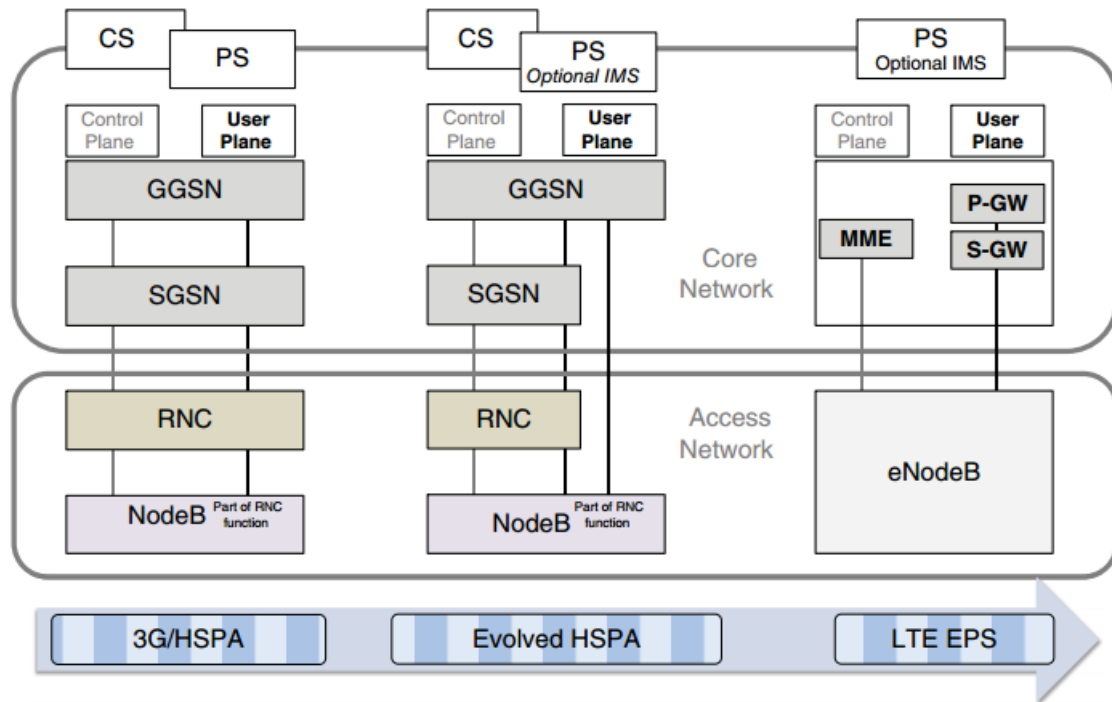


Figure 3 - 3GPP cellular networks evolution [26]

3.1. Core Network

The core network, also called EPC in SAE, includes a *Mobility Management Entity (MME)*, a *Serving-Gateway (S-GW)* and a *Packet-Gateway (P-GW)* entities. These are responsible for functionalities involving call or registration process. Figure 4 shows the simple architecture of the EPS. The connection between UE and EPC is over E-UTRAN (the LTE access network). S1 interface interconnects EPC and E-UTRAN and is responsible for relations between MMEs, S-GWs, and eNodeBs. Also, MME connects to E-UTRAN via a S1 interface (referred to as S1-C or S1-MME).

When UE connects to a LTE network, an UE-specific logical S1-MME connections are established. Also known as EPS bearer, it is used for signalling messages between UE and EPC.

MME is responsible for signalling and security control between the UE and the CN in the *Non-Access Stratum* (NAS) protocol layer. It deals with the EPS bearer management, roaming and authentication and inter core network signalling for mobility between 3GPP access networks [27].

S-GW is connected to P-GW and deals with packet routing and forwarding. According to 23.401 3GPP [28] is responsible for handovers with neighbouring eNodeBs and also for data transfer in terms of all packets across user plane. It also retains information about the bearers when the UE is in idle state because it routes the incoming and upcoming IP packets and temporarily buffers downlink data while the MME initiates paging of the UE to re-establish the bearers.

Like the S-GW, the *Packet Data Network Gateway* (PDN GW) is the termination point of the packet data interface towards the Packet Data Network(s). As an anchor point for sessions towards the external Packet Data Networks, the PDN GW supports:

- Policy enforcement features (applies operator-defined rules for resource allocation and usage);
- Packet filtering (for example, deep packet inspection for application type detection) to meet some QoS requirements;
- Charging support (for example, per-URL charging).

It is the point of connection between the EPC and the external IP networks. It is also responsible to act as an "anchor" of mobility between 3GPP and non-3GPP technologies (such as *Worldwide Interoperability for Microwave Access* (WiMAX) and 3GPP2 (CDMA 1X and EvDO).

HSS

Home Subscriber Server (HSS) provides storage of subscriber data such as users SAE subscription data such as QoS profile and any access restrictions for roaming. It contains the authentication vectors and security keys per UE.

PCRF

With the Release 7 of 3GPP implemented a new converged architecture that optimizes the interactions between the policy and rules functions. This evolution added a new network node, *Policy and Charging Rules Function* (PCRF), which is the junction of *Policy Decision Function* (PDF) and *Charging Rules Function* (CRF).

It provides functions to determine the QoS and charging policy to be applied to data packets sent and received by the user.

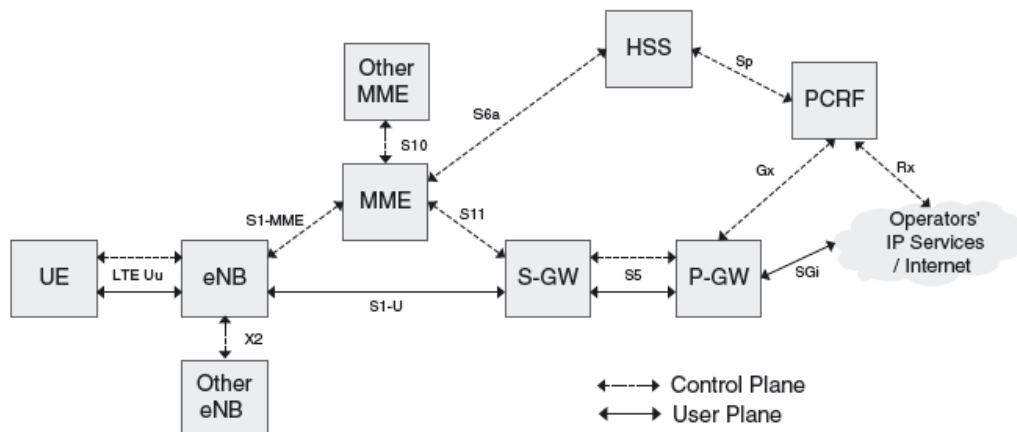


Figure 4 - Evolved Packet System architecture[26]

3.2. Access Network

The architecture of *Evolved-UMTS Terrestrial Radio Access Network* (E-UTRAN) is illustrated in figure 5 (Architecture Description. TS 36.401 V8.8.0).

The E-UTRAN handles the radio communications between the mobile and the EPC [29]. It is constituted of eNodeBs whose interface with the UE. This more simple implementation (there is no need of a centralized controller like older technologies) reduces the latency of all radio interface operations.

The eNodeBs are connected to each other via the X2 interface, which supports active mode mobility. This interface also is used for multi-cell *Radio Resource Management* (RRM) functions such as *Inter-Cell Interference Coordination* (ICIC) [30]. RRM deals with the efficient use of radio resources in order to fulfil users QoS attributes.

The eNodeBs are also connected to the core network via the S1 interface (S1-U for S-GW and S1-MME for MME).

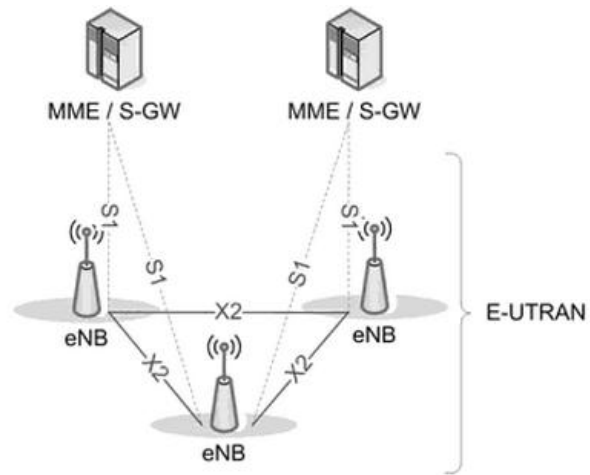


Figure 5 - Evolved UMTS Terrestrial Radio Access Network architecture [29]

In the next chapter, the main technologies referent to LTE's downlink and uplink will be detailed.

Chapter 4

4. OFDM

4.1.1 Basic principles of OFDM

Orthogonal Frequency Division Multiplexing (OFDM) is a technology similar to the conventional FDM which the main difference relies how the signals are modulated and demodulated. Priority is given to minimizing the interference, or crosstalk, among the channels and symbols comprising the data stream. Less importance is given on perfecting individual channels [15].

OFDM originally was used in European digital audio broadcast services but with the evolution of the technology it led itself to digital television and also is considered as the method of obtaining high-speed digital data transmission over conventional telephone lines. It is also used in *Wireless Local Area Networks* (WLAN), *Worldwide Interoperability for Microwave Access* (WIMAX) and *Digital Video Broadcasting* (DVB) broadcast technologies.

Its features worth mentioning are the possible use of several parallel subcarriers that provide longer symbol duration, making the signal inherently robust to time dispersion. *Intersymbol interference* (ISI) can be avoided adding a guard time.

It is possible to have a tight frequency separation and high spectral efficiency because OFDM is constructed with fully orthogonal carriers.

The basic idea of multicarrier modulation is to divide the transmitted bit stream into many different sub-streams over many different sub-channels (figure 6).

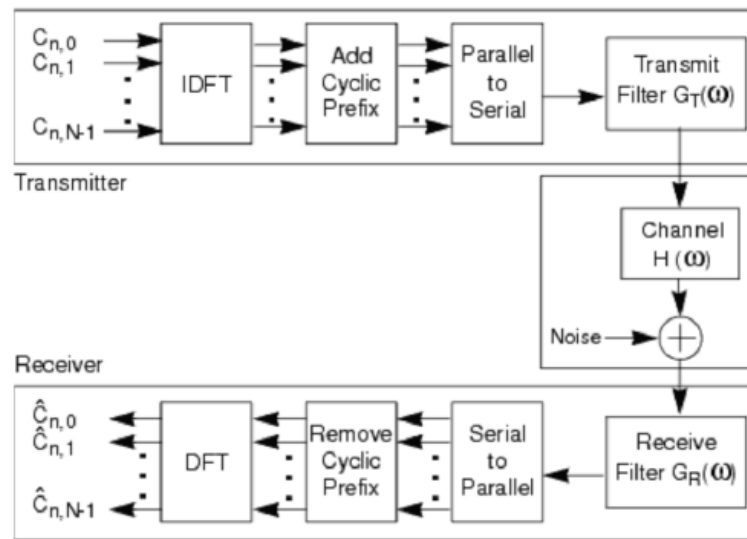


Figure 6 - OFDM system in blocks [31]

The number of sub-streams is chosen to ensure that each sub-channel has lesser bandwidth than the coherence bandwidth of the channel, so the sub-channels experience relatively flat fading. Thus, the inter-symbol interference on each sub-channel is small. The sub-channels in multicarrier modulation don't need to be contiguous which is good for applying in Cognitive Radio Systems [32], and a large continuous quantity of spectrum available is not needed for high rate multicarrier communications (figure 8). Moreover, multicarrier modulation is efficiently implemented digitally. In this discrete implementation, the ISI can be completely eliminated through the use of a cyclic prefix making OFDM relatively insensitive to timing acquisition errors (although there is a need of frequency offset correction). A cyclic prefix is a repetition of the first section of a symbol that is appended to the end of the symbol (explained at Chapter 4.1.3).

The signal can be seen as a simple rectangular pulse shaping (figure 7 a)) corresponding to a sinc-square-shaper per-subcarrier spectrum (figure 7 b)).

At reception OFDM only requires an *Fast Fourier Transform* (FFT) or *Discrete Fourier Transform* (DFT) implementation according to if there is in the transmitted side and *Inverse Fast Fourier Transform* (IFFT) or *Inverse Discrete Fourier Transform* (IDFT) respectively.

In complex baseband notation, during a time interval $mT_a \leq t < (m+1)T_a$, a simple OFDM signal can be denoted as:

$$x(t) = \sum_{n=0}^{N_c-1} x_n(t) = \sum_{n=0}^{N_c-1} a_n^m(t) e^{j2\pi n \Delta f t} \quad (1)$$

$x_n(t)$ represents the n th modulated subcarrier with the frequency $f_n = n \Delta f$ and $a_n^m(t)$ is the given complex that during the m th OFDM symbol interval $mT_a \leq t < (m+1)T_a$, is applied to the n th subcarrier and N_c the number of subcarriers .

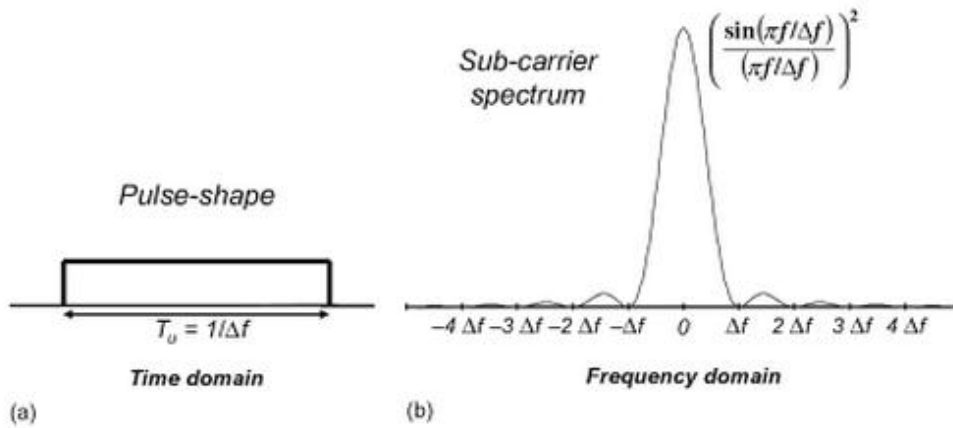


Figure 7 - OFDM symbol in time and frequency domain [15]

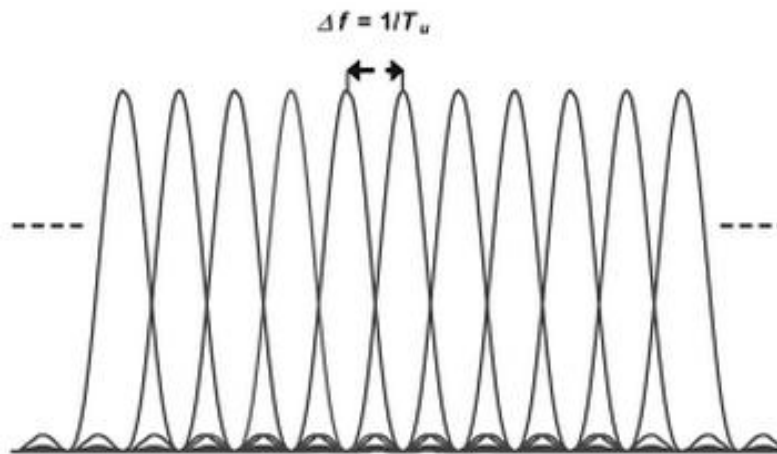


Figure 8 - Bandwidth allocation [15]

During the interval, N_c modulation symbols are transmitted in parallel with the desired modulation (QPSK, 16 QAM, or 64QAM).

The frequency is in order of kHz and the number of subcarrier goes from less than hundreds to thousands. This depends in the conditions we want to operate on, such as radio-channel frequency and channel variations (maximum expected Doppler Spread).

4.1.2 OFDM applied on LTE

For downlink LTE uses *Orthogonal Frequency Division Multiple Access* (OFDMA). For direct link transmission conventional OFDM system is used to divide the spectrum used into multiple orthogonal carriers to each other. Modulation of these subcarriers is done independently using a low rate data stream [33].

This high-rate transmission technique avoids *Inter-Symbol Interference* (ISI) by including a *Cyclic Prefix* (CP) at transmitter side and its removal at receiver side. If the channel delay spread is lesser than the CP's one, ISI will be completely removed. Also, OFDM renders a convolution channel into parallel flat channels, enabling simple one-tap frequency-domain equalization, if the channel remains constant within one OFDM symbol duration.

By the technical recommendation of 3GPP [28], OFDM concept is shown in figure 9.

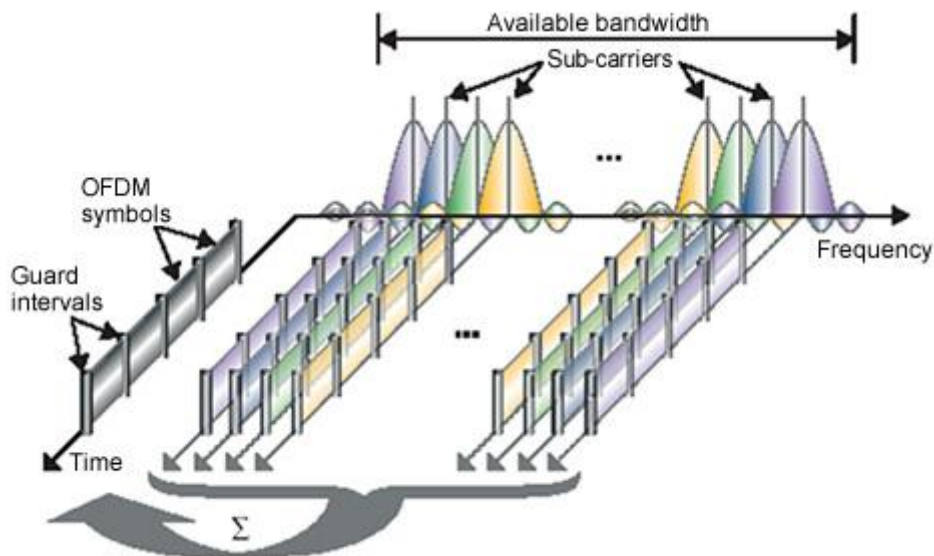


Figure 9 - OFDM concept[35]

There are two different types of frame structures for LTE: LTE *Frequency Division Duplex* (LTE FDD) also known as type 1 and LTE *Time Division Duplex* (LTE TDD) also known as type 2.

Time domain fields are typically defined in terms of T_s which is defined as $T_s = \frac{1}{1500 \times 2048}$ seconds or about 32.6 nanoseconds [36].

Each LTE FDD basic frame has an overall length of 10 ms. It is divided in 20 individual slots (with $T_{slot} = 15360 \times T_s = 0.5$ ms each), numbered from 0 to 19, as shown in figure 10.

Downlink and uplink transmissions are organized into frames with duration of $T_f = 307200 T_s$.

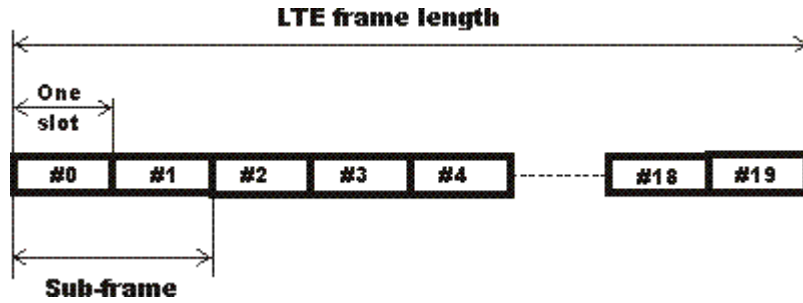


Figure 10- LTE frame [37]

The structure of downlink resource grid is shown in figure 11. Each sub frame divides into two slots. The smallest modulation structure in LTE is the Resource Element which is one 15 kHz subcarrier by one symbol. The resource elements aggregate into *Resource Blocks* (RBs) (figure 11) which each one consists of 12 consecutive sub-carriers in frequency domain.

The transmitted signal in each slot is described by a resource block of $N_{RB}^{DL} N_{SC}^{RB}$ subcarriers with spacing of $\Delta f = 15$ kHz and N_{Symb}^{DL} OFDM symbols. N_{RB}^{DL} is the symbol used to indicate the maximum number of downlink Resource Blocks for a given bandwidth. (N_{RB}^{DL} quantity depends on the downlink transmission bandwidth configured in the cell and shall fulfil the following condition : $6 \leq N_{RB}^{DL} \leq 110$). This consists into a cyclic prefix of 5.2 μs for the first symbol and 4.7 μs for the remaining ones. In time domain, a physical resource block consists of 7 or 6 consecutive OFDM symbols according to cyclic prefix length.

Each UT can assign one or more RBs in each transmission interval of 1 ms depending on the required data rate. The base station makes the scheduling decision and user data or payload is transported on the *Physical Downlink Shared Channel (PDSCH)*. This channel is designed for high data rates and modulation options include QPSK, 16-QAM, and 64-QAM. There are other channel types such as *Physical Control Format Indicator Channel (PCFICH)*, *Physical Broadcast Channel (PBCH)*, *Physical Downlink Control Channel (PDCCH)*, *Physical Multicast Channel (PMCH)* and *Physical Hybrid ARQ Indicator Channel (PHICH)* but less used [38].

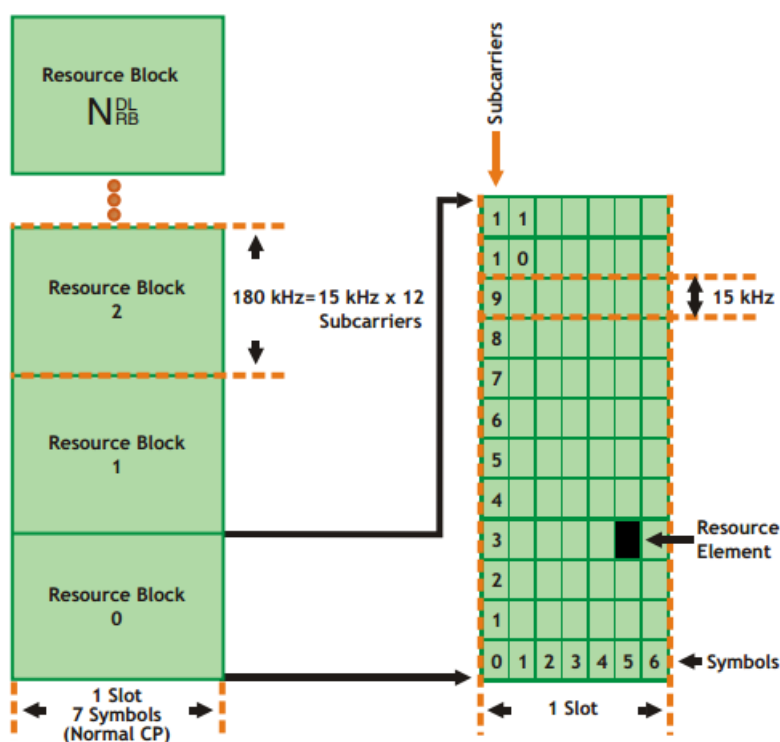


Figure 11 - Relationship between a LTE slot, symbols and Resource Blocks [39]

In order to obtain *Channel State Information (CSI)* [40], OFDM preambles are transmitted at the beginning of the transmission record, or pilot symbols can be integrated in each OFDM slot along symbols. Pilots (complex exponentials in time) are separated from information symbols in the frequency domain [41].

They are used specially to track fast varying channel to make easier channel estimation. Its disadvantage is that it slows the transmission rate, so it is desirable to minimize the number of embedded pilot symbols.

The OFDM frame is divided into a set of orthogonal *Probing Resource Blocks* (PRBs)[42]. The pilot symbols are inserted there [43] and a single antenna transmitter pilot allocation is shown in figure 12.

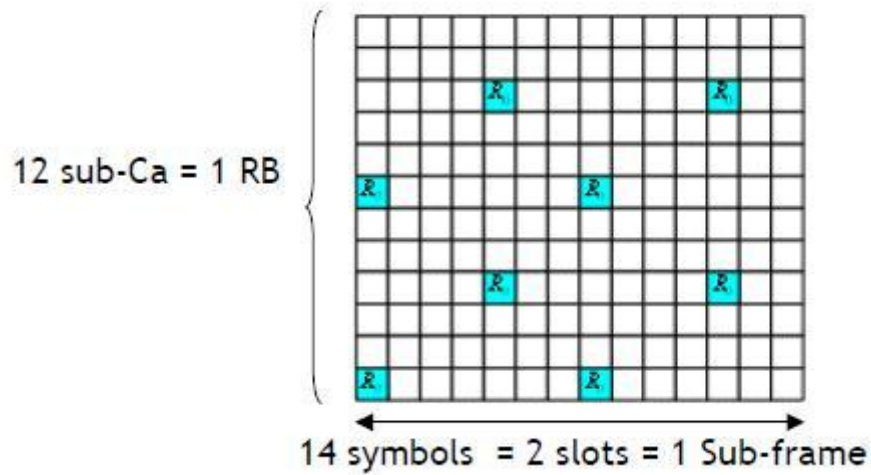


Figure 12- Antenna pilots allocation[44]

In a multiple antenna transmission the pilots of each antenna are transmitted on different sub-carriers to avoid interference between each other.

4.1.2.1 Orthogonality

OFDM is known for its orthogonality between sub-carriers. In opposite to FDM, whose sub-carriers are separated in the frequency domain to avoid interference between the sub channels, OFDM doesn't need the frequency guard band and there is no interference between them. In benefit, more sub-carriers can be sent, allowing to have more symbols. It also brings better spectrum efficiency.

The concept is to modulate N_c data symbols in N_c subcarriers with a spacing Δf given by:

$$\Delta f = \frac{1}{T_u} \quad (2)$$

Where T_u is the time duration of an OFDM symbol.

In figure 8, we can see the frequency spectrum of an OFDM transmission. The symbols overlap. By correlation techniques, the orthogonal signals can be separated at the receiver.

4.1.3. Cyclic prefix

In the case of time-dispersive channels, the subcarrier orthogonality can be lost. The reason for is that the demodulator correlation interval for one path will overlap with the symbol boundary of a different path.

After the insertion of the guard interval T_{CP} [38], the OFDM symbol duration becomes:

$$T_{u'} = T_u + T_{CP} \quad (3)$$

The OFDM sampling frequency is reduced in function of the cyclic prefix duration and it can be expressed as:

$$\beta_{overhead} = \frac{T_{CP}}{T_u + T_{CP}} \quad (4)$$

Cyclic prefix insertion is beneficial because it makes an OFDM signal insensitive to time dispersion as long as the extension of time doesn't exceed the length of the cyclic prefix.

The disadvantages are that only the fraction $\frac{T_{CP}}{T_u + T_{CP}}$ of the received signal power is used by the OFDM demodulator, resulting in some power loss. One solution is to reduce subcarrier spacing Δf , by increasing the OFDM symbol duration T_u . Although this solution, the OFDM transmission will have more sensitivity to fast channel variations (high Doppler spread), as well some frequency errors.

The signal energy dispersed by the multi-path channel should be absorbed by the cyclic prefix, and its length is greater than the channel total delay spread:

$$T_{CP} > \tau \quad (5)$$

where τ is the channel total delay spread and T_{CP} the duration of the cyclic prefix.

4.2.OFDMA and SC-FDMA

4.2.1. OFDMA

In opposite to OFDM whereas only one block is assigned in time per user, *Orthogonal Frequency-Division Multiple Access* (OFDMA) is able to assign different groups of subcarriers in frequency to different users like shown in figure 13.

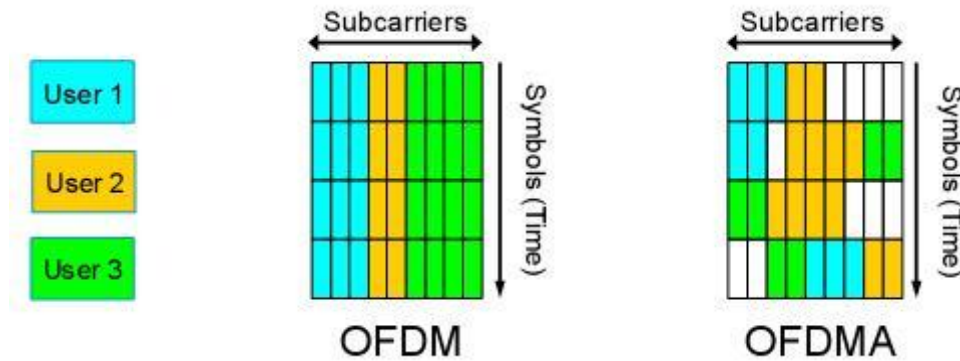


Figure 13 - Difference between OFDM and OFDMA[45]

With the better use of radio resources, the efficiency and robustness of the system is increased. It provides frequency diversity in cases where the data rate is low having narrow frequency allocation (narrow-band fading).

It is effective at combating ISI and multipath fading and requires low-complexity at modulation since it can be implemented using IDFT/DFT (or IFFT/FFT). It also can take advantage of frequency and multiuser diversity through contiguous subcarriers.

OFDMA is used for LTE downlink because it can accommodate many users with widely varying applications, data rates and QoS requirements. The multiple access is done in digital domain (before the IFFT operation), so it allows a flexible, dynamic and efficient use of bandwidth allocation [46].

4.2.2. SC-FDMA

LTE uplink differs from downlink requirements in several ways. Considered as less power hungry due to its low *Peak-to-Average Power Ratio* (PAPR), *Single Carrier-Frequency Domain Multiple Access* (SC-FDMA) is suited for LTE uplink requirements [47].

Although battery performance in mobile devices is improving all over the time, it is still necessary to ensure that the mobile device uses as less battery power as possible. One of the consuming parts from a mobile device to take in consideration is the RF power amplifier that transmits the *Radio Frequency* (RF) signal via the antenna to the base station. This can be much more power hungry depending in the form of radio frequency modulation and signal format. Signals that have a high peak to average ratio and require linear amplification tend to the not efficient use of RF power amplifiers. This is why SC-FDMA is used because it is a system with a constant power level of operating for transmission.

Although SC-FDMA is a MIMO system. LTE uses a SC-FDMA 1x2 configuration, meaning that for one antenna transmitting there are two antennas in the base station receiving.

Its architecture and characteristics are identical to OFDMA differing essentially because its waveform is single carrier where the subcarriers are not independently modulated.

In figure 14 we can see the main differences between the two technologies.

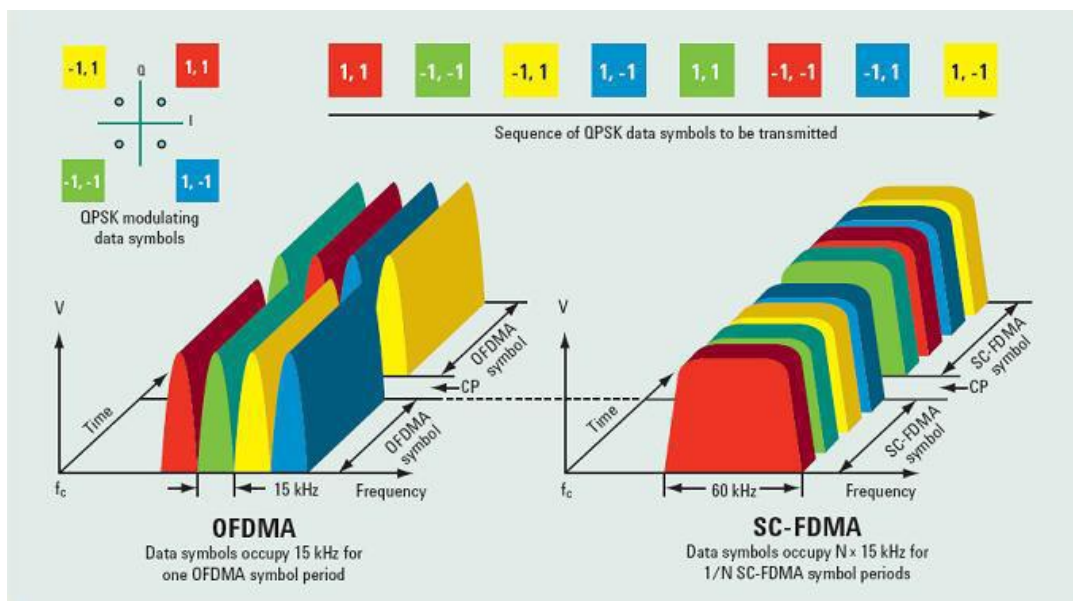
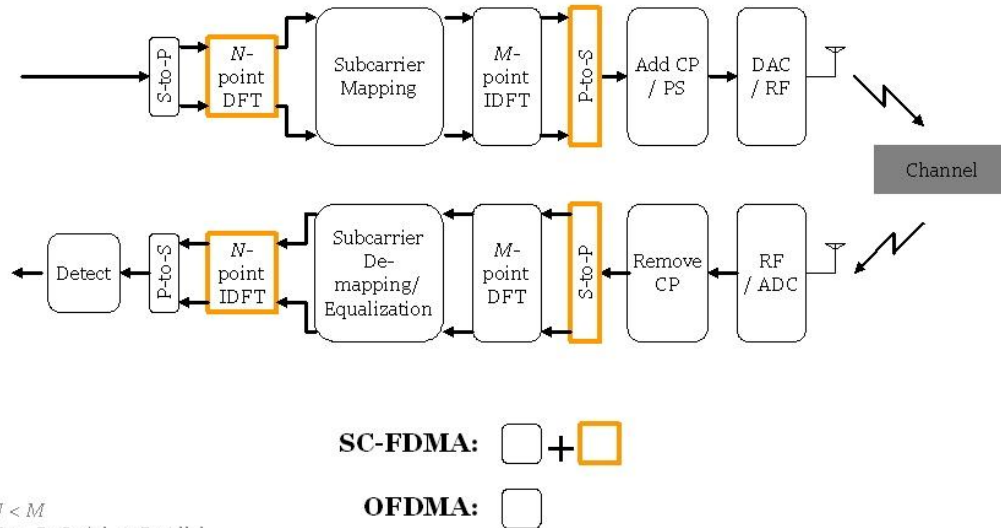


Figure 14- Differences between OFDM and SC-FDMA in terms of frequency/amplitude/time [48]

The main different blocks are according to figure 15:



* $N < M$
 * S-to-P: Serial-to-Parallel
 * P-to-S: Parallel-to-Serial

Figure 15-- Differences between OFDM and SC-FDMA in terms of overall system blocks [49]

The additional different blocks are:

- M-point DFT: Converts in the time domain the Single-Carrier symbol block into M discrete tones mapping the data symbols in the required band;
- Subcarrier mapping: Maps the M-point DFT output tones to specified subcarriers for transmission. SC-FDMA systems either use contiguous tones (localized) or uniformly spaced tones;
- N-point IDFT: Converts mapped subcarriers into time domain for detection.

4.3.MIMO systems

Multiple Input Multiple Output (MIMO) systems with a large number of receive antennas at the *Base Station (BS)* have attracted much attention due to the fact that the spectral efficiency of cellular systems increases only by installing additional antennas at the BS .

With the evolution of wireless communication into broadband systems to support high data rate applications, dealing with frequency-selective fading requires an efficient system leading to the adoption of OFDM systems.

Since the OFDM sub-carriers are constructed as parallel narrow band channels, the fading process experienced by each sub-carrier is close to frequency flat, and therefore, can be modelled as a constant complex gain. This may simplify the implementation of a MIMO scheme if this is applied on a sub-carrier or subset of carrier basis [50].

Diversity[51]:

4.3.1. Multipath diversity

When a *Radio Frequency (RF)* signal is transmitted to a receiver, its behaviour is to grow wider as it is transmitted further. During the transmission the signal can encounter obstacles that can refract, diffract, reflect or interfere with it. When this happens, multiple waves fronts can be created to reach the receiver. This is called multipath distortion.

Some parts go directly to destination while another ones have different paths to get there. This results in a delay in some parts of the signal according to the different paths that some parts of the signal take. Figure 16 shows an example of multipath distortion and the consequences in the received signal.

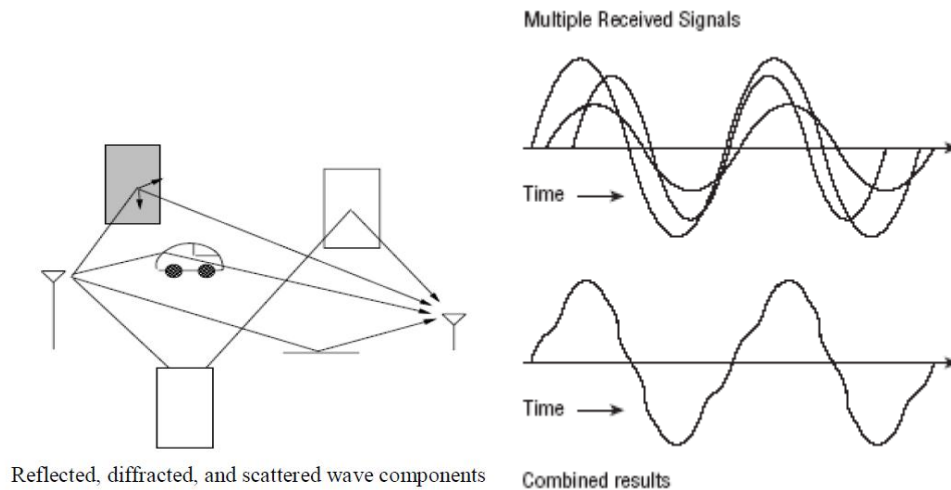


Figure 16- Multipath diversity[52]

4.3.2. Macro diversity

Macro diversity utilizes the network efficiently in order to create antenna diversity. When a signal is uploaded from a mobile station to multiple base stations, it has diversity, since the channel coefficients to each base station are independent. In order to avoid the problem of having a limited bandwidth, it is necessary to have a selection method in order to receive the signal correctly at least at one base station [15].

For downlink the same concept happens but in a different way: various base stations send data to the mobile station, resulting again, in independent fading. This also includes a method used in soft handover mode: *Site Selection Diversity Transmission* (SSDT) [53]. It transmits on the downlink from the best cell, by reducing the interference caused by multiple transmissions in a soft handover mode. Soft handover means that the radio links are added and removed in a way that the UE always keeps at least one radio link to the UTRAN. It also achieves fast site selection without network intervention, thus maintaining the advantage of the soft handover.

4.3.3. Time diversity

Time diversity can be achieved when 2 symbols are transmitted with a separation in time longer than the coherence time of the channel, experiencing uncorrelated channel conditions.

This can be achieved for example by using a repetition coding scheme that would guarantee that symbols will be transmitted over uncorrelated channels. In reception the copies of the symbol will be combined together.

4.3.4. Frequency Diversity

Similar to time diversity, this occurs when the channel coherence bandwidth is smaller than the available bandwidth. The idea is to divide into channels with smaller bandwidth and independent frequency response. This is also used in multicarrier systems, (OFDM), where the wideband channel is divided into non-overlapping narrowband sub-channels. The symbol is transmitted in each sub-channel and has a transmission period long enough for the sub-channel to appear as flat fading channel. This as a small cross-correlation.

4.3.5. Receive Antenna Diversity

Multiple antennas at the receiver are used at base stations to improve uplink capabilities. It gives coverage and performance improvements. On the other hand, it has higher costs and still there are not to many devices with MIMO capabilities. One example of that is the use (only now) in high end smartphones, where Samsung Galaxy S5 and some newer high end devices have that capability giving a streaming experience up to 30% faster (Wi-Fi 802.11ac protocol) [54].

4.3.6. Transmit Diversity

Transmit diversity solutions are used to improve downlink capacity. Typically transmitter antennas are relatively close to each other. The delay parameters are the same for each transmit element. Open loop and close loop concepts transmit diversity solutions are implemented for UTRAs FDD and TDD modes. Some open-loop techniques are *Time Switched Transmit Diversity* (TSTD) which is applied to W-CDMA standard for some common channels. The transmission is switched among various antennas with a periodicity. The same symbol is transmitted among all antennas at low power.

Another solution is *Space Time Transmit Diversity* (STTD) [55], based on a variant of the space–time block code developed by Alamouti, where column 1 is transmitted from antenna 1 and column 2 from antenna 2.

Close loop techniques include such details like co-phasing information, weighting the transmitted signals by evaluating channel conditions experienced or selection of transmit antennas via feedback. WCDMA Release'99 and Release 4 already have close-loop concepts like co-phasing information. They use a fast feedback channel, and it is applied in selecting one of 4 or 16 possible beam weights, respectively.

4.4. Benefits of MIMO technology

Performance gains can be achieved with MIMO technology. These gains are described below[15]:

Array Gain:

It increases the receive *Signal-to-Noise Ratio* (SNR) resulting from a coherent combining effect of the wireless signals at a receiver. This is realized through spatial processing at the receiver array and/or spatial pre-processing at the transmitter array. It improves resistance to noise (improving SNR), improving the coverage and range of the wireless network.

Spatial diversity gain:

Spatial diversity reduces/mitigates fading and is realized by providing the receiver multiple copies of the transmitted signal in space, frequency or time. This increased number of independent copies, increases the probability that at least one of the copies is not experiencing a deep fade, improving the quality and reliability of the reception.

Spatial multiplexing gain:

Transmitting independent, multiple data streams in the bandwidth of operation, MIMO systems offer a linear increase in data rate via spatial multiplexing. Under good channel conditions, the receiver separates the data streams, with the same channel quality as it would be in a *Single Input Single Output* (SISO) system. This Spatial multiplexing gain enhances the capacity of a wireless network.

Interference reduction and avoidance:

Interference in wireless networks appears because multiple users share time and frequency resources. With MIMO systems the spatial dimension can be managed in order to increase the separation between users. Also, the spatial dimension can be managed in order of interference avoidance improving the coverage and range of a wireless network.

4.5. Multiple antenna configurations[56]

The most basic wireless transmission scheme is known as *Single Input Single Output* (SISO).

The received signal can be defined as $r = hs + n$, where h is a deterministic channel, s is the transmitted symbol with symbol energy E_s and n is the zero mean AWGN (Additive Gaussian Noise) noise with power spectrum density N_o . In an wireless system, transmission failures appear mostly when the channel is deep fade. Exploiting different kinds of diversity techniques in space, this failure can be avoided. This scenarios, namely *Single Input Single Output* (SISO), *Multiple Input Single Output* (MISO) and *Multiple Input Multiple Output* (MIMO), are going to be explained above (figure 17).

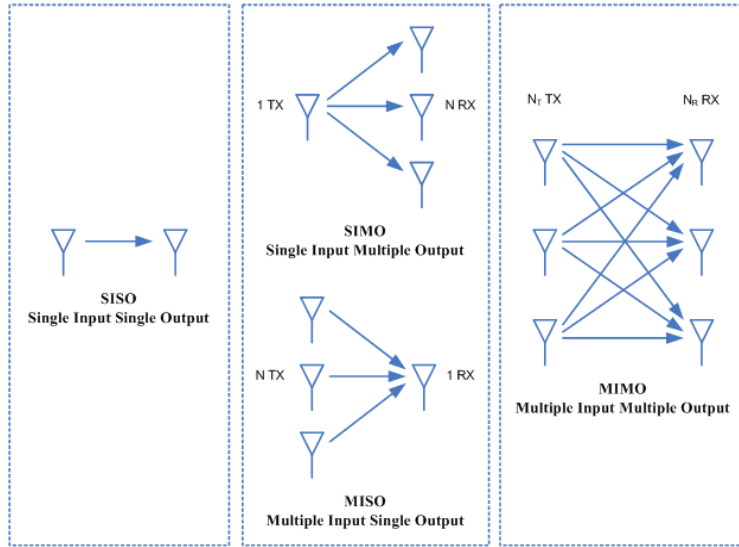


Figure 17- SISO, SIMO, MISO and MIMO[57]

The capacity (C) of the system can be given in order to number of transmit and receive antennas is given by the Shannon Formula :

$$C = B \log_2 \left(1 + nT nR \frac{S}{N} \right) \text{ bits/s} \quad (6)$$

Where nT is the number of transmit antennas, nR the number of receiver antennas and B the bandwidth, S is the average received signal power over the bandwidth (in case of a modulated signal, often denoted C , i.e. modulated carrier), measured in watts (or volts squared), N is the average noise or interference power over the bandwidth, measured in watts (or volts squared) ,and it is called Shannon formula. $\frac{S}{N}$ is also called *Signal-to-Noise Ratio* (SNR).

In a flat-fading scenario, where the coherence bandwidth of the channel is larger than the bandwidth of the signal, and no inter-symbol interference occurs over time , it is assumed that the antennas are located sufficiently away from each other so that channel coefficients between different transmitter and receiver antennas are statistically independent. Combining the signal at the destination or precoding at the transmitter give Spatial diversity gains. With multiple antennas in the receiver it is possible to take advantage of spatial diversity in order to enhance systems performance. Considering the case of a single-antenna transmitting to a receiver with Nr antennas (SIMO) where $x[n]$ is the symbol transmitted in the n -th symbol period and assuming that $E[|x[n]|^2] = 1$. The

received signal at the k -th receiver antenna in the n -th symbol period is expressed as:

$$y_k[n] = \sqrt{P}h_kx[n] + w_k[n] \quad (7)$$

Where P is the transmit power, h_k the channel coefficient seen by the k -th receiver antenna and $w_k[n]$ the AWGN at the k -th receiver antenna. h_k can be expressed as:

$$h_k = |h_k|e^{j\theta_k} \quad (8)$$

Where $|h_k|$ is its amplitude and θ_k its phase for $k = 1, 2, \dots, N_r$.

When we have *Channel State Information* (CSI), the channel coefficients ($h_{1,1}, h_{1,2}, \dots, h_{n,r}$) are known at the receiver. Now the receiver will combine the received symbols $y_1[n], y_2[n], \dots, y_{N_t}[n]$ before reception, with the respective weighting factors $\alpha_1, \alpha_2, \dots, \alpha_{N_t}$ in order to obtain the signal:

$$C[n] = \sum_{k=1}^{N_t} \alpha_k y_k[n] \quad (9)$$

Spatial diversity can also be exploited when there are N_t transmit antennas. The data symbols can be distributed among the multiple transmit antennas. Considering a system with N_t antennas and a single antenna at reception (MISO), transmitting the sequence of data symbols $x[n]$ which are independent and identically distributed over time with zero mean and unit variance. Firstly the data is pre-processed in order the form the sequence of transmit vectors $s[n] = (s_1[n], s_2[n], \dots, s_{N_t}[n])'$ that are going to be transmitted over the N_t antennas in the n th symbol period. The transmitted symbols satisfy the sum power constraint:

$$E[|x[n]|^2] = \sum_{k=1}^{N_t} E[|s_k[n]|^2] \leq 1 \quad (10)$$

And the signal obtained in the receiver during the n-th symbol period is:

$$y(n) = \sum_{k=1}^{N_t} \sqrt{P} h_k s_k[n] + w[n] \quad (11)$$

Where P is the transmit power, h_k the channel coefficient seen by the k-th transmit antenna and the receiver, and $w_k[n]$ the AWGN with zero mean and variance σ_w^2 .

Equipping with multiple antenna elements both in transmitter and receiver leads to multiple-input multiple-output (MIMO) scheme. The signal sent by N_t antennas and received at N_r antennas, is dealt in such a way it will improve the quality (*Bit-Error Rate* (BER)) or the data rate (bits/sec).

4.5.1. Practical implementation

Matlab simulations were made, proving that systems with more antennas lead to a smaller BER (number of bit errors divided by the total number of bits transferred (Figure 18) (Annex A).

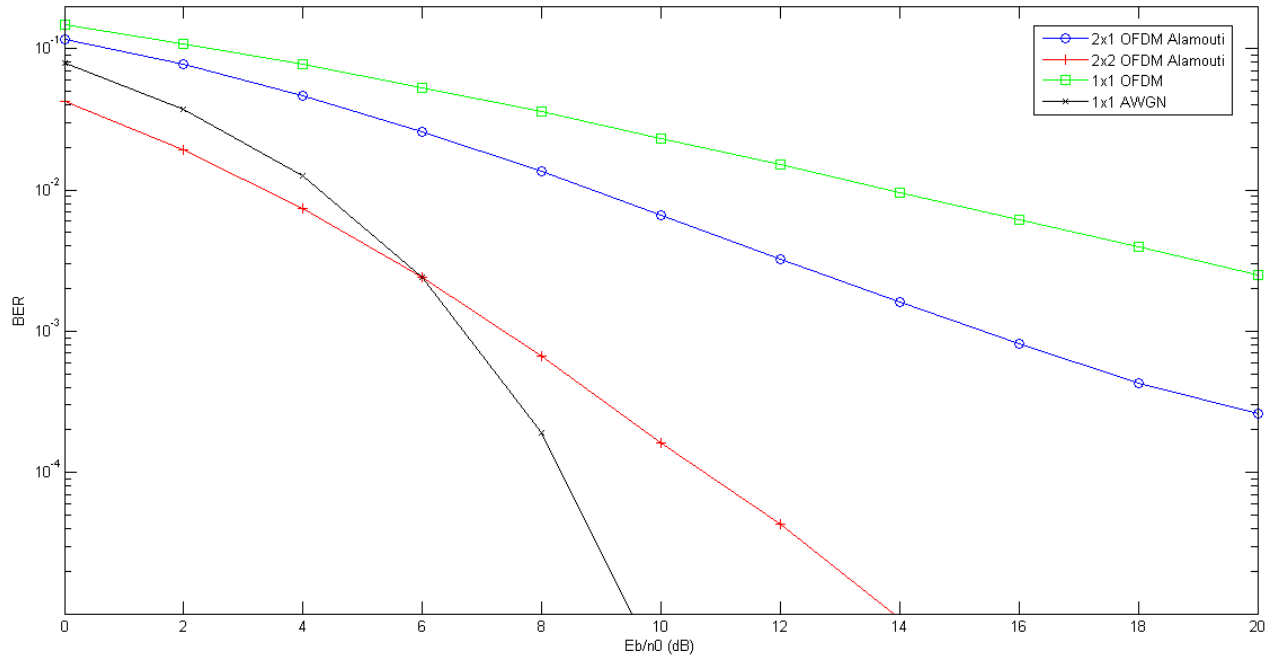


Figure 18- BER for 2x1, 2x2 and 1x1 systems

In the previous figure it is modified the number of antennas in reception and transmission of OFDM modulation and *Space-Frequency Block Coding* (SFBC) Alamouti scheme (table 3). 1x1 AWGN (*Additive White Gaussian Noise*) channel is chosen just in terms of comparison. A AWGN channel is known for its characteristics as noise added to the signal (addictive) that has a "flat" power spectral density (white) independent of frequency as it only varies randomly in time (Gaussian).

There is a big jump in performance of Alamouti scheme when the number of antennas is increased to 2 in transmission and reception (BER is much smaller). MIMO takes advantage of random fading and multipath delay spread (when available) increasing transfer rate[58]. Improving magnitude without spectrum cost led into progress in areas as channel modelling, antenna design, or signal processing.

In the next chapter, Alamouti's encoding and decoding is described with a practical system implemented in Xilinx System Generator.

Chapter 5

5 Alamouti's encoding and decoding

5.1.Space-Time Block Coding Alamouti

One of the ways to exploit the capacity of a MIMO system is to had additional diversity [59], in order to combat channel fading. It can be achieved by transmitting several replicas of the same information through each antenna.

Alamouti published its first technique *Space Time Block Coding* (STBC) into W-CDMA and CDMA-2000 schemes [60].

The first release was for 2 transmit antennas and 1 receive antenna. It has full rate since it transmits 2 symbols every 2 time intervals. The Alamouti scheme encoding operation is given by equation 12:

$$G = \begin{bmatrix} s_1 & s_2 \\ -s_2^* & s_1^* \end{bmatrix} \quad (12)$$

Where s_1, s_2 represent transmitted symbols, and s_1^*, s_2^* their complex conjugates respectively. At a given time t , symbol s_1 and s_2 are transmitted through antenna 1 and antenna 2 respectively. Assuming the duration time of a symbol is T , then at time $t + T$, the symbols $-s_2^*$ and s_1^* are transmitted through antenna 1 and antenna 2 respectively.

The received signals at the antenna, at time t and $t + T$ are given by :

$$r_1(t) = h_{1,1}s_1 + h_{1,2}s_2 + n(t) \quad (13.1)$$

$$r_1(t + T) = -h_{1,1}s_2^* + h_{1,2}s_1^* + n(t + T) \quad (13.2)$$

Where, r_1 represents the received signal at antenna 1 , $h_{i,j}$ the channel transfer function from the j^{th} transmit antenna and the i^{th} receive antenna and n is the complex random variable that represents noise.

Before being sent to the decoder the signals are combined and it is given by:

$$\tilde{s}_1 = h_{1,1}^* r_1(t) + h_{1,2} r_1^*(t + T) \quad (14.1)$$

$$\tilde{s}_2 = h_{1,2}^* r_1(t) + h_{1,1} r_1^*(t + T) \quad (14.2)$$

In the case of 2 receive antennas the received symbols are given by:

$$r_1(t) = h_{1,1} s_1 + h_{1,2} s_2 + n_1(t) \quad (15.1)$$

$$r_1(t + T) = -h_{1,1} s_2^* + h_{1,2} s_1^* + n_1(t + T) \quad (15.2)$$

$$r_2(t) = h_{2,1} s_1 + h_{2,2} s_2 + n_2(t) \quad (15.3)$$

$$r_2(t + T) = -h_{2,1} s_2^* + h_{2,2} s_1^* + n_2(t + T) \quad (15.4)$$

Where r_2 represents the received signal at antenna 2, r_2^* its complex conjugate and n_2 a complex random variable that represents noise in antenna 2.

And the combined signals are given by:

$$\tilde{s}_1 = h_{1,1}^* r_1(t) + h_{1,2} r_1^*(t + T) + h_{2,1}^* r_2(t) + h_{2,2} r_2^*(t + T) \quad (16.1)$$

$$\tilde{s}_2 = h_{1,2}^* r_1(t) + h_{1,1} r_1^*(t + T) + h_{2,2}^* r_2(t) + h_{2,1} r_2^*(t + T) \quad (16.2)$$

5.2.Space-Frequency Block Coding Alamouti [61]

Alamouti *Space-Frequency Block Coding* (SFBC) is similar to STBC with the exception of symbols being encoded across space and frequency rather than space and time. At the transmitter side, a block of N modulation symbols, s_1, \dots, s_n goes to the encoder which generates 2 or more output sequences according to a SFBC algorithm[62] (table 2).

Frequency	Antenna 1	Antenna 2
n	s_n	$-s_{n+1}^*$
$n + 1$	s_{n+1}	s_n^*

Table 2 - Alamouti code 1

Each sequence is converted from serial to parallel and then each one go through *Inverse Fast Fourier Transform* (IFFT) blocks. All subcarriers in different frequencies that come from SFBC block are converted into time domain by the IFFT block. Cyclic Prefix can be inserted in this stage. Before going to each transmit antenna, all sub streams from each symbol are converted to serial.

At reception CP is removed if it was inserted at transmission, and then the received signal is converted from serial to parallel in order to obtain again the sub-streams and convert them into frequency domain by the *Fast Fourier Transform* (FFT) block. Demodulated signal at channel n and $n + 1$ is expressed as:

$$r_n = h_{1,n}s_n - h_{2,n}s_{n+1}^* + n_n \quad (17.1)$$

$$r_{n+1} = h_{2,n+1}s_{n+1} + h_{1,n+1}s_n^* + n_{n+1} \quad (17.2)$$

Where $h_{m,n}$ represents the flat fading coefficient of the sub-channel n in the antenna m and n_n AWGN noise with zero mean and a given value of variance in sub-carrier n .

Now all sub streams are converted again from parallel to serial so then can be decoded by the SFBC decoder. Here, channel estimation (*Channel State Information* (CSI)) is also made, which estimates frequency response of the channel for every output

from the SFBC decoder (equations 17.1 and 17.2). In the end, the modulated symbols can be demodulated in order to obtain the original transmit bit sequence:

$$\tilde{s}_n = h_{1,n}^* r_n + h_{2,n} r_{n+1}^* \quad (18.1)$$

$$\tilde{s}_{n+1} = -h_{2,n} r_n^* + h_{1,n}^* r_{n+1} \quad (18.2)$$

It is assumed that the channels between two adjacent frequencies are highly correlated from the start so $h_n = h_{n+1}$. From the last equations it is possible to conclude that noise is fully removed.

5.3. Practical system

MISO 2x1 chain using SFBC Alamouti Simulink model was projected in System Generator from Xilinx and it will be explained bellow. All chains were built using System Generator Xilinx design.

It uses Alamouti coding algorithm 2 according to table 3:

Frequency	Antenna 1	Antenna 2
n	S_n	S_{n+1}
$n + 1$	$-S_{n+1}^*$	S_n^*

Table 3- Alamouti code 2

The transmitter system is shown in figure 19:

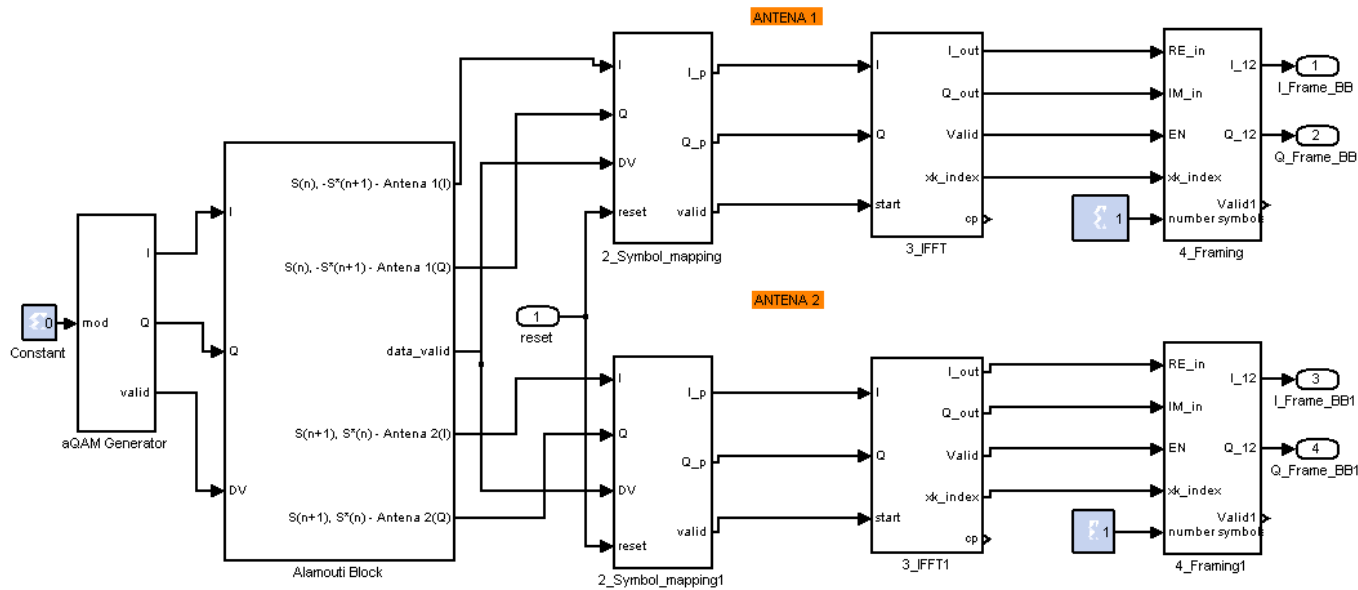


Figure 19- Transmitter side System Generator's Xilinx design

Where I represents In-phase element, Q represents Quadrature element and DV/valid represents Data Valid signal that control the system and guarantees its desired performance.

The block aQAM generator represents the modulation block and the options can be the output of QPSK or 16-QAM symbols. The Alamouti block encodes data through

Alamouti code 2. Symbol mapping block guarantees the sending of pilots or symbols. Framing blocks construct the organized LTE frames to be sent.

Reception:

The Alamouti reception scheme is shown in the figure 20. As the data is received (RX) with a real and imaginary part, it only goes through decoding when the control block signals it is possible to go to next stage. This involves synchronization between data and channel estimation. When pilots are ready to be transmitted, an enable signal is activated and all the data goes through. After decoding we have everything all the parameters ready and then after a normalization we can have the data at reception shown as I_desc (in-phase) and Q_desc (quadrature).

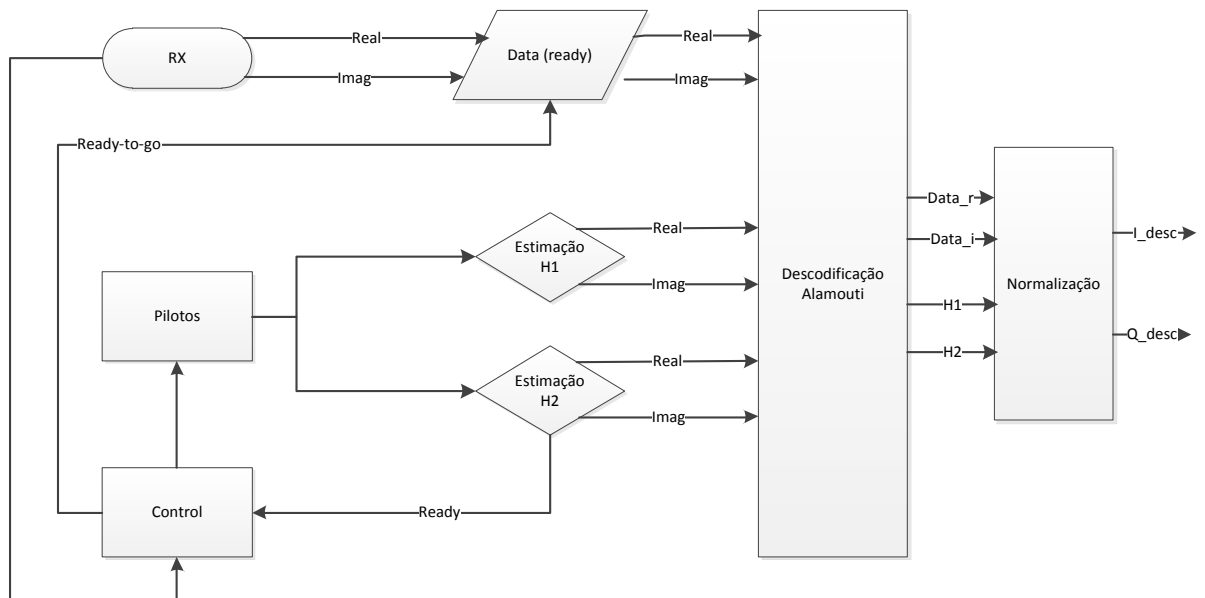


Figure 20- System reception block diagram

The system is now organized so it is possible to distinguish in reception where data and channel parameters (H1 and H2) go (figure 21). Each values start from a *Random Access Memory* (RAM) and go through according to a control signal that is given when pilots are detected and channel estimation is finished.

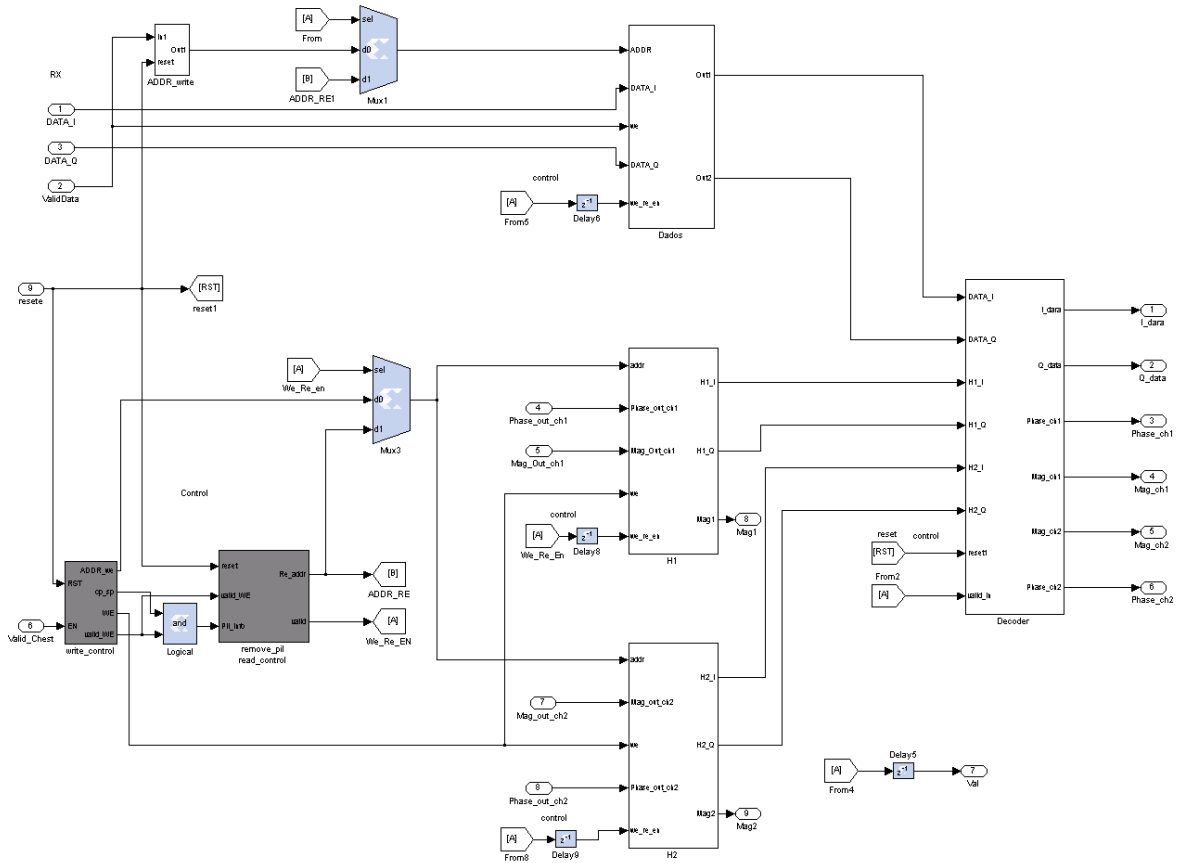


Figure 21 - Alamouti decoder Xilinx System Generator design

Decoding is made and CSI at the receiver in order to obtain the combined signals given by the equations 19.1 and 19.2:

$$\tilde{s}_n = h_{1,n+1}^* r_n + h_{2,n} r_{n+1}^* \quad (19.1)$$

$$\tilde{s}_{n+1} = -h_{1,n} r_{n+1}^* + h_{2,n+1}^* r_n \quad (19.2)$$

The channels are aligned in both instants/frequencies. From the equations above, the block needs to have knowledge of the channel coefficients (h_1 and h_2), thus we assume that they are recovered perfectly at the receiver.

It is assumed that the channels between two adjacent frequencies are highly correlated from the start so $h_n = h_{n+1}$.

Before going to output the data is normalized in a subsystem.

In the next chapter, precoding methods are going to be introduced, as well some practical implementations.

Chapter 6

6. Precoding – Practical implementation

Due to the increasing demand on data throughput and *Quality of Service* (QoS), *Multiple Input Multiple Output* (MIMO) wireless systems are used because of its benefits.

Transmitter design is a problem taken in consideration for MIMO standards. Design algorithms are used, in particular precoding schemes which provide a good tradeoff between performance and complexity. Some of this algorithms are Zero-forcing (ZF) precoding and *Minimum Mean Square Error* (MMSE).

In conventional single-stream beamforming, the same signal is emitted from each of the transmit antennas with appropriate weighting (phase and gain) such that the signal power is maximized at the receiver output. When the receiver has multiple antennas, single-stream beamforming cannot simultaneously maximize the signal level at all of the receive antennas. In order to maximize the throughput in multiple receive antenna systems, multi-stream transmission is generally required. In point-to-point systems, some of the benefits of precoding can be realized without requiring *Channel State Information* (CSI) at the transmitter, while such information is essential to handle the inter-user interference in multi-user systems.

There are several methods like *Zero Forcing* (ZF), *Minimum Mean Square Estimation* (MMSE) ,*Brute Force ML decoding*, and they can be used for Alamouti decoding.

Zero-forcing

Zero-forcing precoding design is highly related to matrix inversion in linear algebra. Basically ZF precoder inverts the multiuser channel [63].

The zero forcing approach tries to find a matrix W which satisfies $WH=I$. The *Zero Forcing* (ZF) linear detector for meeting this constraint is given by [64]:

$$W = H'(H H')^{-1} \quad (20)$$

MMSE

The *Minimum Mean Square Error* (MMSE) approach tries to find a coefficient W which minimizes the criterion:

$$E\{[W - x][W - x]'\} \quad (21)$$

Where x is a random vector variable.

Solving:

$$W = [H'H + \text{var}(n)I]^{-1}H' \quad (22)$$

Where H is the channel matrix, $\text{var}(n)$ the symbol variance where n goes from 1 to E_b/N_o length and I the identity matrix.

Matlab simulations were made and it is possible to see the BER difference between both precoding schemes (figure 22). SISO system's BER is also shown as comparison (Annex B) .

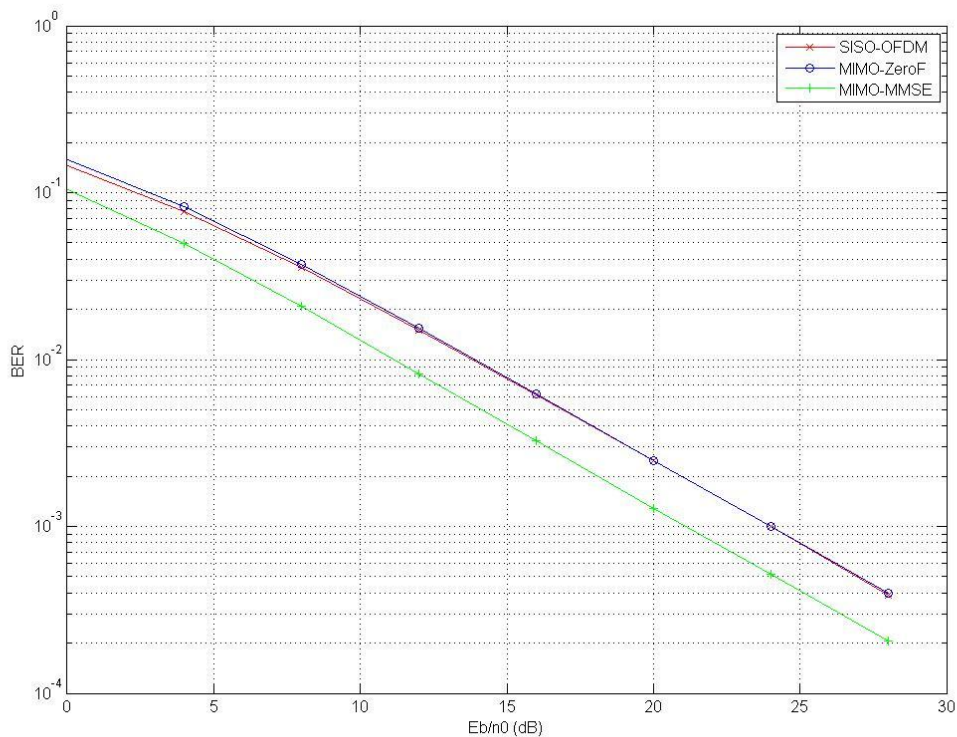


Figure 22 - BER comparing SISO to MIMO systems with ZF and MMSE precoders

It is possible to conclude that MMSE precoding gives better results than ZF, although it is a more complex algorithm and requires more computational intensity. ZF is a little better than a normal SISO system.

6.1.Celcop chain practical implementation

Using matlab's Celcop chain implementation it is possible to implement a MIMO system that makes Power allocation and precoding (Zero-forcing or MMSE) in the block Central_Unitf (Annex C).

Simulation parameters are shown in figure 23:

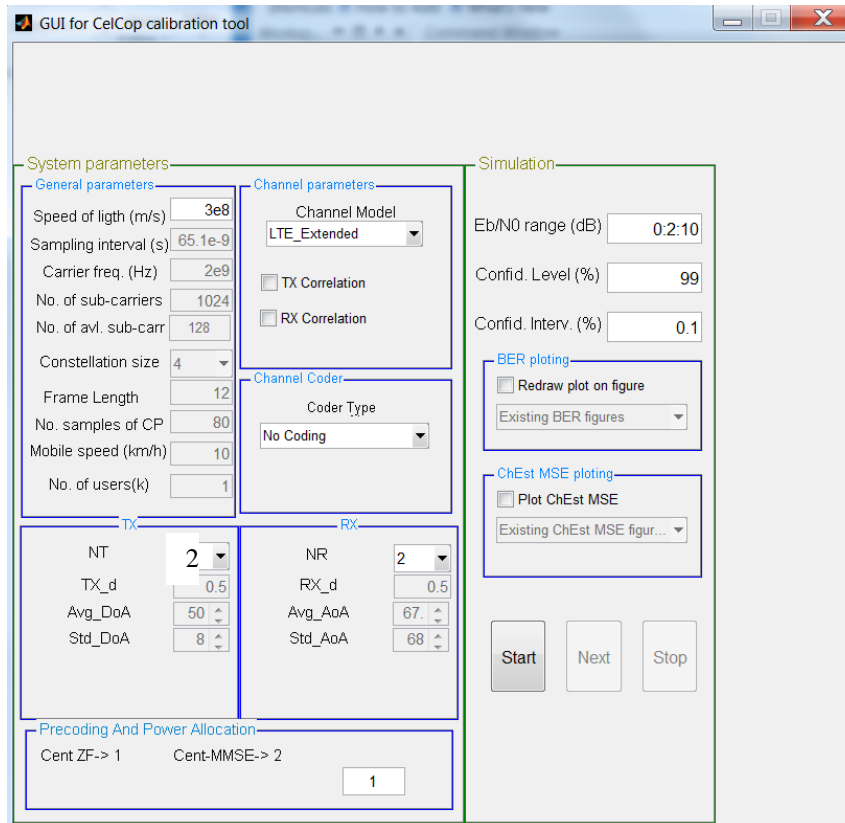


Figure 23-Celcop Calibration tool V5

Where simulation parameters are:

Eb/n0: 0 to 10 dB

Channel model: LTE_Extended

Transmission antennas: 2

Reception antennas: 2

Precoding e Power allocation: Zero-forcing and MMSE

In block diagram (figure 24) it is shown Data_User1 which represents the data transmitted by users. It goes through block Central_Unitf where ZF or MMSE was implemented and can be chosen as an option in the calibration tool. Then it goes through BS1 (base station) and data is divided through 2 antennas creating channels H11, H21, H12 and H22. In the end data is received in block Frame errors and compared to the original, and BER is calculated.

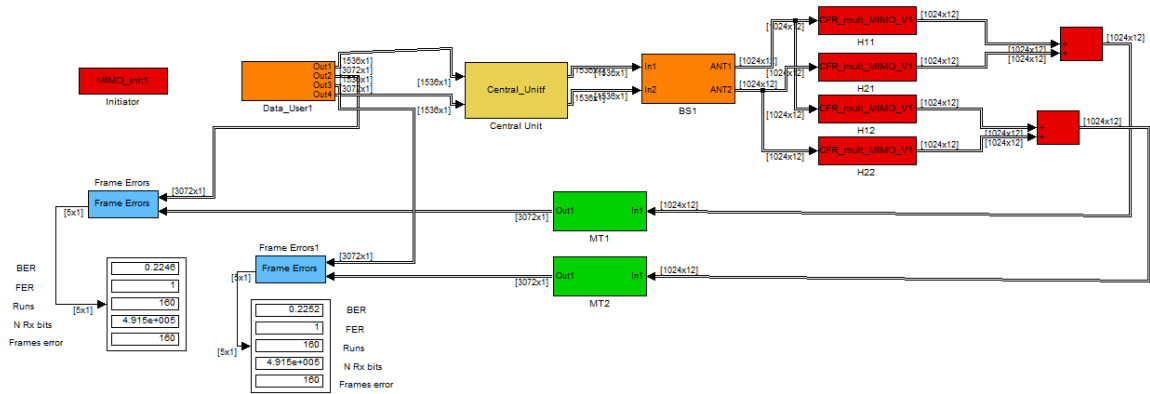


Figure 24- Celcop chain overall block diagram

The implemented/programmed block Central unit processes the precoding and power allocation with the chosen option (ZF or MMSE). The modulation used is *Quadrature Pulse Shift Keying (QPSK)*.

Central Unit parameters are shown below:

Input parameters: NcAv, Frame_Length, Precoding Scheme

Output parameters: (NcAv x Frame_Length) x 1 => 128*12, Total number of data carrying subcarriers in a OFDM frame

The precoding matrix $W(2x2)$ fits dimensions $2x2$ in order to have 4 coefficients that characterizes the 4 channels of each of the 128 sub carriers. *Frame_Length* is the number of OFDM symbols in each frame and *NcAv* the number of sub-carriers in 1 frame.

$W(2x2)$ => Pre-coding matrix (Zero Forcing or MMSE) :

Each Precoding matrix can be defined by:

Zero Forcing:

$$W = H'(H H')^{-1} \quad (23)$$

MMSE:

$$W = H'(H H' + eye(2,2) var(n_{symbols}))^{-1} \quad (24)$$

Where var represents the variance and goes ($n_{symbols}$) from 1 to E_b/N_o length, and $eye(2,2)$ the identity matrix with 2x2 dimensions.

To counter the effect of channel correlation, it is introduced beamforming with precoding where the transmitter sends αW instead of sending W . By requiring that α we maintain the power constraint on the input [65]:

$$\alpha_{zf} = \frac{2}{trace(W W')} \quad (25.1)$$

$$\alpha_{mmse} = \frac{2}{trace(W W')} \quad (25.2)$$

And then multiplying by W matrix we get the precoding matrix required denoted in matlab as $W_{novo}(2 \times 2)$ in the code at annex C.

The channel coefficients matrix is defined by:

H => Carriers matrix => each H with length of 128.

H_{11} => Channel of user 1

H_{21} => Channel of user 1

H_{12} => Channel of user 2

H_{22} => Channel of user 2

Dt_1 / Dt_2 => Data from user 1 / 2 => Length of 128x2 QPSK

Y_1 / Y_2 => Reception at antenna 1 / 2 (length of 128 for each antenna)

N_1 / N_2 => Gaussian noise => length of 128

The reception is done according to:

$$\begin{bmatrix} Y_1 \\ Y_2 \end{bmatrix} = \begin{bmatrix} W_{11} & W_{21} \\ W_{12} & W_{22} \end{bmatrix} \begin{bmatrix} H_{11} & H_{21} \\ H_{12} & H_{22} \end{bmatrix} x \begin{bmatrix} Dt_1 \\ Dt_2 \end{bmatrix} + \begin{bmatrix} N_1 \\ N_2 \end{bmatrix} \Leftrightarrow \quad (26)$$

$$\begin{bmatrix} Y_1 \\ Y_2 \end{bmatrix} = \begin{bmatrix} W_{11}H_{11} + W_{21}H_{12} & W_{11}H_{21} + W_{21}H_{22} \\ W_{12}H_{11} + W_{22}H_{12} & W_{12}H_{21} + W_{22}H_{22} \end{bmatrix} x \begin{bmatrix} Dt_1 \\ Dt_2 \end{bmatrix} + \begin{bmatrix} N_1 \\ N_2 \end{bmatrix}$$

Separating the data we obtain the data for:

User 1:

$$Y_1 = (W_{11}H_{11} + W_{21}H_{12})Dt_1 + (W_{11}H_{21} + W_{21}H_{22})Dt_2 + N_1 \quad (27)$$

User 2:

$$Y_2 = (W_{12}H_{11} + W_{22}H_{12})Dt_1 + (W_{12}H_{21} + W_{22}H_{22})Dt_2 + N_2 \quad (28)$$

Where Y_1 and Y_2 represent the data for user 1 and 2 respectively, with a dimension of 128 each one.

Simulink results are shown in figures 25 and 26. MMSE results give a better BER proving the results already shown at Chapter 6 are right:

Centmmse:

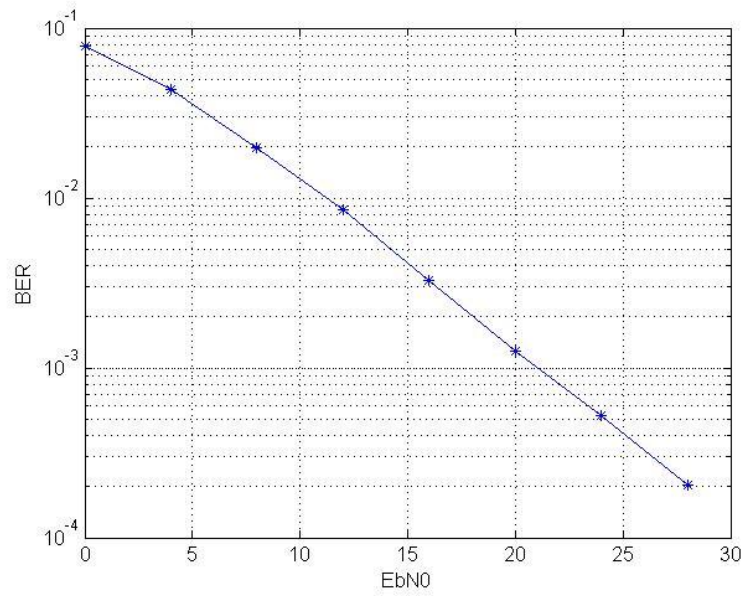


Figure 25 - BER for cent-mmse precoding

Zero-forcing:

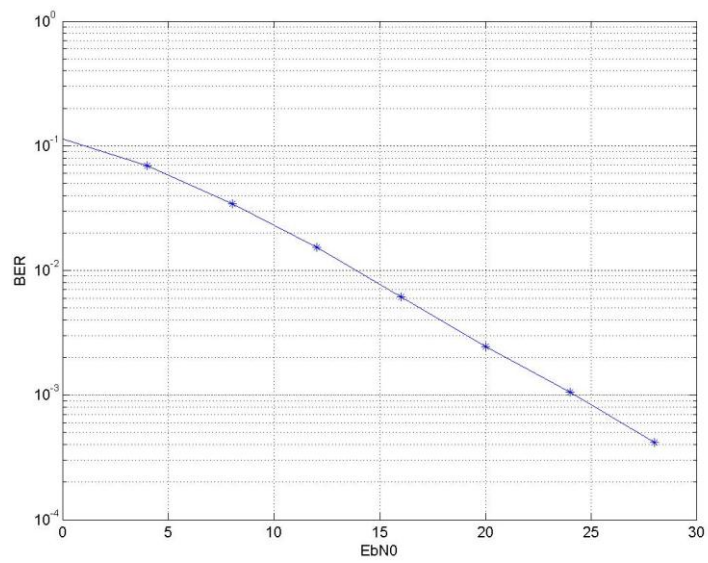


Figure 26 - BER for ZF precoder

6.2.Zero-forcing practical implementation - System generator

A zero forcing solution was made for FPGA implementation. Zero forcing matrix (W) can be achieved by equation 29:

$$W = H'(H H')^{-1} \quad (29)$$

Where H represents the channels matrix coefficients.

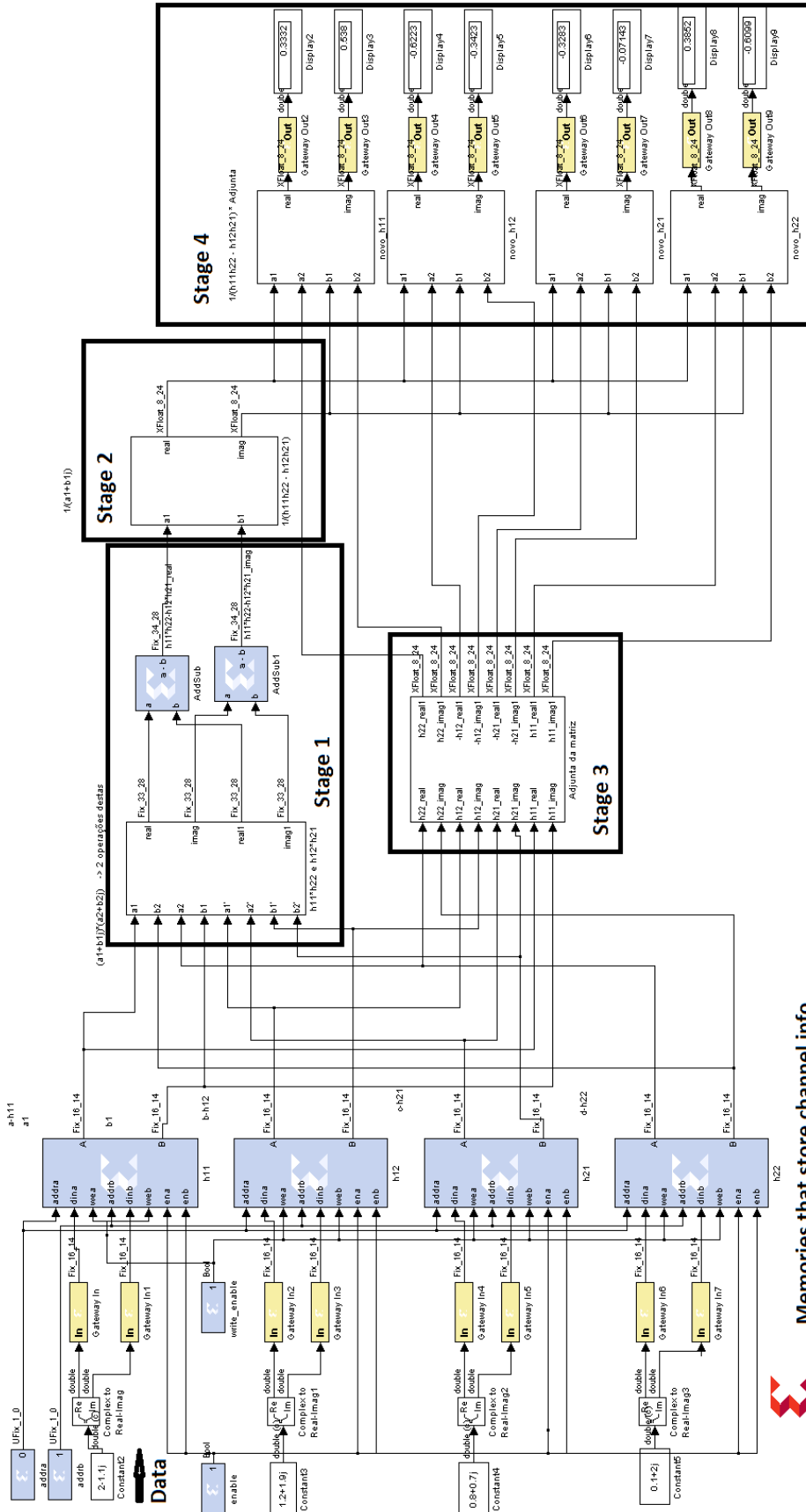
Simplifying the previous equation turns out that it is possible to achieve W by inverting H matrix.

Implementation in system generator can be done with the use of mainly add, subtract, multiply and division blocks. The main equation :

$$W = \frac{1}{h_{1,1}h_{2,2} - h_{1,2}h_{2,1}} \begin{bmatrix} h_{2,2} & -h_{1,2} \\ -h_{2,1} & h_{1,1} \end{bmatrix} \quad (30)$$

Where $h_{i,j}$ represents channel coefficient of the j th user through the i th channel. All of them represented by complex numbers with real and imaginary parts. Convert blocks are used to convert the values into floating point in order to work with the *Field Programmable Gate Array* (FPGA).

The main system is shown in figure 27. Real and imaginary parts are separated and saved in 4 ram (each one with 2 entries to separate real and imaginary parts). Memories represent the 4 channel coefficients. When enable is on, real and imaginary parts are read and treated independently by the system. The system is divided in subsystems which can be seen as stages explained below.



Memories that store channel info




Figure 27- ZF Xilinx design system blocks

Adding and subtracting complex part can be done directly with real with real part, and imaginary with imaginary parts.

Multiplying complex numbers is shown according to equation 31:

$$(a_1 + b_1i)(a_2 + b_2i) = (a_1a_2 - b_1b_2) + (a_1b_2 + b_1a_2)i \quad (31)$$

Its Xilinx design in System generator subsystem is illustrated in figure 28:

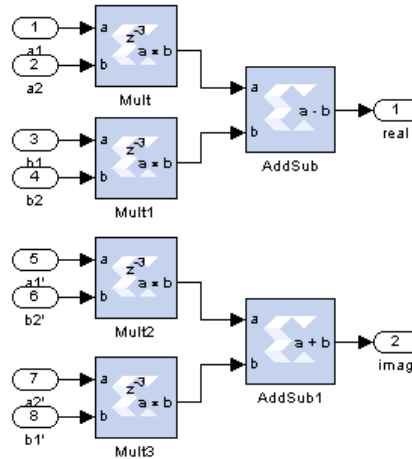


Figure 28 - Complex multiplier system blocks

Stage one deals with the operation $h_{1,1}h_{2,2}$ and $h_{1,2}h_{2,1}$ and subtracts them in order to achieve the denominator $h_{1,1}h_{2,2} - h_{1,2}h_{2,1}$.

Stage two deals with division operation. It calculates $\frac{1}{h_{1,1}h_{2,2} - h_{1,2}h_{2,1}}$ reciprocal.

Dividing complex numbers is done by rationalize the denominator by multiplying the numerator and the denominator by the conjugate of the denominator. The calculation of $1/y$ can be done like:

$$\frac{1}{a_1 + b_1i} = \frac{a_1 - b_1i}{(a_1 + b_1i)(a_1 - b_1i)} = \frac{a_1 - b_1i}{a_1^2 + b_1^2} = \frac{a_1}{a_1^2 + b_1^2} - \frac{b_1}{a_1^2 + b_1^2} \cdot i \quad (32)$$

Its Xilinx design System Generator subsystem is represented in figure 29:

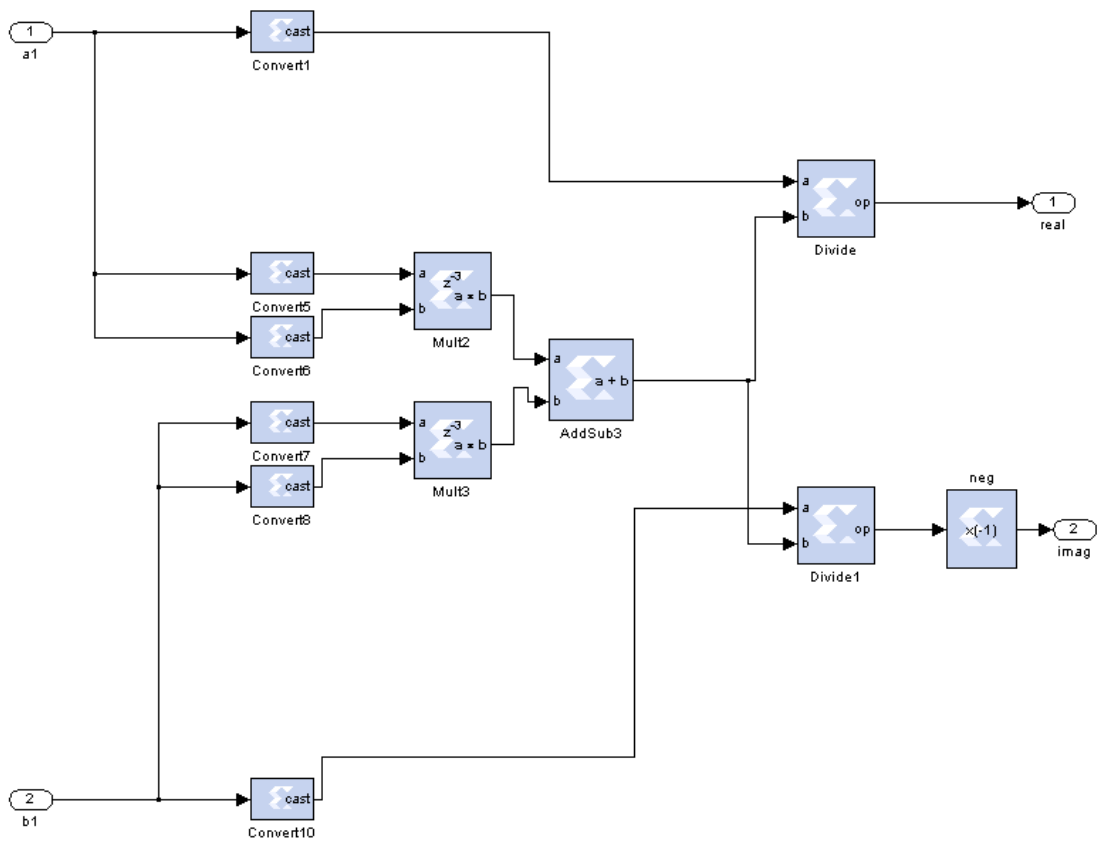


Figure 29- Complex Division system blocks

Third stage determines H Matrix adjunct. It can be achieved by negating some values and changing their place in the matrix.

The Xilinx design in System Generator subsystem is represented in figure 30:

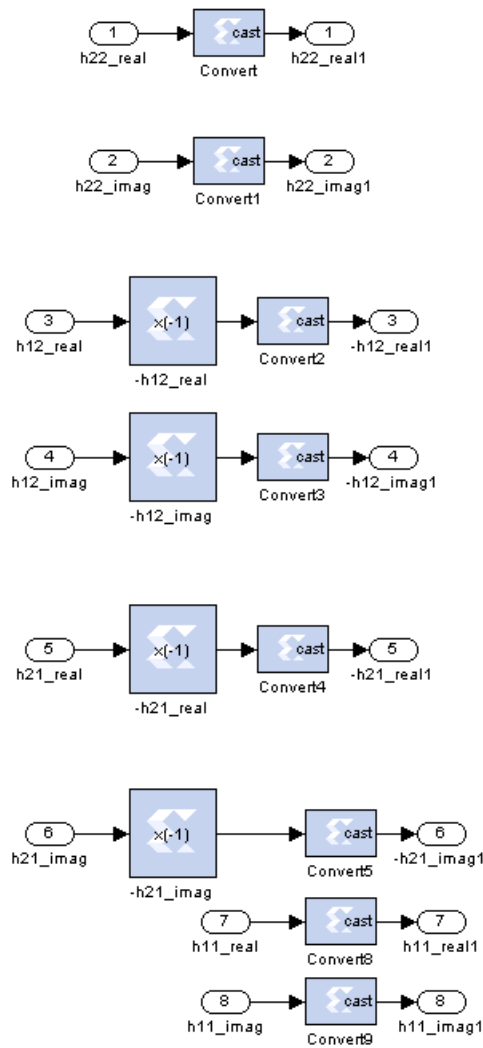


Figure 30- Adjunct matrix creator system blocks

The fourth and last stage makes the middle multiplication of equation 30 in order to output the new matrix H coefficients.

Results:

Transmitting to memories 4 (input) complex numbers representing $h_{1,1}$, $h_{1,2}$, $h_{2,1}$ and $h_{2,2}$, we get as output the 8 new values representing real and imaginary parts of the precoding matrix W (figure 31):

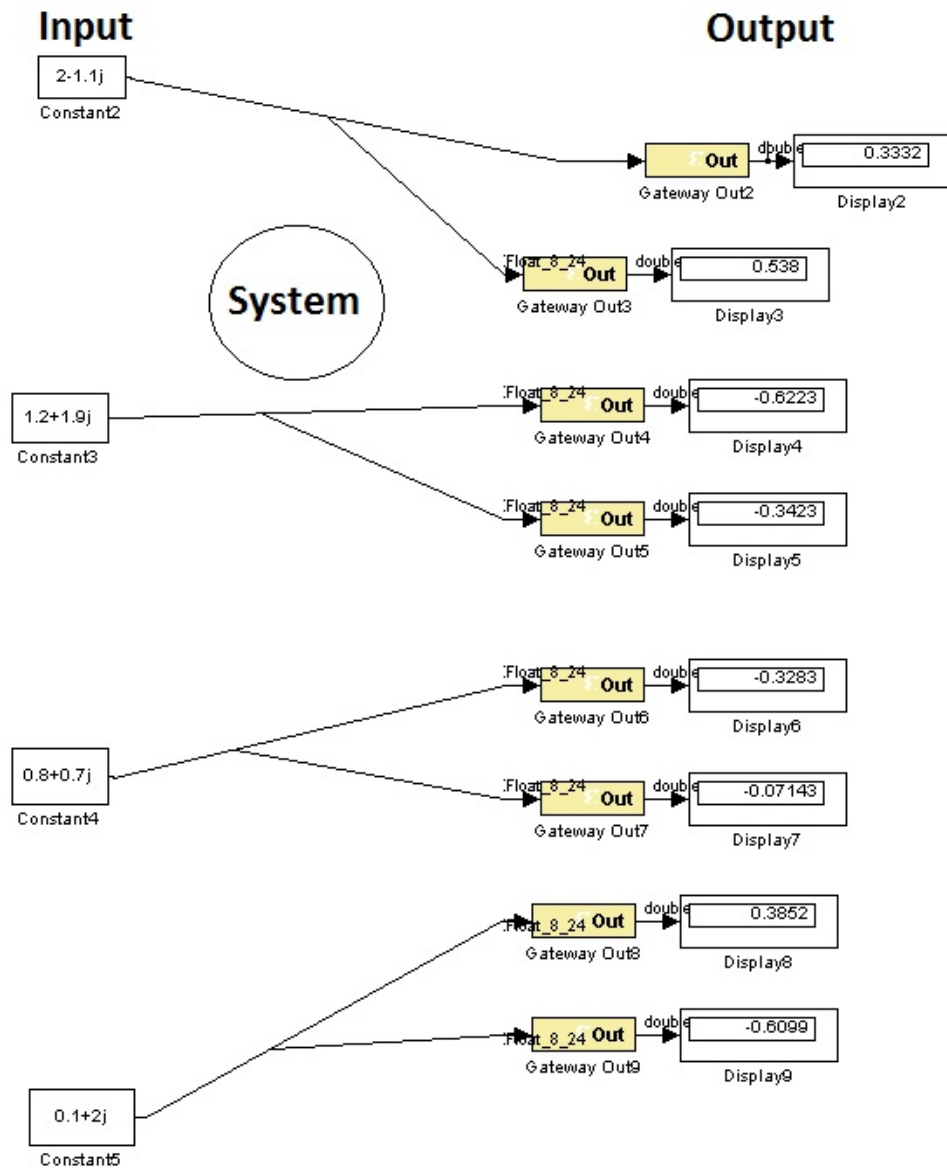


Figure 31- Input and Output system results

Since:

$$\begin{bmatrix} 2 - 1.1j & 1.2 + 1.9j \\ 0.8 + 0.7j & 0.1 + 2j \end{bmatrix}^{-1} = \begin{bmatrix} 0.3332 + 0.5380j & -0.6222 - 0.3422j \\ -0.3282 - 0.0714j & 0.3852 - 0.6099j \end{bmatrix} \quad (33)$$

The system is working correctly.

In the next chapter a PAPR reduction technique will be shown for the Alamouti's chain implemented in System Generator.

Chapter 7

7. PAPR (Peak-to-Average Power Ratio)

One of the major practical difficulties involving OFDM modulation is High *Peak-to-Average Power Ratio* (PAPR). According to [66] and [67] this results from the modulation where all subcarriers are added forming the signal to be transmitted. For example, an input sequence that requires the maximum amplitude values of its subcarriers would result in higher PAPR. High PAPR signals require a large range of dynamic linearity from the analogue circuits with the consequence of more "power hungry" devices.

By limiting the input sequences to a smaller subset, it would be possible to obtain outputs with low PAPR and resiliency in the presence of noise. All these involves a selection of code words based on their PAPR and minimum distance performance.

Several schemes for reducing peak amplitude were introduced as *clipping* [68], *coding* [69], *interleaving* [70], *Active Constellation Extension* (ACE) [71], *partial transmit sequences* [72] or *Turbo Coded OFDM* [73].

The PAPR of the signal $x(t)$ is the ratio of the peak instantaneous power to the average power, given as:

$$PAPR = \max_{0 \leq t \leq (m+1)T_a} \frac{|x(t)|^2}{E[|x(t)|^2]} \quad (34)$$

Where $E[.]$ is the expectation operator and $(m + 1)T_a$ the signal period. If N_c is large enough, based on the central limit theorem, the real and imaginary parts of $x(t)$ have Gaussian distribution [74] and its envelope is similar to a Rayleigh distribution [75] leading to high PAPR.

A dynamic estimation of channel is necessary before the demodulation of OFDM signals since the radio channel is frequency selective and time-varying for wideband mobile communication systems.

The channel estimation can be is done by either inserting pilot tones into all of the subcarriers of OFDM symbols with a specific period or inserting pilot tones into each OFDM symbol (chapter 4.1.2). In the present chain (chapter 5.3), the known pilots are multiplexed into the data stream, and channel estimation is performed by interpolation between pilots.

7.1.Reducing PAPR – Random reference Pilots generation practical implementation (Transmitter side)

Practical considerations:

- Necessary to load random I, Q vectors through symbol_gen.m file;
- Necessary to sum the 2 signals at transmitter side in order to receive it (somaçanais.mdl) because it is a MISO chain;
- Doesn't follow LTE PHY at its full extent. the bandwidth is close to 10 MHz just for testing. Resulting 50 PRBs per slot. The frame is based in the first transmission slot;
- Each sequence contains 6 OFDM symbols.

In the previous system (chapter 5.3), pilots (sent by signal that selects in the multiplexers) have the constant value of approximately (1,0), 1 for in-phase and 0 for quadrature. Due to this, it tends to have higher PAPR values.

In the new system, pilots are sent in blocks symbolmapping and symbolmapping1 (figure 19) for antenna 1 and 2 respectively (figure 32 and 33 respectively).

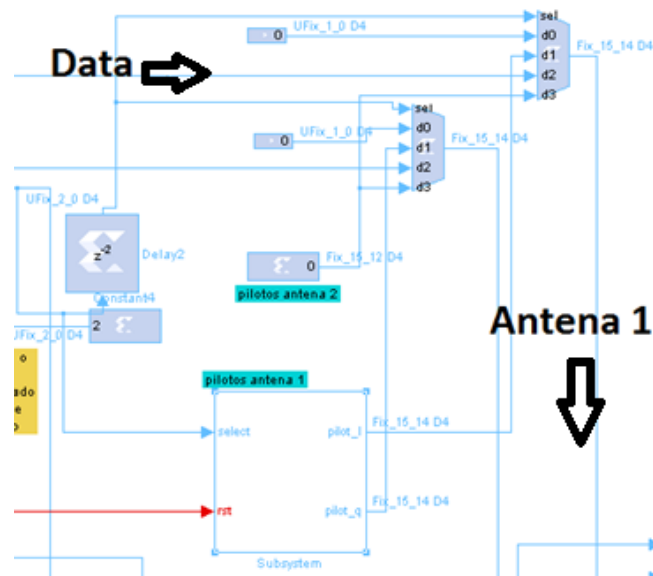


Figure 32 - Pilots insertion subsystem in antenna 1

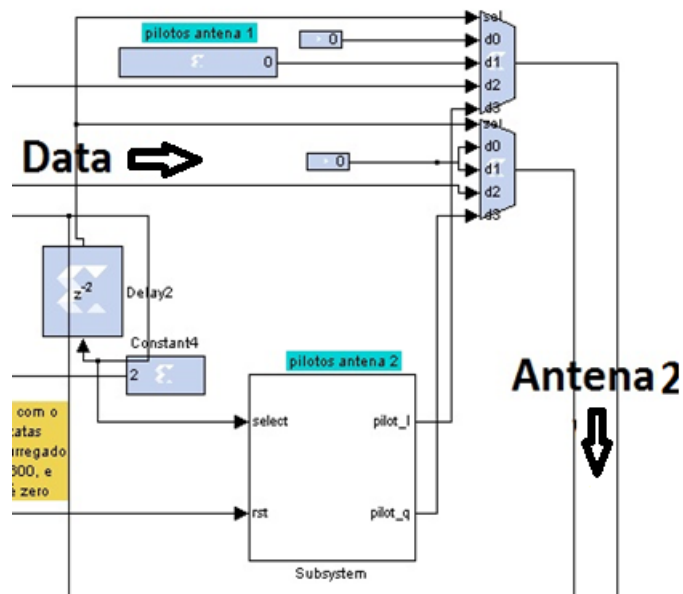


Figure 33- Pilots insertion subsystem in antenna 2

In each slot (period), there are sent 6 symbols with pilots (each radio frame has 10 ms long, being composed by 20 slots of length each one with 6 or 7 OFDM symbols). In the end we can see some peak values. This leads to higher PAPR. Reducing these values would lead to a more efficient use of power in the FPGA.

Using LFSR it is possible to generate random values when pilots need to be sent.

Linear-Feedback Shift Register (LFSR) are Xilinx design blocks that output '0' and '1'. It is a shift register whose input bit is a linear function of its previous state. Along the time they output sequences according to the initial value and the linear function that it is done. Usually it is an *exclusive-or* (XOR) or *exclusive-nor* (XNOR) [76].

The gates can be inserted in the bits position we would like.

They are attractive structures for the following reasons:

- LFSRs have a simple structure;
- Their shift property is easily inserted in the scan design environment;
- They are capable of generating exhaustive and/or vector;
- Their error detection and correction properties make them good for signature analysis applications.

The LFSR sending bits for in-phase values for pilots, has 4 bits to combine, deals with a XNOR gate and its initial value is 0x1.

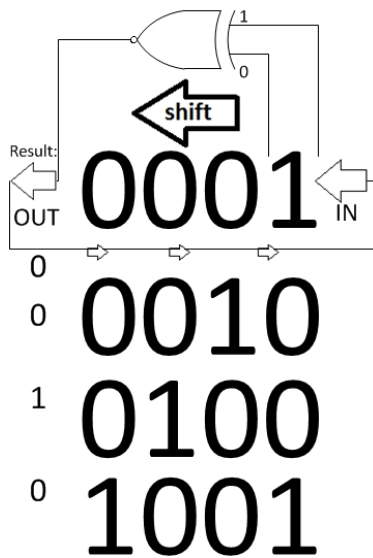


Figure 34 - LFSR example sending in-phase values

The LFSR sending bits for quadrature values for pilots, has 5 bits to combine, deals with a XOR gate and its initial value is 0x09.

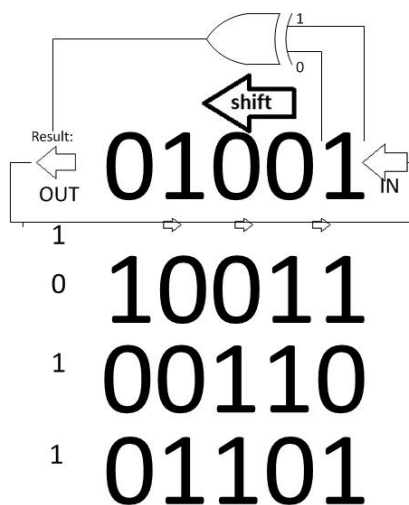


Figure 35-LFSR example sending quadrature values

They have an enable port synchronized when the frame is starting to be sent or received and a reset port to start again at the initial value.

Using a LFSR for inphase with 5 bits and starting at 0x1 value, and another LSFR with 6 bits starting at value 0x9, it is possible to generate random values sent by both of (0,0), (0,1), (1,0) and (1,0). To guarantee that the values are inside the circle it is assumed

that 0 is equivalent to -0.7 and 1 equivalent to 0.7. The whole system for 1 antenna is represented in figure 36.

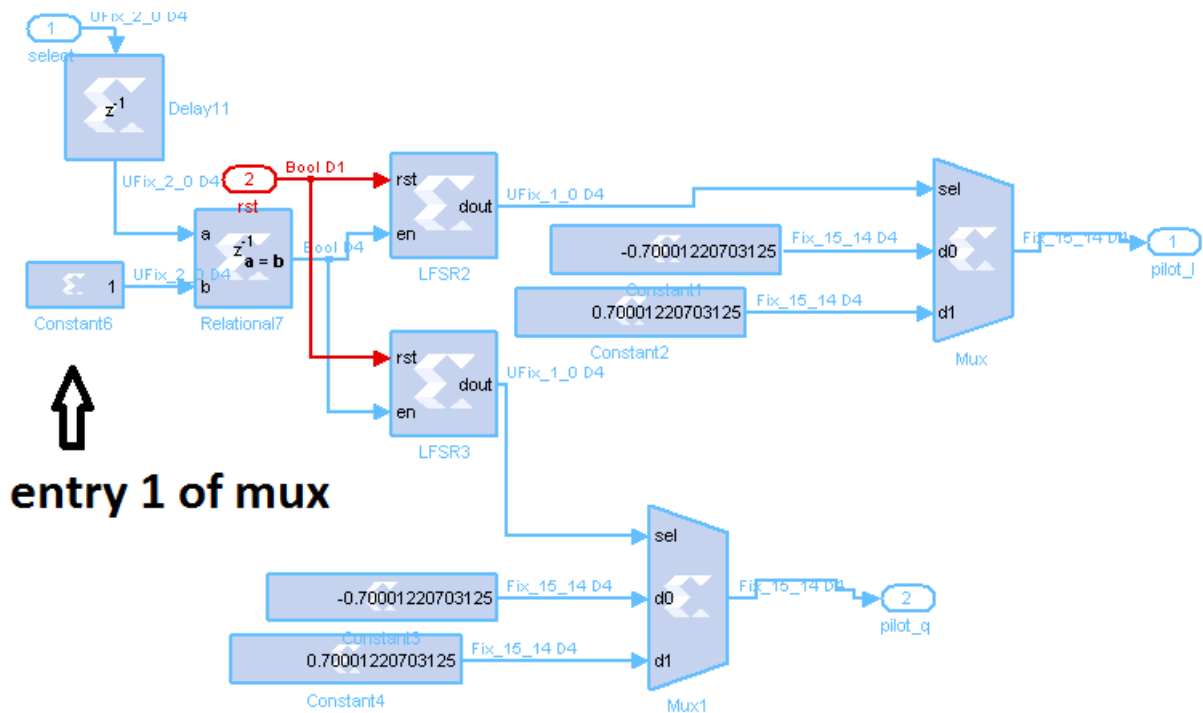


Figure 36 - Inside view of the pilots insertion subsystem

The main difference between the subsystem for antenna 1 and 2 is that pilots go through the number 1 and number 3 entry of the multiplexer in antenna 1 and 2 respectively. The selection and enabling of the LFSRs is done via an relational that compares the select signal and decides if it is the chosen option to activate pilots sending or not.

To guarantee that the systems works correctly in transmitter side, it is compared the signal at the receiver antenna with itself but at different times (figure 37). As we can see, the same sequence is being transmitted all over again because the red (signal at time $t1$) and blue (signal at time $t2$) lines overlap when put together at the same start point. In conclusion this means that the system is transmitted correctly and the pilots and being inserted in the right places even when system resets.

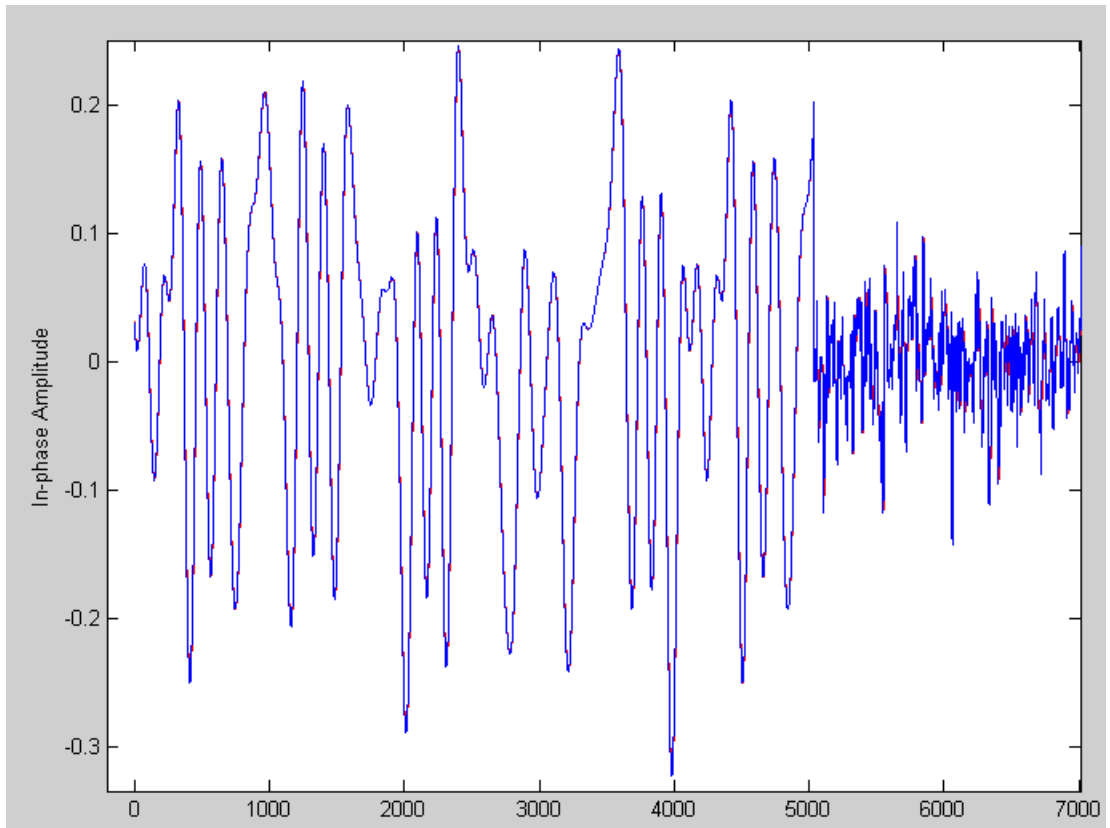


Figure 37- OFDM signals comparison at different time samples

7.2.Reducing PAPR – Random reference Pilots generation practical implementation (Receiver side)

In this implementation, an phase is being added due to the in-phase values added, so it needs to be later discovered and be taken/corrected from the signal before channel estimation. Concatenating each pair of the values from both LFSRs before will lead to values from 0 to 3. This values select the phase value to add or subtract according to the values given by the LFSRs (note that 2 identical LSFRs to the ones in transmission are inserted in reception so it is possible to know before estimation which value was transmitted at the given time), so the pilot would be in x axis. It is illustrated in figure 39 a). In table 4 the values are expressed according to LFSRs output:

LFSRs output concatenated (MS,LS):	Correction needed (rad):
(0,0)	$+3/4\pi$
(0,1)	$-3/4\pi$
(1,0)	$+\pi/4$
(1,1)	$-\pi/4$

Table 4 - Phase correction values

Where MS is the output bit from the LFRS that outputs for in-phase (real) values and LS is the output bit from the LFRS that outputs for quadrature (imaginary) values, according to a) in figure 38.

In next stage, it is added 2π or -2π to guarantee the phase value is between values of π and $-\pi$ of the circle, according to b) in figure 38. This is an additional correction but in theory the phase value will be the same. It corrects the interpolation.

The whole system is shown in figure 38. This represents the one used for antenna 2. Note that the system is the same for antenna 1.

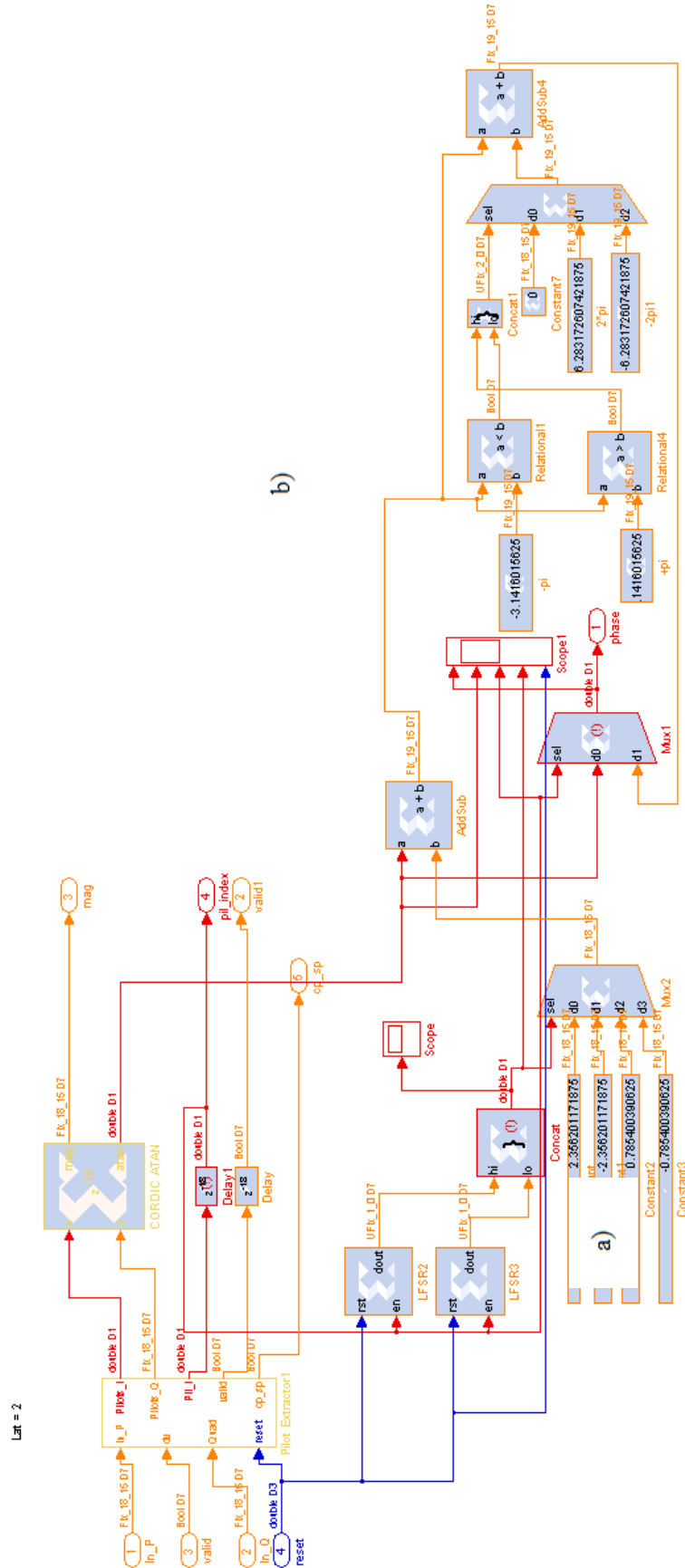


Figure 38 - Overall system blocks of phase correction at reception

7.3. Practical Results (Receiver side)

The corrected Phase values are correctly shown at 1st line graphic of figure 39. They have a linear variation. For comparison it is shown the phase values before correction in the 2nd plot. Graphic in 3rd plot confirms that the system is synchronized and the 4th plot shows a graphic with the values of both LFSRs concatenated in order to choose the right value to add or subtract to the original phase.

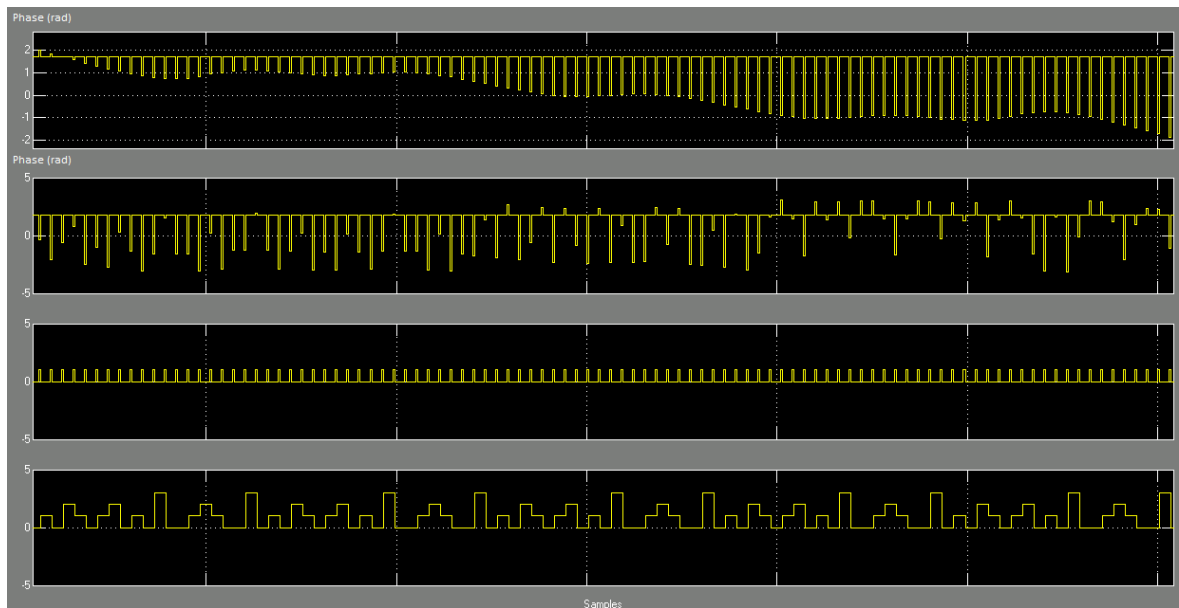


Figure 39 - Scope values

Next to that, it goes through phase interpolation that estimates the phase for 6 points and varies if the distance between 2 symbols that are next to each other, is bigger than values 5 and -5 (first stage) , π and π (2nd stage) , and 2π and -2π (3rd stage).

The figure 40 shows the values of phase (rad) After phase interpolation and estimation. Note that the system is always estimating for 6 points.

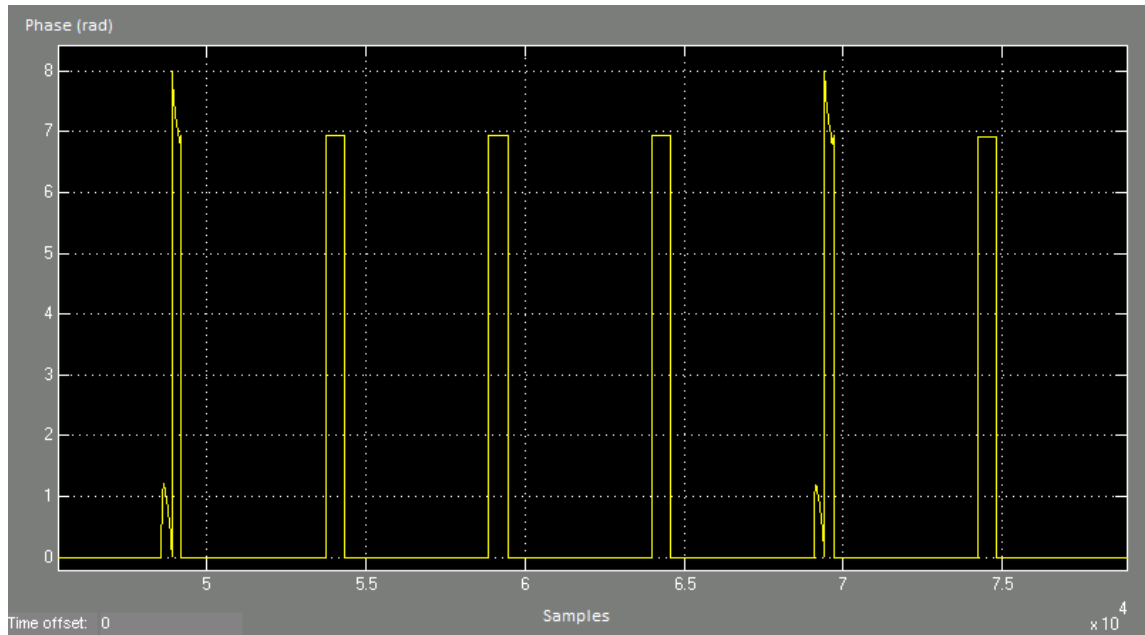


Figure 40 - Scope values for phase interpolation

To prove that the system is working well it is compared the frame when both systems start to receive symbols. At figure 41 it is possible to conclude that the original system (in red) has much higher peak values (pilots), proving that the new system (in blue) with random values for pilots leads to lower PAPR.

It was considered a sequence were we know that pilots are being sent in the antenna we are analysing.

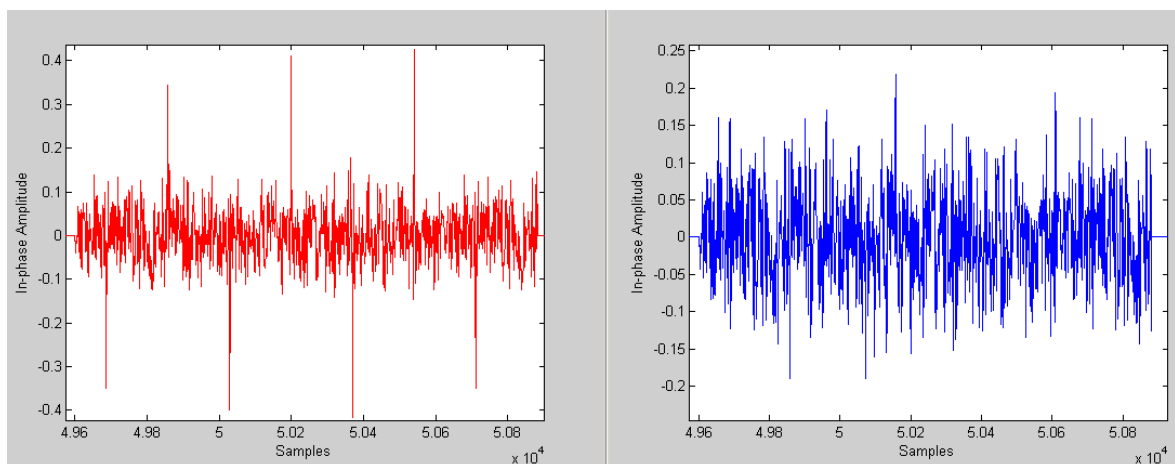


Figure 41 - Pilots peak values comparison between old (red) and new system (blue)

Comparing to original system, as shown in figure 42 and figure 43, the signals are received correctly either QPSK or 16-QAM.

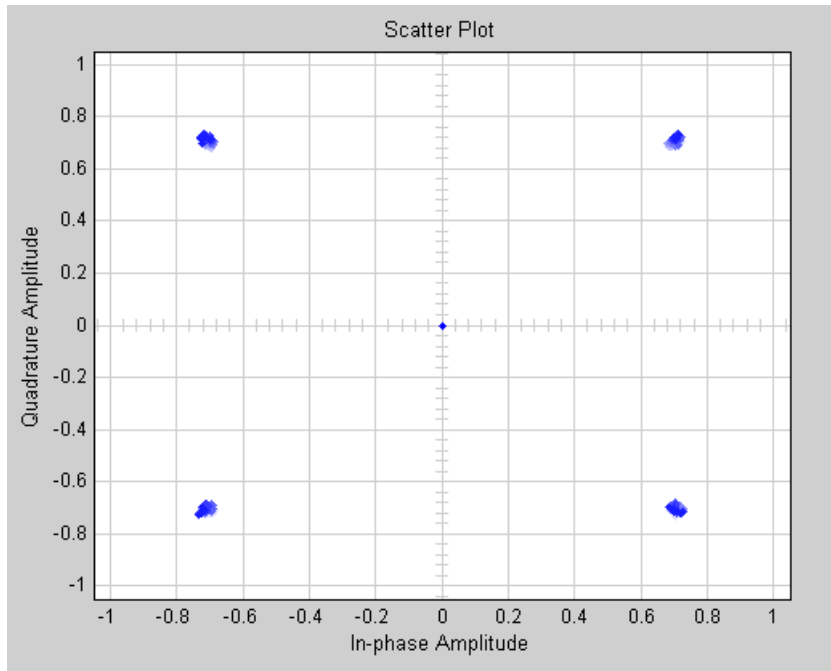


Figure 42- QPSK output signal

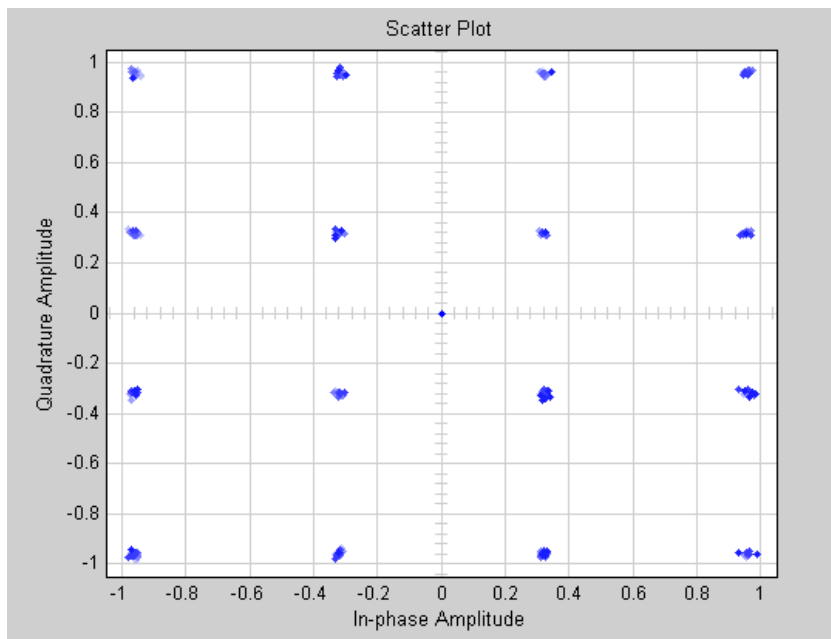


Figure 43 - 16-QAM output signal

Running the script biterror.m it is possible to conclude that the symbols transmitted are correctly received (figure 44).

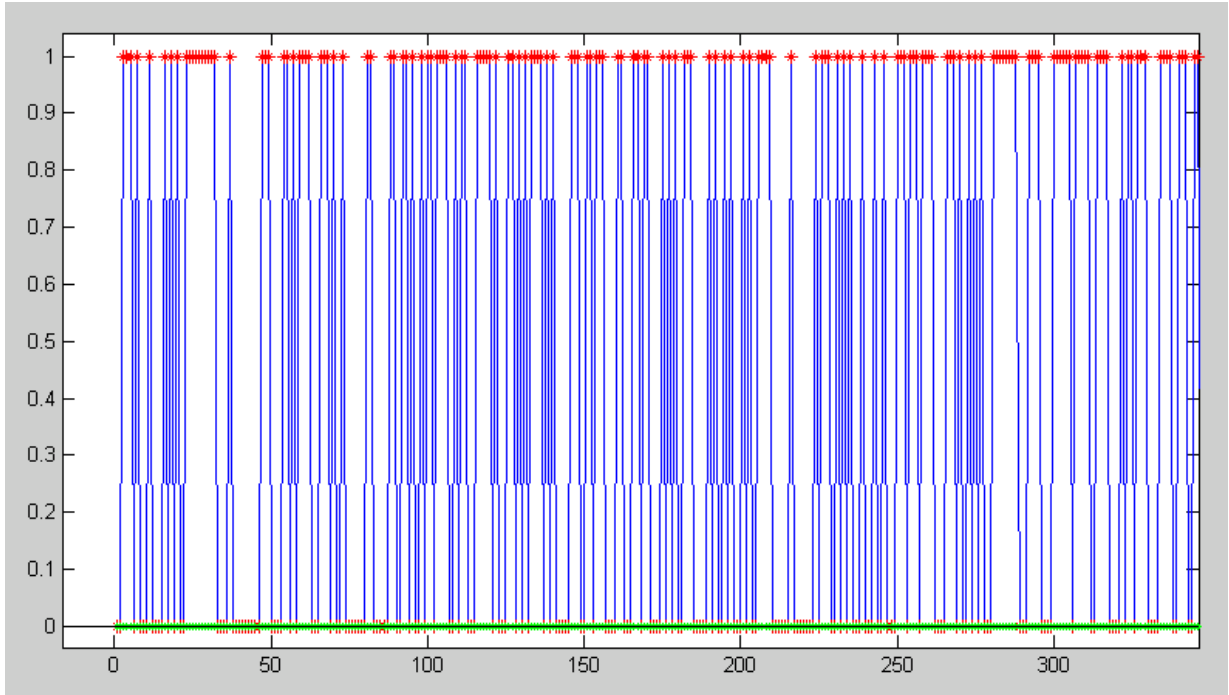


Figure 44- Testing graphic / received bits vs transmitted bits

Where green marks represent the transmitted signal and the reception is represented by red marks.

PAPR is taken from the signals after IFFT block, in transmitter side, for the same time period and the results were (Annex D):

PAPR Antenna 1:

Original Inphase: 2.284064

Inphase with Isfr: 1.065235

Difference for the best (lower PAPR): 1.218829

Original Quadrature: 0.575619

Quadrature with Isfr: 0.667664

Difference for the best (lower PAPR): -0.092045

PAPR Antenna 2:

Original Inphase: 3.746221

Inphase with Isfr: 1.384695

Difference for the best (lower PAPR): 2.361527

Original Quadrature: 1.301353

Quadrature with Isfr: 1.449414

Difference for the best (lower PAPR): -0.148061

The PAPR gets lower for inphase values for both antennas, as expected. It is a little bigger for quadrature values, but irrelevant to the values of improvement gained in inphase values.

The PAPR efficiency for inphase values for antenna 1 is increasing for 46,64% and 63,03% for antenna 2 in some frame transmissions .

The next chapter talks about conclusions about all this work and future work to take in consideration for future.

Chapter 8

8. Conclusion and future work

With this thesis it is possible to conclude that there are different ways to process a LTE system following its physical layer specifications. Different ways can be exploited according to what efficiency or QoS we want.

The Alamouti decoder was organized in order to be easily understood.

Other less complex and power hungry ways can be exploited like the Zero-forcing precoder. It was implemented in Xilinx System Generator and for future work is to implement it in a MIMO chain. Changing from Cartesian coordinates to Polar values is also a future work to be proposed in order to study the impact in the efficiency of the system.

In the last stage of the work, it was possible to conclude that there are several ways to reduce the power consumption of a systems, reducing the PAPR, turning into having much more efficient devices. For future work it is proposed to study a method of reducing the Quadrature values instead of only the in-phase ones.

Bibliography

- [1] D. Agrawal and Q.-A. Zeng, *Introduction to Wireless and Mobile Systems*. Cengage Learning, 2010, p. 582.
- [2] “Global mobile statistics 2014 Part A: Mobile subscribers; handset market share; mobile operators | mobiForge.” [Online]. Available: <http://mobiforge.com/research-analysis/global-mobile-statistics-2014-part-a-mobile-subscribers-handset-market-share-mobile-operators?mT>. [Accessed: 13-Oct-2014].
- [3] Xilinx, “Product brief,” 2012. [Online]. Available: http://www.xilinx.com/publications/prod_mktg/ml605_product_brief.pdf.
- [4] “First Generation Cellular.” [Online]. Available: http://www.pitt.edu/~dtipper/2720/2720_Slides5.pdf. [Accessed: 20-Jul-2014].
- [5] “1G.” [Online]. Available: <http://en.wikipedia.org/wiki/1G>.
- [6] “What is 1G or First generation of wireless telecommunication technology?”
- [7] “Cellular Generations,” *Telecommun. Internet, Wirel. Technol.*
- [8] “3GPP Organizational Partners.” [Online]. Available: <http://www.3gpp.org/about-3gpp/partners>.
- [9] R. Ganesh, K. Pahlavan, and Z. Zvonar, Eds., *Wireless Multimedia Network Technologies*, vol. 524. Boston: Kluwer Academic Publishers, 2002.
- [10] L. MILSTEIN, *Wideband code division multiple access*, 18th ed. 2000, pp. 1344–1354.
- [11] A. Graven, “3G The Next Wave.”
- [12] S. M. and G. J. R. P. H. Haas, “Capacity-coverage analysis of TDD and FDD mode in UMTS at 1920MHz,” 2002.

- [13] X. J. Ingo Forkel, *Performance Comparison Between UTRA-TDD High Chip Rate And Low Chip Rate Operation*. 2002.
- [14] and V. HARRDT, M., KLEIJN, A., KOHEN, R., OESTRICH, S. and T. U. SAMMER, *The TD-CDMA based UTRA TDD mode*, 18th ed. 2000, pp. 1375–1385.
- [15] E. Dahlman, S. Parkvall, J. Skold, and P. Beming, *3G Evolution: HSPA and LTE for Mobile Broadband (Google eBook)*. Academic Press, 2010, p. 648.
- [16] “LTE.” [Online]. Available: <http://www.3gpp.org/technologies/keywords-acronyms/98-lte>. [Accessed: 11-Oct-2014].
- [17] R. Research, “Mobile Broadband Explosion: The 3GPP Wireless Evolution,” 2012.
- [18] “LTE Relay | 4g LTA Advanced Relaying | Tutorial - Radio-Electronics.Com.” [Online]. Available: <http://www.radio-electronics.com/info/cellulartelecomms/lte-long-term-evolution/4g-lte-advanced-relaying.php>. [Accessed: 11-Oct-2014].
- [19] A. Silva and A. Gameiro, “4G Cellular Systems (LTE),” 2012.
- [20] “ZON Optimus reforça liderança na inovação - NOS.” [Online]. Available: <http://news.cision.com/pt/nos/r/zon-optimus-reforca-lideranca-na-inovacao,c63529456134000000>. [Accessed: 11-Oct-2014].
- [21] “LTE-Advanced.” [Online]. Available: <http://www.3gpp.org/technologies/keywords-acronyms/97-lte-advanced>. [Accessed: 11-Oct-2014].
- [22] H. Holma and A. Toskala, *LTE for UMTS: Evolution to LTE-Advanced*. John Wiley & Sons, 2011, p. 576.
- [23] L. Alcatel, “The LTE Network Architecture A comprehensive tutorial.”
- [24] M. Poikselkä, H. Holma, J. Hongisto, J. Kallio, and A. Toskala, *Voice over LTE (VoLTE)*. John Wiley & Sons, 2012, p. 264.
- [25] Qualcomm and Ericsson, “Circuit-switched fallback. The first phase of voice evolution for mobile LTE devices.,” 2012.

- [26] A. EINashar, M. El-saidny, and M. Sherif, *Design, Deployment and Performance of 4G-LTE Networks: A Practical Approach*. Wiley, 2014, p. 608.
- [27] "LTE AND BEYOND | Tech-blog on LTE/4G and more.." [Online]. Available: <http://www.lteandbeyond.com/2012/01/functions-of-main-lte-packet-core.html>. [Accessed: 11-Oct-2014].
- [28] "3GPP specification: 23.401." [Online]. Available: <http://www.3gpp.org/DynaReport/23401.htm>. [Accessed: 11-Oct-2014].
- [29] T. Ali-Yahiya, *Understanding LTE and its Performance*. Springer Science & Business Media, 2011, p. 280.
- [30] "3GPP Long Term Evolution (LTE): ICIC and eICIC." [Online]. Available: <http://4g-lte-world.blogspot.pt/2012/06/icic-and-eicic.html>. [Accessed: 10-Sep-2014].
- [31] "The Block Diagram of a Basic OFDM System." [Online]. Available: <http://sna.csie.ndhu.edu.tw/~cnyang/MCCDMA/sld020.htm>. [Accessed: 11-Oct-2014].
- [32] L. L. Jie DING, Daiming QU, "A Robust Frequency Synchronization Method for Non-Contiguous OFDM-Based Cognitive Radio Systems," 2012.
- [33] 3GPP, "3GPP TR 25.892 V6.0.0," 2004.
- [34] "3GPP specification: 25.892." [Online]. Available: <http://www.3gpp.org/DynaReport/25892.htm>. [Accessed: 11-Oct-2014].
- [35] "LTE: Powerful processors and new horizons implement the next generation in communication | Renesas Electronics." [Online]. Available: http://www.renesas.com/edge_ol/technology/03/index.jsp. [Accessed: 08-Sep-2014].
- [36] T. I. Inc., "LTE in a Nutshell: The Physical Layer," 2010.
- [37] "LTE Frame Structure | Frame Subframe Type 1 & 2| Tutorial - Radio-Electronics.Com." [Online]. Available: <http://www.radio->

electronics.com/info/cellulartelecomms/lte-long-term-evolution/lte-frame-subframe-structure.php. [Accessed: 08-Sep-2014].

- [38] E. Dahlman, S. Parkvall, and J. Skold, *4G: LTE/LTE-Advanced for Mobile Broadband: LTE/LTE-Advanced for Mobile Broadband (Google eBook)*. Academic Press, 2011, p. 455.
- [39] Anritsu, "LTE Resource Guide," 2009.
- [40] M. Ozdemir and H. Arslan, *Channel estimation for wireless OFDM systems*. 2007.
- [41] Y. Li, *Pilot-symbol-aided channel estimation for OFDM in wireless systems*. 2000.
- [42] S. Rahman and D. Remein, "Wideband Channel Estimation in Upstream EPoC."
- [43] S. Ohno and E. M. M. Nakamoto, "Preamble and pilot symbol design for channel estimation in OFDM systems with null subcarriers," *EURASIP J. Wirel. Commun. Netw.*, 2011.
- [44] "Measurement Report For UE in LTE." [Online]. Available: <http://telecomyou.com/blogs/entry/Measurement-Report-For-UE-in-LTE>. [Accessed: 11-Oct-2014].
- [45] "OFDM vs OFDMA." [Online]. Available: <http://www.eefocus.com/article/08-04/40838s.html>.
- [46] S. F. B. R. Access, *LTE for UMTS - OFDMA and SC-FDMA Based Radio Access*. 2009, p. 450.
- [47] "LTE Modulation | OFDM OFDMA SC-FDMA | Radio-Electronics.com." [Online]. Available: <http://www.radio-electronics.com/info/cellulartelecomms/lte-long-term-evolution/lte-ofdm-ofdma-scdma.php>. [Accessed: 11-Oct-2014].
- [48] "New Page 1." [Online]. Available: <http://ecee.colorado.edu/~ecen4242/LTE/radio.htm>. [Accessed: 11-Oct-2014].
- [49] "File:Scfdma.jpg - Wikipedia, the free encyclopedia." [Online]. Available: <http://en.wikipedia.org/wiki/File:Scfdma.jpg>. [Accessed: 11-Oct-2014].

- [50] E. Biglieri, R. Calderbank, A. Constantinides, A. Goldsmith, A. Paulraj, and H. V. Poor, *MIMO Wireless Communications*. Cambridge University Press, 2007.
- [51] Y. Li, N. Seshadri, and S. Ariyavisitakul, *Transmitter diversity of OFDM systems with dispersive fading channels*. .
- [52] "Multipath interference." [Online]. Available: [http://mobile.ztopics.com/Multipath interference/](http://mobile.ztopics.com/Multipath%20interference/). [Accessed: 11-Oct-2014].
- [53] "Improvements to Site Selection Diversity Transmission (SSDT)," 1999.
- [54] Samsung, "Samsung S5 features," 2014. [Online]. Available: <http://www.samsung.com/global/microsite/galaxys5/features.html>.
- [55] M. France, "Extended STTD with Switching for Open Loop Transmit Diversity for more than 2 Antennas," 1999.
- [56] A. R. S. Bahai and B. R. Saltzberg, *Multi-Carrier Digital Communications: Theory and Applications of OFDM*. 1999.
- [57] "Understanding of SISO, SIMO, MISO and MIMO | telecom and telephone." [Online]. Available: <http://tele-information.com/2012/07/understanding-of-iso-simo-miso-and-mimo/>. [Accessed: 11-Oct-2014].
- [58] *Multiband Integrated Antennas for 4G Terminals*. Artech House, 2008, p. 317.
- [59] S. M. Alamouti, "A Simple Diversity Technique for Wireless Communication," 1998.
- [60] L. M. Cortes-Peña, "MIMO Space-Time Block Coding (STBC): Simulations and Results," 2009.
- [61] V. Kambale, K. Djouani, and A. Kurien, "Toward an FPGA Hardware Implementation of the Alamouti 4x2 Space-time Block Coding," 2013.
- [62] J. R. Hampton, *Introduction to MIMO Communications*, vol. 28. Cambridge University Press, 2013, p. 300.
- [63] A. Wiesel, Y. C. Eldar, and S. Shamai, *Zero forcing precoding and generalized inverses*. 2007.

- [64] "Six equalizers for V-BLAST." [Online]. Available: <http://www.dsplog.com/2009/04/21/six-equalizers-for-v-blast/>. [Accessed: 11-Oct-2014].
- [65] T. Y. Al-Naffouri, "Opportunistic Random Beamforming with Precoding for Spatially Correlated Channels."
- [66] R. Winoto, "Peak-to-Average Power Control in OFDM Systems."
- [67] H. Y. Sakran, M. Shokair, and A. A. Elazm, "An efficient technique for reducing PAPR of OFDM system in the presence of nonlinear high," *Prog. Electromagn. Res. C*, vol. 2, 2008.
- [68] R. Gross and D. Veeneman, *Clipping distortion, in DMT ADSL systems*. .
- [69] J. A. Davis and J. Jedwab, *Peak-to-mean power control in OFDM, Golay complementary sequences, and Reed-Muller codes*. .
- [70] A. D. S. Jayalath and C. Tellambura, *Use of data permutation to reduce the peak-to-average power ratio of an OFDM signal*. 2002.
- [71] B. S. Krongold and D. L. Jones, *PAR reduction in OFDM via active constellation extension*. 2003.
- [72] S. H. Muller and J. B. Huber, *OFDM with reduced peak-to-average power ratio by optimum combination of partial transmit sequences*. .
- [73] C. Yung, K. Shang, C. Kuan, and C. Mao, *Turbo coded OFDM for reducing PAPR and error rates*. .
- [74] "Gaussian Distribution." [Online]. Available: <http://hyperphysics.phy-astr.gsu.edu/hbase/math/gaufcn.html>. [Accessed: 11-Oct-2014].
- [75] "Rayleigh Distribution." [Online]. Available: <http://www.math.wm.edu/~leemis/chart/UDR/PDFs/Rayleigh.pdf>.
- [76] K. K. Saluja, "Linear Feedback Shift Registers Theory and Applications," Wisconsin-Madison, 1991.

Annex

Annex A

```
function ofdm_alamouti_variasantenas2122

clear;
close all;
clc;

N_bits=768;      % Numero de simbolos a criar
N_simbolos=10000;
m=4; % modulaçao QPSK
SampFreq=15.36e6;

pdp=[0 -1; 50 -1; 120 -1; 200 0; 230 0; 500 0; 1600 -3; 2300 -5; 5000 -
7];

Ebn0=0:2:20;

var=(1*(10.^(-Ebn0/10)))/(log2(m));

for n=1:length(Ebn0)
    for p=1:N_simbolos

        % ***** Modulador (OFDM (tempo e frequencia)) *****
        data=data_gen(2*N_bits);          % gera 2*N_bits simbolos 0 ou 1
        com igual probabilidade

        data_symbol=mod_data(data, m); % 768 simbolos

        % ***** Space-frequency coding *****
        ant1_n = zeros(1,768);

        ant1_n(1:2:768) = data_symbol(1:2:end);
        ant2_n(1:2:768) = data_symbol(2:2:end);
        ant1_n(2:2:768) = -conj(data_symbol(2:2:end));
        ant2_n(2:2:768) = conj(data_symbol(1:2:end));

        ant1_n = ant1_n./sqrt(2);
        ant2_n = ant2_n./sqrt(2);

        % ***** Calculo do ERRO (OFDM) *****

        ngauss_freq=(sqrt(var(n)/2))*(randn(1,length(data_symbol))+(1j*randn(1,length(data_symbol)))); % erro na frequencia

        ngauss_freq2=(sqrt(var(n)/2))*(randn(1,length(data_symbol))+(1j*randn(1,length(data_symbol)))); % erro na frequencia
    end
end
```

```

% ***** CANAL (OFDM) *****
[ht11, h11]=channel_gen(pdp,SampFreq, 1024);
[ht21, h21]=channel_gen(pdp,SampFreq, 1024);
[ht12, h12]=channel_gen(pdp,SampFreq, 1024);
[ht22, h22]=channel_gen(pdp,SampFreq, 1024);

[ht2, HF]=channel_gen(pdp,SampFreq, 1024);

h11 = h11(129:896);
h21 = h21(129:896);
h12 = h12(129:896);
h22 = h22(129:896);
HF = HF(129:896);

DATA_canal_OFDM_freq=ant1_n.*h11; % OFDM
com canal, mas na frequencia
DATA_canal_OFDM_freq2=ant2_n.*h21;
DATA_canal_OFDM_freq12=ant1_n.*h12; %
OFDM com canal, mas na frequencia
DATA_canal_OFDM_freq22=ant2_n.*h22;
DATA_canal_OFDM_freq3=data_symbol.*HF;

% ***** Ruido (OFDM) *****

DATA_OFDM_canalRuido_freq3=DATA_canal_OFDM_freq3+ngauss_freq;
% OFDM com ruido e canal, mas na frequencia

% ***** Equalizador (OFDM) *****

g2=conj(HF)./((abs(HF)).^2); % equalizador 768 simbolos

data_OFDM_canalRuido_freq_equal=g2.*DATA_OFDM_canalRuido_freq3;
% OFDM com erro e canal multipercurso (na frequencia)

% ***** Recepcao na antena *****

yn = DATA_canal_OFDM_freq + DATA_canal_OFDM_freq2 +ngauss_freq;
yn2 = DATA_canal_OFDM_freq12 + DATA_canal_OFDM_freq22
+ngauss_freq2;

% ***** Space-frequency Decoding *****
sn = zeros(1,768);
sn2 = zeros(1,768);

sn(1:2:end) = (1/sqrt(2)).* (conj(h11(2:2:end)).* yn(1:2:end)) +
(1/sqrt(2)).* (h21(1:2:end).*conj(yn(2:2:end)));
sn(2:2:end) = (1/sqrt(2)).* (conj(h21(2:2:end)).* yn(1:2:end)) -
(1/sqrt(2)).* (h11(1:2:end).*conj(yn(2:2:end)));
sn2(1:2:end) = (1/sqrt(2)).* (conj(h12(2:2:end)).* yn2(1:2:end))
+ (1/sqrt(2)).* (h22(1:2:end).*conj(yn2(2:2:end)));

```



```

        sn2(2:2:end) = (1/sqrt(2)).* (conj(h22(2:2:end)).* yn2(1:2:end))
- (1/sqrt(2)).*(h12(1:2:end).*conj(yn2(2:2:end)));

        sntotal = sn+sn2;

        % ***** Desmodulador (OFDM) *****

        decoded_data_OFDM_canalRuido_freq=demod_data(sn, m, 2*N_bits); %
OFDM com erro e canal multipercurso (na frequencia)
        decoded_data_OFDM_canalRuido_freq2=demod_data(sntotal, m,
2*N_bits);

        decoded_data_OFDM_canalRuido_freq3=demod_data(data_OFDM_canalRuido_freq_e
qual, m, 2*N_bits); % OFDM com erro e canal multipercurso (na frequencia)

        % ***** BER *****

        Cop_BER_OFDM_canalRuido_freq
=(sum(data~=decoded_data_OFDM_canalRuido_freq)/length(data)); % OFDM com
erro e canal multipercurso (na frequencia)
        Cop_BER_OFDM_canalRuido_freq2
=(sum(data~=decoded_data_OFDM_canalRuido_freq2)/length(data));
        Cop_BER_OFDM_canalRuido_freq3
=(sum(data~=decoded_data_OFDM_canalRuido_freq3)/length(data)); % OFDM com
erro e canal multipercurso (na frequencia)

        BER_OFDM4(p)=Cop_BER_OFDM_canalRuido_freq; % OFDM com
erro e canal multipercurso (na frequencia)
        BER_OFDM5(p)=Cop_BER_OFDM_canalRuido_freq2;
        BER_OFDM6(p)=Cop_BER_OFDM_canalRuido_freq3;

        end

        BER4(n)=mean(BER_OFDM4); % OFDM com erro e canal multipercurso
(na frequencia)
        BER5(n)=mean(BER_OFDM5);
        BER6(n)=mean(BER_OFDM6);

        end

        figure(1)
        semilogy(Ebn0,BER4,'o-',Ebn0,BER5,'+-r', Ebn0,BER6,'s-g')
        xlabel('Eb/n0 (dB)');
        ylabel('BER');
        hold on

        % ***** AWGN *****
        SNR = 0:2:10;
        SNR_L = 10.^(SNR./10);
        Pavg = qfunc(sqrt(2*SNR_L));
        semilogy(SNR,Pavg,'x-k');

```

```

legend('2x1 Alamouti','2x2 Alamouti','SISO','AWGN')
axis([0 20 10E-6 0.2])

end

%% ***** Funções Auxiliares *****

function array = data_gen (n_bits)
% cria n_bits (0 ou 1) com a mesma probabilidade
array=randi([0,1],1,n_bits);

end

function data_symbol=mod_data(data, m)
% Data Modulation
%BPSK, m=2
%QPSK, m=4,
%16-QAM, m=16

switch m
case 2
    data_symbol = -data*2+1; %mapping of 1->-1 and 0->1

case 4
    % Coding of data bits in QPSK symbols - using Grey coding
    % (00->1+i; 01->1-i; 10->-1+i; 11->-1-i)
    % bit MS defines real polarity
    % bit LS defines imag polarity
    data_temp = reshape(data,2,length(data)/2);
    data_real = data_temp(1,:);
    data_imag = data_temp(2,:);
    data_symbol = sqrt(2)/2*((-1).^(data_real)+i*(-1).^(data_imag));

case 16
    data_temp = reshape(data,4,length(data)/4);
    data_r1 = data_temp(1,:);
    data_i1 = data_temp(2,:);
    data_r2 = data_temp(3,:);
    data_i2 = data_temp(4,:);
    data_symbol = 2/sqrt(10).*(0.5*(-1).^(data_r2).*(-
1).^(data_r1)+(-1).^( data_r1)+i.*(0.5*(-1).^(data_i2).*(-1).^(data_i1)+
(-1).^(data_i1)));
    otherwise
        helpdlg('Constellation size (m) not available');
end
end

function decoded_data=demod_data(data_symbol, m, N_Data)

vect_IMAG = imag(data_symbol);
vect_REAL = real(data_symbol);
coder_type_value=0;
switch m

```

```

    case 2
        if (coder_type_value==0)
            %hard decision
            decoded_data= ceil(-
vect_REAL./(1.00000000000001.*max(abs(vect_REAL))));

        else
            %soft decision
            decoded_data = vect_REAL;
        end

    case 4
        % Decoding of data bits in QPSK symbols - using Grey coding
        % (1+i->00; 1-i->01; -1+i->10; -1-i->11)
        % real polarity defines bit MS
        % imag polarity defines bit LS
        if (coder_type_value==0)
            %hard decision
            vect_REAL_1 = ceil(-
vect_REAL./(1.00000000000001.*max(abs(vect_REAL))));
            vect_IMAG_1 = ceil(-
vect_IMAG./(1.00000000000001.*max(abs(vect_IMAG))));
            decoded_data = reshape([vect_REAL_1; vect_IMAG_1],1,N_Data);
        else
            %soft decision
            decoded_data = reshape([vect_REAL; vect_IMAG],1,N_Data);
        end
    case 16
        P_1= vect_REAL;
        P_2= vect_IMAG;
        P_3= abs(vect_REAL)-2/sqrt(10);
        P_4= abs(vect_IMAG)-2/sqrt(10);
        if (coder_type_value==0)
            %hard decision
            vect_IMAG_1 = ceil(-P_2./(1.00000000000001.*max(abs(P_2))));
            vect_IMAG_2 = ceil(-P_4./(1.00000000000001.*max(abs(P_4))));
            vect_REAL_1 = ceil(-P_1./(1.00000000000001.*max(abs(P_1))));
            vect_REAL_2 = ceil(-P_3./(1.00000000000001.*max(abs(P_3))));
            decoded_data = reshape([vect_REAL_1; vect_IMAG_1;
vect_REAL_2; vect_IMAG_2],1,N_Data);
        else
            %soft decision
            decoded_data = reshape([P_1; P_2; P_3; P_4],1,N_Data);
        end
    end

    otherwise
        helpdlg('Constellation size (m) not available');
end
end

function [ht, Hf]=channel_gen(pdp,samp_freq, Nc)

delta_t=1/samp_freq; %sample duration
Npaths = length(pdp(:,1)); % No. of paths considered for the
channel
deltans=delta_t/1e-9; % Sampling interval in ns

path_pot_lin=10.^(pdp(:,2)/10);

```

```

path_pot_lin=path_pot_lin./sum(path_pot_lin);

delays = pdp(:,1);
delays = round(delays./(deltans))+1;

multipath = zeros(1,Npaths);

for n=1:Npaths
    pot_componente=0.5;

multipath(n)=sqrt(pot_componente)*randn(1,1)+j*sqrt(pot_componente)*randn
(1,1);
    multipath(n)=multipath(n).*sqrt(path_pot_lin(n));

end

RI=zeros(1,Nc);
RI(delays) = RI(delays) + multipath;

ht=RI;
Hf=fft(ht);
end

function y=conv_s_h(s,h,pdp,Nc,samp_freq,tg)
%tg=5.21e-6; % guerad time -> 80 samples

delays=pdp(:,1);
delta_t=1/samp_freq;
Npaths = length(delays); % No. of paths considered
for the channel
deltans=delta_t/1e-9; % Sampling interval in ns

delays = round(delays/(deltans))+1;
Ng= round(tg/(delta_t))+1;
f_zeros=find(h==0);
h(f_zeros)=[];

aux = zeros(Npaths,Nc+Ng);

for n=1:Npaths

    conv_sh=h(n)*s;

    aux(n,delays(n):Nc+Ng-1+delays(n)-1)=conv_sh;

end

y=sum(aux);
y=y(1:Nc+Ng-1);

end

```

Annex B

```
function precodersZFMMSE

clear;
close all;
clc;

N_bits=128;      % Numero de simbolos a criar
N_simbolos=10000;
m=4; % modulaçao QPSK
SampFreq=15.36e6;

pdp=[0 -1; 50 -1; 120 -1; 200 0; 230 0; 500 0; 1600 -3; 2300 -5; 5000 -
7];

%Eb/n0
Ebn0=0:4:28;

%Variância
var=(1*(10.^(-Ebn0/10)))/(log2(m));

for n=1:length(Ebn0)
    for p=1:N_simbolos

        % ***** Modulador (OFDM (tempo e frequencia)) *****
        %data=zeros(128*2,1);
        %SISO
        datasiso = data_gen(2*N_bits);
        data_symbolsiso = mod_data(datasiso,m);

        %MIMO
        data(:,1)=data_gen(2*N_bits);          % gera 2*N_bits simbolos 0
ou 1 com igual probabilidade
        data(:,2)=data_gen(2*N_bits);          %n . utilizador 2
        data_symbol=mod_data(data(:,1), m);    % 128 simbolos
        data_symbol2=mod_data(data(:,2), m);    % 128 simbolos

        % ***** Calculo do ERRO (OFDM) *****
        %SISO

        ngauss_freqsiso=(sqrt(var(n)/2))*(randn(1,length(data_symbolsiso))+(1j*randn(1,length(data_symbolsiso)))); % erro na frequencia

        %MIMO

        ngauss_freq(1,:)=(sqrt(var(n)/2))*(randn(1,length(data_symbol))+(1j*randn(1,length(data_symbol)))); % erro na frequencia

        ngauss_freq(2,:)=(sqrt(var(n)/2))*(randn(1,length(data_symbol2))+(1j*randn(1,length(data_symbol2)))); % erro na frequencia

        %SISO
```

```

[ht2, Hf2]=channel_gen(pdp,SampFreq, 128);           % canal para
128
DATA_canal_OFDM_freq=data_symbolsiso.*Hf2;           % OFDM
com canal, mas na frequencia
DATA_OFDM_canalRuido_freq=DATA_canal_OFDM_freq+ngauss_freqsiso;
% OFDM com ruido e canal, mas na frequencia

%SISO- Equalizador OFDM
g=conj(Hf2)./((abs(Hf2)).^2);           % equalizador 128 simbolos
%recepcao na antena
data_OFDM_canalRuido_freq_equal=g.* DATA_OFDM_canalRuido_freq;
% OFDM com erro e canal multipercurso

%MIMO
% ***** CANAL (OFDM) *****
%h11 -> canal de comunicação utilizador 1
[ht11, h11]=channel_gen(pdp,SampFreq, 128);
%h21 -> canal de comunicação utilizador 1
[ht21, h21]=channel_gen(pdp,SampFreq, 128);
%h12 -> canal de comunicação utilizador 2
[ht12, h12]=channel_gen(pdp,SampFreq, 128);
%h22 -> canal de comunicação utilizador 2
[ht22, h22]=channel_gen(pdp,SampFreq, 128);

%MIMO
W=zeros(2,2,128);
W1=zeros(2,2,128);
alfa=zeros(2,2,128);

% 128 * 2 antenas
for i=1:128
    H1 = [h11(i) h21(i); h12(i) h22(i)];

    %Zero-forcing
    %W1 -> matriz precoding zf
    W1(:, :, i)=H1'*(H1*H1')^-1;
    alfa_zf=sqrt(2/trace((W1(:, :, i)*W1(:, :, i)'))); %2 é o numero
de utilizadores
    %Wfinal = alfa*W1
    W_zf(:, :, i) = alfa_zf* W1(:, :, i);

    %MMSE
    %W2 -> matriz precoding mmse
    W2(:, :, i) = H1'*(H1*H1' + eye(2,2).*var(n))^-1;
    alfa_mmse=sqrt(2/trace((W2(:, :, i)*W2(:, :, i)'))); %2 é o
numero de utilizadores
    W_mmse(:, :, i) = alfa_mmse* W2(:, :, i);

end

% ***** Recepcao naS antenaS *****
for nx=1:128

```

```

H=[h11(nx) h21(nx) ;h12(nx) h22(nx)];

%Zero-forcing
zf=H*W_zf(:, :, nx)*[data_symbol(nx);data_symbol2(nx)] +
[ngauss_freq(1, nx) ;ngauss_freq(2, nx)] ;

yzf1(nx, 1)=zf(1, :);
yzf2(nx, 1)=zf(2, :);

%mmse
mmse = H*W_mmse(:, :, nx)*[data_symbol(nx);data_symbol2(nx)] +
[ngauss_freq(1, nx) ;ngauss_freq(2, nx)] ;
ymmse1(nx, 1)=mmse(1, :);
ymmse2(nx, 1)=mmse(2, :);
end

% ***** Desmodulador (OFDM) *****

%SISO
decoded_data_OFDM_canalRuido_freq=demod_data(data_OFDM_canalRuido_freq_eq
ual, m, 2*N_bits); % OFDM com erro e canal multipercurso (na frequencia)

%MIMO-ZF
decoded_data_canalRuido_freqZF=demod_data(yzf1.', m, 2*N_bits); %
OFDM com erro e canal multipercurso (na frequencia)
decoded_data_canalRuido_freqZF2=demod_data(yzf2.', m, 2*N_bits);

%MIMO-MMSE
decoded_data_canalRuido_freqmmse=demod_data(ymmse1.', m,
2*N_bits); % OFDM com erro e canal multipercurso (na frequencia)
decoded_data_canalRuido_freqmmse2=demod_data(ymmse2.', m,
2*N_bits);

% ***** BER *****
%SISO
Cop_BER_OFDM_canalRuido_freq
=(sum(datasiso~=decoded_data_OFDM_canalRuido_freq)/length(datasiso)); %
OFDM com erro e canal multipercurso (na frequencia)

%MIMO
Cop_BER_canalRuido_freq
=(sum(data(:, 1).~=decoded_data_canalRuido_freqZF)/length(data(:, 1).));
% OFDM com erro e canal multipercurso (na frequencia)
Cop_BER_canalRuido_freq2
=(sum(data(:, 2).~=decoded_data_canalRuido_freqZF2)/length(data(:, 2).));
% - Cop_BER_OFDM_canalRuido_freq3
=(sum(data~=decoded_data_OFDM_canalRuido_freq3)/length(data)); % OFDM com
erro e canal multipercurso (na frequencia)
Cop_BER_canalRuido_freq3
=(sum(data(:, 1).~=decoded_data_canalRuido_freqmmse)/length(data(:, 1).))
; % OFDM com erro e canal multipercurso (na frequencia)
Cop_BER_canalRuido_freq4
=(sum(data(:, 2).~=decoded_data_canalRuido_freqmmse2)/length(data(:, 2).)
);

```

```

BER_SISO3(p)=Cop_BER_OFDM_canalRuido_freq;

BER_MIMO4(p)=(Cop_BER_canalRuido_freq+Cop_BER_canalRuido_freq2)/2;
% OFDM com erro e canal multipercurso (na frequencia)
% BER_MIMO5(p)=Cop_BER_canalRuido_freq2;

BER_MIMO6(p)=(Cop_BER_canalRuido_freq3+Cop_BER_canalRuido_freq4)/2;
% BER_MIMO7(p)=Cop_BER_canalRuido_freq4;

    ['teste: BER_OFDM_SISO= ' , num2str(BER_SISO3(p),5), '
Received Bits= ', num2str(p), ' Stop: Ctrl+c ']
    % ['teste: BER_zf= ' , num2str(BER_MIMO4(p),5), ' Received
Bits= ', num2str(p), ' Stop: Ctrl+c ']
    % ['teste: BER_mmse= ' , num2str(BER_MIMO6(p),5), ' Received
Bits= ', num2str(p), ' Stop: Ctrl+c ']

end

BER3(n)=mean(BER_SISO3); % OFDM com erro e canal multipercurso
(na frequencia)

BER4(n)=mean(BER_MIMO4);
% BER5(n)=mean(BER_MIMO5);
BER6(n)=mean(BER_MIMO6);
% BER7(n)=mean(BER_MIMO7);
end

figure(1)
semilogy(Ebn0,BER3,'xr-',Ebn0,BER4,'o-',Ebn0,BER6,'+-g')
grid on
xlabel('Eb/n0 (dB)');
ylabel('BER');
legend('SISO-OFDM','MIMO-ZeroF','MIMO-MMSE')
% hold on

end

%% ***** Funções Auxiliares *****

function array = data_gen (n_bits)
% cria n_bits (0 ou 1) com a mesma probabilidade
array=randi([0,1],1,n_bits);

end

function data_symbol=mod_data(data, m)
% Data Modulation
%BPSK, m=2
%QPSK, m=4,
%16-QAM, m=16

switch m

```



```

case 2
    data_symbol = -data*2+1; %mapping of 1->-1 and 0->1

case 4
    % Coding of data bits in QPSK symbols - using Grey coding
    % (00->1+i; 01->1-i; 10->-1+i; 11->-1-i)
    % bit MS defines real polarity
    % bit LS defines imag polarity
    data_temp = reshape(data,2,length(data)/2);
    data_real = data_temp(1,:);
    data_imag = data_temp(2,:);
    data_symbol = sqrt(2)/2*((-1).^(data_real)+i*(-1).^(data_imag));

case 16
    data_temp = reshape(data,4,length(data)/4);
    data_r1 = data_temp(1,:);
    data_i1 = data_temp(2,:);
    data_r2 = data_temp(3,:);
    data_i2 = data_temp(4,:);
    data_symbol = 2/sqrt(10).*(0.5*(-1).^(data_r2).*(-
1).^(data_r1)+(-1).^( data_r1)+i.*(0.5*(-1).^(data_i2).*(-1).^(data_i1)+
(-1).^(data_i1)));
    otherwise
        helpdlg('Constellation size (m) not available');
end
end

function decoded_data=demod_data(data_symbol, m, N_Data)

vect_IMAG = imag(data_symbol);
vect_REAL = real(data_symbol);
coder_type_value=0;
switch m
    case 2
        if (coder_type_value==0)
            %hard decision
            decoded_data= ceil(-
vect_REAL./(1.00000000000001.*max(abs(vect_REAL))));

        else
            %soft decision
            decoded_data = vect_REAL;
        end

    case 4
        % Decoding of data bits in QPSK symbols - using Grey coding
        % (1+i->00; 1-i->01; -1+i->10; -1-i->11)
        % real polarity defines bit MS
        % imag polarity defines bit LS
        if (coder_type_value==0)
            %hard decision
            vect_REAL_1 = ceil(-
vect_REAL./(1.00000000000001.*max(abs(vect_REAL))));
            vect_IMAG_1 = ceil(-
vect_IMAG./(1.00000000000001.*max(abs(vect_IMAG))));
            decoded_data = reshape([vect_REAL_1; vect_IMAG_1],1,N_Data);
        else
            %soft decision

```

```

        decoded_data = reshape([vect_REAL; vect_IMAG],1,N_Data);
    end
    case 16
        P_1= vect_REAL;
        P_2= vect_IMAG;
        P_3= abs(vect_REAL)-2/sqrt(10);
        P_4= abs(vect_IMAG)-2/sqrt(10);
        if (coder_type_value==0)
            %hard decision
            vect_IMAG_1 = ceil(-P_2./(1.000000000000001.*max(abs(P_2))));
            vect_IMAG_2 = ceil(-P_4./(1.000000000000001.*max(abs(P_4))));
            vect_REAL_1 = ceil(-P_1./(1.000000000000001.*max(abs(P_1))));
            vect_REAL_2 = ceil(-P_3./(1.000000000000001.*max(abs(P_3))));
            decoded_data = reshape([vect_REAL_1; vect_IMAG_1;
vect_REAL_2; vect_IMAG_2],1,N_Data);
        else
            %soft decision
            decoded_data = reshape([P_1; P_2; P_3; P_4],1,N_Data);
        end

    otherwise
        helpdlg('Constellation size (m) not available');
    end
end

function [ht, Hf]=channel_gen(pdp,samp_freq, Nc)

delta_t=1/samp_freq; %sample duration
Npaths = length(pdp(:,1)); % No. of paths considered for the
channel
deltans=delta_t/1e-9; % Sampling interval in ns

path_pot_lin=10.^(pdp(:,2)/10);
path_pot_lin=path_pot_lin./sum(path_pot_lin);

delays = pdp(:,1);
delays = round(delays./(deltans))+1;

multipath = zeros(1,Npaths);

for n=1:Npaths
    pot_componente=0.5;

    multipath(n)=sqrt(pot_componente)*randn(1,1)+j*sqrt(pot_componente)*randn
(1,1);
    multipath(n)=multipath(n).*sqrt(path_pot_lin(n));

end

RI=zeros(1,Nc);
RI(delays) = RI(delays) + multipath;

ht=RI;
Hf=fft(ht);
end

function y=conv_s_h(s,h,pdp,Nc,samp_freq,tg)

```

```

%tg=5.21e-6; % guard time -> 80 samples

delays=pdp(:,1);
delta_t=1/samp_freq;
Npaths = length(delays); % No. of paths considered
for the channel
deltans=delta_t/1e-9; % Sampling interval in ns

delays = round(delays/(deltans))+1;
Ng= round(tg/(delta_t))+1;
f_zeros=find(h==0);
h(f_zeros)=[];

aux = zeros(Npaths,Nc+Ng);

for n=1:Npaths

    conv_sh=h(n)*s;

    aux(n,delays(n):Nc+Ng-1+delays(n)-1)=conv_sh;

end

y=sum(aux);
y=y(1:Nc+Ng-1);

end

```

Annex C

```

function SF_Processing(block)
% Implements the Space-Time block coding for 2 transmitting antennas
% according to the scheme proposed by Alamouti. Does not code the pilot
% subcarriers.
% Input parameters:
% Nc - no. of subcarriers
% Frame_Length - no. of OFDM symbols in the frame
% Inputs:
% InputPort(1) - OFDM frame to be coded
% Outputs:
% OutputPort(1) - Coded frame to be transmitted by antenna 1
% OutputPort(2) - Coded frame to be transmitted by antenna 2

setup(block);

%endfunction

%Put auxiliar functions in here
%-----
%function N_Data_Carriers = Data_Dim(block)

```

```

% Calculation of number of data sub-carriers in the OFDM frame
%NcAv = block.DialogPrm(1).Data;
%Frame_Length = block.DialogPrm(2).Data;
%
%
%N_Data_Carriers = NcAv*Frame_Length; % Total number of data carrying
subcarriers in a OFDM frame

%endfunction
%-----

function setup(block)

% Calculation of data sub-carriers position on the OFDM frame
NcAv = block.DialogPrm(1).Data;
Frame_Length = block.DialogPrm(2).Data;
%NT = block.DialogPrm(3).Data;
k_users = block.DialogPrm(4).Data;
N_Data_Carriers = NcAv*Frame_Length; % Total number of data carrying
subcarriers in a OFDM frame

% Register sample times
% [0 offset]           : Continuous sample time
% [positive_num offset] : Discrete sample time
% [-1, 0]             : Port-based sample time
% [-2, 0]             : Variable sample time
block.SampleTimes = [-1 0];

%% Register parameters
block.NumDialogPrms = 14;
%NcAv,Frame_Length,NT,k,Matrix_H,Matrix_H_2,Matrix_H_3,Matrix_H_4,Matrix_
H_5,Matrix_H_6,Matrix_H_7,Matrix_H_8,power, EbN0

%% Register number of ports
block.NumInputPorts = 2;
block.NumOutputPorts = 2;

block.SetPreCompOutPortInfoToDynamic;
block.SetPreCompInpPortInfoToDynamic;

% Setup InputPort properties
block.InputPort(1).DirectFeedthrough = true;

block.InputPort(1).DatatypeID = 0; % double
block.InputPort(1).Complexity = 'Complex';
block.InputPort(1).SamplingMode = 1; % frame
block.InputPort(1).Dimensions = [k_users*N_Data_Carriers , 1];

block.InputPort(2).DirectFeedthrough = true;

block.InputPort(2).DatatypeID = 0; % double
block.InputPort(2).Complexity = 'Complex';
block.InputPort(2).SamplingMode = 1; % frame

```

```

block.InputPort(2).Dimensions = [k_users*N_Data_Carriers , 1];
% Setup OutputPort properties
block.OutputPort(1).DatatypeID = 0; % double
block.OutputPort(1).Complexity = 'Complex';
block.OutputPort(1).SamplingMode = 1; % frame
block.OutputPort(1).Dimensions = [k_users*N_Data_Carriers , 1];

block.OutputPort(2).DatatypeID = 0; % double
block.OutputPort(2).Complexity = 'Complex';
block.OutputPort(2).SamplingMode = 1; % frame
block.OutputPort(2).Dimensions = [k_users*N_Data_Carriers, 1];

%% Register methods
block.RegBlockMethod('Outputs', @Output);

%endfunction

function Output(block)

% Calculation of data sub-carriers position on the OFDM frame
NcAv = block.DialogPrm(1).Data;
Frame_Length = block.DialogPrm(2).Data;
NT = block.DialogPrm(3).Data;
N_Data_Carriers = NcAv*Frame_Length; % Total number of data carrying
subcarriers in a OFDM frame
Ntb=2; %antennas per basestation;
EbN0=block.DialogPrm(14).Data;
power=block.DialogPrm(13).Data;
k_users = block.DialogPrm(4).Data;
Pt=1;

H111 = evalin('base', block.DialogPrm(5).Data);
H121 = evalin('base', block.DialogPrm(6).Data);
H112 = evalin('base', block.DialogPrm(7).Data);
H122 = evalin('base', block.DialogPrm(8).Data);
H211 = evalin('base', block.DialogPrm(9).Data);
H221 = evalin('base', block.DialogPrm(10).Data);
H212 = evalin('base', block.DialogPrm(11).Data);
H222 = evalin('base', block.DialogPrm(12).Data);

noise_variance = Pt.*10.^(-EbN0./10);
dt_out1=zeros(128,12);
dt_out2=zeros(128,12);

data_in=block.InputPort(1).Data; % Vector in
data_frame1=reshape(data_in,128,12);
data_in2=block.InputPort(2).Data; % Vector out
data_frame2=reshape(data_in2,128,12);

ww11=zeros(12,128);
ww22=zeros(12,128);

a_bs1=zeros(12,128);

```

```

a_bs2=zeros(12,128);

switch power

    case 1
        %zero forcing
        Wnc=zeros(2,2,128,12);

        for c=1:12
            p=0;
            for n=1:128
                %user1;
                ni=(n-1)*8 + 1;

                %BS1
                h11=H111(ni,c);
                h12=H112(ni,c);

                %BS2;

                h21=H121(ni,c);
                h22=H122(ni,c);

                %Zero-forcing
                Ht=[h11.' h21.'; h12.' h22.']; % Ht Matrix

                W1=Ht'*(Ht*Ht')^-1;
                Wnc(:,:,n,c) = W1;
                alfa_zf=sqrt(2/trace((Wnc(:,:,n,c)*Wnc(:,:,n,c)'))); %2 é o
numero de utilizadores?
                W_zf(:,:,n,c) = alfa_zf* Wnc(:,:,n,c);
                z1=W_zf(:,:,n,c)*[data_frame1(n,c);data_frame2(n,c)];
                %antes :
                z1=Ht*W_zf(:,:,n,c)*[data_frame1(n,c);data_frame2(n,c)];
                %
                %           Ht=[h11.' h21.'; h12.' h22.']; % Ht Matrix
                %
                %           Wt=Ht'*(Ht*Ht')^-1;
                %           Wnc(:,:,n,c)=Wt;
                %
                %           z1=Wnc(:,:,n,c)*[data_frame1(n,c);data_frame2(n,c)];
                %

                dt_out1(n,c)=z1(1,:);
                dt_out2(n,c)=z1(2,:);

            end

        end

    case 2
        %MMSE
        Wnc=zeros(2,2,128,12);

```

```

for c=1:12
    p=0;
    for n=1:128
        %user1;

        ni=(n-1)*8 + 1;

        %BS1
        h11=H111(ni,c);
        h12=H112(ni,c);

        %BS2;

        h21=H121(ni,c);
        h22=H122(ni,c);

        Ht=[h11.' h21.'; h12.' h22.']; % Ht Matrix
        Id = eye(2);
        W2(:, :, n, c) = Ht'*(Ht*Ht' + Id*noise_variance)^-1;
        alfa_mmse=sqrt(2/trace((W2(:, :, n, c)*W2(:, :, n, c)'))); %2 é o
numero de utilizadores?
        W_mmse(:, :, n, c) = alfa_mmse* W2(:, :, n, c);

        z1 = W_mmse(:, :, n, c)*[data_frame1(n,c);data_frame2(n,c)] ;
        %antes: z1 = Ht*W_mmse(:, :, n, c)*[data_frame1(n,c);data_frame2(n,c)]
;

        % Ht=[h11.' h21.'; h12.' h22.']; % Ht Matrix
        % Id=eye(2);
        % Wt=Ht'*(Ht*Ht'+ Id*noise_variance)^-1;
        % Wnc(:, :, n, c)=Wt;
        %
        % z1=Wnc(:, :, n, c)*[data_frame1(n,c);data_frame2(n,c)];
        %

        dt_out1(n,c)=z1(1, :);
        dt_out2(n,c)=z1(2, :);

    end

end

vsinrflag=0;
centflag=1;
assignin('base', 'vsinrflag', vsinrflag);
assignin('base', 'centflag', centflag);
end

data_out1=reshape(dt_out1,1536,1);
data_out2=reshape(dt_out2,1536,1);

block.OutputPort(1).Data=data_out1;
block.OutputPort(2).Data=data_out2;

```

Annex D

```
clear all
clc
load('valores_original.mat')
load('valores_lsfr.mat')

rms_x = sqrt(mean(papr_1_i_original.signals.values(32323:33602).^2));
peak = max(papr_1_i_original.signals.values(32323:33602).^2);
PAPR_original1_i = abs(peak) / rms_x;
paproriginal1_i_db =
10*log10(max(abs(papr_1_i_original.signals.values).^2) /
mean(abs(papr_1_i_original.signals.values).^2));
m = 0;
for i = 1 : length(papr_2_i_original.signals.values)

    if papr_2_i_original.signals.values(i) ==
papr_2_i.signals.values(i)

        else
            i;

                m=m+1;
        end

end

for i = 1 : length(papr_2_q_original.signals.values)

    if papr_2_q_original.signals.values(i) ==
papr_2_q.signals.values(i)

        else
            i;
            break
            m=m+1;
        end

end

%%32323:33602

%2q 247476:252866
rms_x = sqrt(mean(papr_1_i.signals.values(32323:33602).^2));
peak = max(papr_1_i.signals.values(32323:33602).^2);
PAPR_novo1_i = abs(peak) / rms_x;
papr_novo1_i_db = 10*log10(max(abs(papr_1_i.signals.values).^2) /
mean(abs(papr_1_i.signals.values).^2));

rms_x = sqrt(mean(papr_1_q_original.signals.values(32323:33602).^2));
peak = max(papr_1_q_original.signals.values(32323:33602).^2);
PAPR_original1_q = abs(peak) / rms_x;
```



```

%paproriginal1_q_db =
10*log10(max(abs(papr_1_q_original.signals.values.^2) /
mean(abs(papr_1_q_original.signals.values).^2)));

rms_x = sqrt(mean(papr_1_q.signals.values(32323:33602).^2));
peak = max(papr_1_q.signals.values(32323:33602).^2);
PAPR_novo1_q = abs(peak) / rms_x;
papr_novo1_q_db =
10*log10(max(abs(papr_1_q.signals.values(32323:33602)).^2) /
mean(abs(papr_1_q.signals.values(32323:33602)).^2)));

fprintf('PAPR Antena 1:\nInphase original: %f\n',PAPR_original1_i)
fprintf('Inphase com lsfr: %f\n',PAPR_novo1_i)
fprintf('Diferença para melhor (PAPR menor): %f \n \n', PAPR_original1_i-
PAPR_novo1_i)

fprintf('Quadrature original: %f\n',PAPR_original1_q)
fprintf('Quadrature com lsfr: %f\n',PAPR_novo1_q)
fprintf('Diferença para melhor (PAPR menor): %f \n \n', PAPR_original1_q-
PAPR_novo1_q)
%antena2%%

rms_x = sqrt(mean(papr_2_i_original.signals.values(247476:252866).^2));
peak = max(papr_2_i_original.signals.values(247476:252866).^2);
PAPR_original2_i = abs(peak) / rms_x;
papr_original2_i_db =
10*log10(max(abs(papr_2_i_original.signals.values(247476:252866)).^2) /
mean(abs(papr_2_i_original.signals.values(247476:252866)).^2)));

rms_x = sqrt(mean(papr_2_i.signals.values(247476:252866).^2));
peak = max(papr_2_i.signals.values(247476:252866).^2);
PAPR_novo2_i = abs(peak) / rms_x;
papr_novo2_i_db =
10*log10(max(abs(papr_2_i.signals.values(247476:252866)).^2) /
mean(abs(papr_2_i.signals.values(247476:252866)).^2)));

rms_x = sqrt(mean(papr_2_q_original.signals.values(247476:252866).^2));
peak = max(papr_2_q_original.signals.values(247476:252866).^2);
PAPR_original2_q = abs(peak) / rms_x;
papr_original2_q_db =
10*log10(max(abs(papr_2_q_original.signals.values(247476:252866)).^2) /
mean(abs(papr_2_q_original.signals.values(247476:252866)).^2)));

rms_x = sqrt(mean(papr_2_q.signals.values(247476:252866).^2));
peak = max(papr_2_q.signals.values(247476:252866).^2);
PAPR_novo2_q = abs(peak) / rms_x;
papr_novo2_q_db =
10*log10(max(abs(papr_2_q.signals.values(247476:252866)).^2) /
mean(abs(papr_2_q.signals.values(247476:252866)).^2)));

fprintf('PAPR Antena 2:\nInphase original: %f\n',PAPR_original2_i)
fprintf('Inphase com lsfr: %f\n',PAPR_novo2_i)
fprintf('Diferença para melhor (PAPR menor): %f \n \n', PAPR_original2_i-
PAPR_novo2_i)

```

```
fprintf('Quadrature original: %f\n',PAPR_original2_q)
fprintf('Quadrature com lsfr: %f\n',PAPR_novo2_q)
fprintf('Diferença para melhor (PAPR menor): %f \n \n', PAPR_original2_q-
PAPR_novo2_q)
```